EUMETSAT Satellite Application Facility on Climate Monitoring

Requirements Review

AVHRR GAC Edition 3.5 CDR and ICDR

(CLARA-A3.5)

	CDR	ICDR
Fractional Cloud Cover	**CM-11013**	**CM-6012**
Joint Cloud property Histogram	**CM-11023**	**CM-6022**
Cloud Top Level	**CM-11033**	**CM-6032**
Cloud Phase	**CM-11043**	**CM-6042**
Liquid Water Path	**CM-11053**	**CM-6052**
Ice Water Path	**CM-11063**	**CM-6062**
Surface Incoming Shortwave Radiation	**CM-11203**	**CM-6212**
Surface Downward Longwave Radiation	**CM-11263**	**CM-6262**
Surface Radiation Budget	**CM-11273**	**CM-6272**
Surface Net Shortwave Radiation	**CM-11282**	**CM-6282**
Surface Net Longwave Radiation	**CM-11292**	**CM-6292**
Black-sky albedo from AVHRR-GAC	**CM-11226**	**CM-6226**
White-sky albedo from AVHRR-GAC	**CM-11227**	**CM-6227**
Blue-sky albedo from AVHRR-GAC	**CM-11228**	**CM-6228**
TOA Reflected Solar Flux (RSF)	**CM-11313**	**CM-6332**
TOA Outgoing Longwave Radiation (OLR)	**CM-11343**	**CM-6322**

Reference Number:	SAF/CM/SMHI/RR/4.2
Issue/Revision Index:	1.1
Date:	15.04.2024

Document Signature Table

	Name	Function	Signature	Date
Author	Karl-Göran Karlsson	CM SAF Scientists		15.04.2024
Editor	Marc Schröder	CM SAF Science Coordinator		15.04.2024
Approval	CM SAF Steering Group			
Release	Rainer Hollmann	CM SAF Project Manager		

Distribution List

Internal Distribution	
Name	**No. Copies**
CM SAF Project Manager	1
CM SAF Project Team	1

External Distribution		
Company	**Name**	**No. Copies**
EUMETSAT		1

Document Change Record

Issue/ Revision	Date	DCN No.	Changed Pages/Paragraphs
1.0	29-12-2023	SAF/CM/SMHI/RR/4.2	Original version, with editorial changes from 16.02.2024
1.1	15.04.2024	SAF/CM/SMHI/RR/4.2	Results from RID discussions implemented

Applicable documents

Reference	Title	Code
AD 1	CM SAF CDOP4 Project Plan	SAF/CM/DWD/PP/1.0

Reference Documents

Reference	Title	Code
RD 1	CM SAF Product Requirements Document	SAF/CM/DWD/PRD/4.2
RD 2	Requirements Review for the AVHRR GAC Edition 3 data records	SAF/CM/CDOP3/SMHI/RR32
RD 3	Validation Report CLARA-A3 Cloud Products	SAF/CM/DWD/VAL/GAC/CLD
RD 4	Validation Report CLARA-A3 Surface Radiation Products	SAF/CM/DWD/VAL/CLARA/RAD
RD 5	Validation Report CLARA-A3 Surface Albedo Products	SAF/CM/DWD/VAL/CLARA/SAL
RD 6	Validation Report CLARA-A3 Top-of-Atmosphere Radiation Products	SAF/CM/RMIB/VAL/GAC/TOA

Table of Contents

List of Figures:

List of Tables:

1 Purpose of the document

This document consolidates the position of the CM SAF project team concerning the product requirements for the CLARA-A3.5 CDR and ICDR products. The CDR product identifiers are CM-11013, CM-11023, CM-11033, CM-11043, CM-11053, CM-11063, CM-11203, CM-11263, CM-11273, CM-11282, CM-11292, CM-11226, CM-11227, CM-11228, CM-11313, and CM-11343. The corresponding ICDR product identifiers are CM-6012, CM-6022, CM-6032, CM-6042, CM-6052, CM-6062, CM-6212, CM-6262, CM-6272, CM-6282, CM-6292, CM-6226, CM-6227, CM-6228, CM-6332, and CM-6322.

2 Introduction

2.1 The Climate Monitoring SAF (CM SAF)

The EUMETSAT Satellite Application Facility on Climate Monitoring (CM SAF, https://www.cmsaf.eu), together with the EUMETSAT Secretariat, holds the role as main implementer of EUMETSAT's commitments in support to climate monitoring.

Since the beginning in 1999, CM SAF has developed and will continue to develop capabilities for a sustained generation and provision of Climate Data Records (CDR's) of Essential Climate Variables (ECVs) as defined by the Global Climate Observing System (GCOS), derived from operational meteorological satellites. In particular, the generation of long-term data records is pursued that are suitable for the analysis of climate variability and potentially the detection of climate trends. Here, the main focus in CM SAF is on those ECVs that describe important components of the Earth's energy budget and its water cycle.

Another essential task of CM SAF is to produce data records that can serve applications related to the Global Framework of Climate Services initiated by the WMO World Climate Conference-3 in 2009. For this, CM SAF is supporting climate services at national meteorological and hydrological services with long-term data records but also with data sets produced in a seamless and coherent way close to real time that can be used to, e.g., prepare monthly/annual updates of the state of the climate. These so-called Interim Climate Data Records (ICDRs) together with the CDRs allow for a consistent description of mean values, anomalies, variability and potential trends for the considered ECVs. CM SAF CDRs also facilitate scientific applications such as for example process studies and evaluation of climate models at regional and global scales.

Furthermore, CM SAF contributes to advancing the availability, quality and usability of Fundamental Climate Data Records (FCDRs) in close collaboration with the EUMETSAT Secretariat and other satellite operators.

CM SAF is connected to the global scientific community ensuring a steady exchange of knowledge to continuously improve the data records and services, among others, through its engagement in international data assessments and through taking over responsibility in various international coordination bodies.

The international consortium of CM SAF currently comprises the Deutscher Wetterdienst (DWD) as host institute, the Royal Meteorological Institute of Belgium (RMIB), the Finnish Meteorological Institute (FMI), the Royal Meteorological Institute of the Netherlands (KNMI), the Swedish Meteorological and Hydrological Institute (SMHI), the Meteorological Service of Switzerland (MeteoSwiss), the Meteorological Service of the United Kingdom (UK Met Office) and the Centre National de la Recherche Scientifique (CNRS).

More information, including a complete catalogue of all CM SAF products, can be found at CM SAF's webpage, https://www.cmsaf.eu. Accessing all data products is facilitated through the CM SAF web user interface: https://wui.cmsaf.eu/.

3 Background of product under review

For RR 4.2 the following products as listed in Table 3-1 from PRD 4.2 (RD 1) are under review:

Table 3-1: CM SAF products under review.

Product Family	GCOS ECV	CM SAF Product Identifier (CDR, ICDR)	Product Name
CLARA-A3.5	Cloud properties	CM-11013, CM-6012	Cloud Fractional Cover (CFC)
	n/a	CM-11023, CM-6022	Joint Cloud Histogram (JCH)
	Cloud properties	CM-11033, CM-6032	Cloud Top (CTO)
	Cloud properties	CM-11043, CM-6042	Cloud Phase (CPH)
	Cloud properties	CM-11053, CM-6052	Liquid Water Path (LWP)
	Cloud properties	CM-11063, CM-6062	Ice Water Path (IWP)
	Albedo	CM-11226, CM-6226	Surface Albedo (SAL)
	Albedo	CM-11227, CM-6227	White-sky Surface Albedo (WAL)
	Albedo	CM-11228, CM-6228	Blue-sky Surface Albedo (BAL)
	Radiation budget	CM-11203, CM-6212	Surface Incoming Solar radiation (SIS)
	Radiation budget	CM-11263, CM-6262	Surface Downwelling Longwave radiation (SDL)

	Radiation budget	CM-11273, CM-6272	Surface Radiation Budget (SRB)
	Radiation budget	CM-11282, CM-6032	Surface Net Solar radiation (SNS)
	Radiation budget	CM-11292, CM-6292	Surface Net Longwave radiation (SNL)
	Earth radiation budget	CM-11313, CM-6332	ToA Reflected Solar Flux (RSF)
	Earth radiation budget	CM-11343, CM-6322	ToA Outgoing Longwave Radiation (OLR)

The CLARA-A3.5 ICDRs extend the associated CLARA-A3.5 CDRs until present time. To the maximum extent possible the ICDR is based on the same scientific and technical approaches as the CDR. In that sense, the combined CDR and ICDR data records are considered as a unit and consequently they share a common DOI. The CDR itself consists of consistently processed satellite data of a defined period in the past.

3.1 History of products/precursors

The first effort to retrieve cloud properties, surface radiation and surface albedo from the historic global NOAA AVHRR data record took place during the CM SAF CDOP-1 phase. The first data record was produced in 2011 and was named the CM SAF Cloud, Albedo and Radiation dataset, AVHRR-based; abbreviated CLARA-A1 (Karlsson et al., 2013). The second edition of the CLARA data record (CLARA-A2) was developed in the CDOP-2 phase and was released in 2016 (Karlsson et al., 2017). The third edition (CLARA-A3) was developed in the CDOP-3 phase but was not released until the first year of the CDOP-4 phase (Karlsson et al., 2023b).

3.2 Structure and content of this document

The products under review basically concern a completion and/or an extension of the CLARA-A3 climate data record. The extension comes from inclusion of products based on AVHRR-heritage channels of the Visible Infrared Imaging Radiometer Suite (VIIRS) resampled to approximately the same horizontal resolution as AVHRR GAC in the VGAC (VIIRS Global Area Coverage) format. Thus, CLARA-A3.5 is not an entirely new edition of CLARA. This means that product accuracy, precision and stability requirements should stay the same since a large part of CLARA-A3 will remain untouched in CLARA-A3.5. In other words, additional products must fulfil the same requirements as the remaining untouched products. However, a recalibration correction to the products' underlying visible radiances from 2017 onwards is envisaged, thereby correcting the original CLARA-A3 products. This recalibration also ensures a smooth transition to new products after 2020.

Finally, this document covers the requirements for the CDR and the ICDR, i.e., the continuous temporal extension of the CDR.

From these conditions, it follows that large parts of this document are identical to the prevous RR document for CLARA-A3 (RD 2) while additions mainly concern the modifications and extensions mentioned above.

3.3 Product status

Table 3-2 and Table 3-3 provide an overview of the relation of the CM SAF products under review in this RR to those in CLARA-A3, including the achieved accuracy in the CLARA-A3 DRR review.

Table 3-2 describes all cloud products where accuracy is generally measured by the bias (mean error) for level-2 (L2) and level-3 (L3) products, and precision is measured with the Hanssen-Kuipers Skill Score (KSS) for L2 and bias-corrected root-mean-square deviation (bc-RMS) for L3. Stability is measured as the change in bias per decade for L3 products. The reference instruments or data records given between brackets are: Cloud-Aerosol Lidar with Orthogonal Polarisation (CALIOP) v4 cloud products, surface synoptic observations (SYNOP), Moderate Resolution Imaging Spectroradiometer (MODIS) Collection 6.1, and the microwave-imager-based Multisensor Advanced Climatology of LWP (MAC-LWP).

Table 3-3 describes all remaining products, i.e., surface radiation, surface albedo and top of atmosphere radiation products.The reference for surface radiation products is BSRN stations and accuracies and precision are given by the mean absolute deviation. For surface albedo (SAL) and white sky albedo (WAL) references are also BSRN stations, accuracies are given as relative biases and precision as bc-RMS. For blue sky albedo (BAL), an additional reference is the Programme for the Monitoring of the Greenland Ice Sheet (PROMICE), accuracies are given as relative biases and precision as bc-RMS. For top of atmosphere radiation products the reference is CERES and ERA5 for reflected solar flux (RSF) and HIRS for outgoing longwave radiation (OLR). For both products the accuracy and precision parameters are given by the mean absolute deviation.

Table 3-2: Relation of CLARA-A3.5 cloud product identifiers (IDs) and CLARA-A3 product IDs and achieved accuracy, precision and stability as presented in the validation report (RD-3) of CLARA-A3. Corresponding validation results for CLARA-A2 are summarized in RD-2 for comparison.

Product Name	**CLARA Ed. 3.5** **CM SAF ID**	**CLARA Ed. 3**	
		CM SAF ID	**Achieved accuracy, precision and stability**
Fractional Cloud Cover	CM-11013	CM-11012	**Bias:** L2: -3.2 % (CALIOP, all clouds) -0.1 % (CALIOP, COT>0.217) L3: 2.0 % (SYNOP), -5.0 % (CALIOP, all clouds 2,4 % (CALIOP, COT>0.3) **bc-RMS or KSS:** L2: 0.6 (CALIOP, KSS) L3: 8.8 % (SYNOP) 8.9 % (CALIOP, all clouds) 6.9 % (CALIOP, COT>0.3) **Stability (trend per decade):** -1.3 % (SYNOP) 0.0 % (MODIS)
Joint Cloud property Histogram	CM-11023	CM-11022	n/a
Cloud top Level	CM-11033	CM-11032	**Bias**: L2, cloud top height: -898 m (CALIOP, all clouds) 250 m (CALIOP, COT>0.4) L3, cloud top pressure: 27 hPa (CALIOP, all clouds) -50 hPa (CALIOP, COT>0.3 **bc-RMS:**

Product Name	CLARA Ed. 3.5 CM SAF ID	CLARA Ed. 3	
		CM SAF ID	**Achieved accuracy, precision and stability**
			L2, cloud top height: 3236 m (CALIOP, all clouds) 1244 m (CALIOP, COT>0.4 L3, cloud top pressure: 41 hPa (CALIOP, all clouds) 66 hPa (CALIOP, COT>0.3 **Stability, cloud top pressure:** -4.7 hPa (MODIS)
Cloud Phase	CM-11043	CM-11042	**Bias:** L2: -2 % (CALIOP, all clouds) L3: -4.9 % (MODIS) **bc-RMS or KSS:** L2: 0.67 (CALIOP, KSS) L3: 13.1 % (MODIS) **Stability:** 2.5 % (MODIS)
Liquid Water Path	CM-11053	CM-11052	**Bias:** L3 : -0.7 to 8.1 gm^{-2} (MAC-LWP), -4.9 gm^{-2} (MODIS), **bc-RMS :** L3 : 11.7-16.1 gm^{-2} (MAC-LWP) 13.4 gm^{-2} (MODIS) **Stability :** 1.8 gm^{-2} (MODIS) (-6.9)-(-4.8) (MAC-LWP)
Ice Water Path	CM-11063	CM-11062	**Bias:**

Product Name	CLARA Ed. 3.5 CM SAF ID	CLARA Ed. 3	
		CM SAF ID	Achieved accuracy, precision and stability
			L3 : -0.4 gm^{-2} (MODIS) **bc-RMS :** L3 : 22.5 gm^{-2} (MODIS) **Stability :** -0.8 gm^{-2} (MODIS)

Table 3-3: Relation of remaining CLARA-A3.5 product identifiers (IDs) with CLARA-A3 product IDs and achieved accuracy, precision and stability as presented in the validation reports (RD 4, RD 5 and RD 6) of CLARA-A3.

Product Name	CM SAF ID in CLARA Ed. 3.5	CLARA Ed. 3	
		CM SAF ID	Achieved accuracy, precision and stability
Surface Incoming Solar radiation	CM-11203	CM-11202	**Meanabsolute deviation**: 7.3 Wm^{-2} Stability (after 1994): -0.13 $Wm^{-2}dec^{-1}$
Surface Albedo	CM-11226	CM-11222	**Relative bias:** -10.2 % **Mean RMSD**: 6.7 % **Stability**: -1.49 $\%dec^{-1}$
White-sky surface albedo	CM-11227	CM-11223	**Relative Bias:** -11.4 % **Mean RMSD:** 8.3 % **Stability:** 2.14 %
Blue-sky surface albedo	CM-11228	CM-11224	**Relative Bias:** -4.12-3.55 % **Mean RMSD:** 6-19 % **Stability:** +0.26-(-1.01) $\%dec^{-1}$
Surface Downwelling Longwave radiation	CM-11263	CM-11262	**Mean absolute deviation**: 7.2 Wm^{-2} **Stability (after 1994):** -0.17 $Wm^{-2}dec^{-1}$

Surface Radiation Budget	CM-11273	CM-11272	**Mean absolute deviation:** 9.7 Wm^{-2}
Surface Net Shortwave Radiation	CM-11282	CM-11281	**Mean absolute deviation:** 10.8 Wm^{-2}
Surface Net Longwave Radiation	CM-11292	CM-11291	**Mean absolute deviation:** 6.8 Wm^{-2}
ToA Reflected Solar radiation	CM-11313	CM-11312	*Mean bias ('accuracy'): (not evaluated)* **Mean Absolute Deviation** ('precision'): 3.2 Wm^{-2} **Stability:** Bias within +/-2W/m² for 94% of the RSF data, and for 98% of the OLR data
ToA Emitted Thermal radiation	CM-11343	CM-11342	*Mean bias ('accuracy'): (not evaluated)* **Mean Absolute Deviation** ('precision'): 1.8 Wm^{-2} **Stability**: Bias within +/-2W/m² for 94% of the RSF data, and for 98% of the OLR data

3.4 Related open actions from previous meetings and SGs

Various actions were issued during previous reviews for future CLARA editions. They are given in **Table 3-4**. Most of them, if not all of them, are valid for the entire CDR/ICDR dataset and not exclusively for the extension with VGAC-based products. Consequently, (most of) these actions are suggested to be applicable not before the Requirements Review for the next full reprocessing of the CLARA CDR (to be named CLARA-A4).

Table 3-4: List of open actions on CLARA-A3.5 from previous reviews and SG meetings. Due date might be after RR 4.2.

Action	Actionnee	Description	Due Date	Related RID
DRR3.2_001	PT	PT to quantify the error that was introduced with the approximation made by the retrieval of the algorithm of black-sky albedo.	PCR CLARA-A4	[034]
DRR3.2_002	PT	PT to consider how to provide global averages for CDRs.	RR CLARA-A4	[004]
DRR3.2_003	PT	PT to consider for the next version of CLARA (CLAR-A4), to document the assessment of the quality of surface clear-sky solar radiation.	DRR CLARA-A4	[005]
DRR3.2_004	PT	PT to identify suitable stations for validation of upward solar radiation fluxes.	RR CLARA-A4	[017]
DRR3.2_005	PT	PT to check and discuss with the method developers that ice sheets (Antarctic and Greenland) can be used as invariants for solar AVHRR channels.	PCR CLARA-A4	-
PCR3.2_001	PT	PT to account for CLARA-A4 using satellite observations also for clear-sky conditions (surface radiation products)	PCR CLARA-A4	[006]
PCR3.2_002	PT	PT to assess the sensitivity of the LUT and consider LUT with different effective radius (surface radiation products)	PCR CLARA-A4	[007]
PCR3.2_005	PT	PT to consider the aerosol correction as a part of ADM for the next version of CLARA (CLARA-A4). (TOA radiation products)	PCR CLARA-A4	[051]
PCR3.2_007	PT	PT to consider for the next CLARA release (A4), applying more "analytic" methods following e.g. the FIDUCEO approach or the even previous paper: https://agupubs.onlinelibrary.wiley.com/doi/full/10.1029/2006JD007313 in order to have a more sound and improved uncertainties estimation. Areas of elevated uncertainties shall be identified alerting the users for this areas. (Surface Albedo Products	PCR CLARA-A4	[154]
PCR3.2_009	PT	PT to consider including a long-term solar irradiance data product (TSI) for the next version of CLARA (A4). (TOA radiation products)	RR CLARA-A4	[129]
RR3.2_001	PT	PT to consider to provide simultaneous retrievals of Aerosols and Surface Albedo for future Releases.	RR CLARA A4	[009]

Action	Actionnee	Description	Due Date	Related RID
RR3.2_003	PT	PT to consider including clear-sky estimates of TOA fluxes to the product.	RR CLARA-A4	[013]

3.5 Current Planning

The CM SAF Project Plan [AD 1] provides the CM SAF review schedule. The part relevant for RR 4.2 is recalled in Table 3-5.

Table 3-5: Planned schedule for data records under review (from Project Plan). Proposed updates are given in red.

Family	RR4.2	PCR4.2	DRR4.2	Release
TCDR Global clouds and radiation (CLARA)	~~Q4 2018~~ Q1 2024	~~Q1~~ Q1 2025	Q4 2025	Q2 2026

4 Definition of product requirements

4.1 CDR

The CDR consists of consistently processed satellite data of a defined period in the past, ideally based on quality controlled, recalibrated and intercalibrated Level 1 data, i.e., an FCDR. The quality of the CDR is assessed during Delivery Readiness Reviews (DRRs).

4.2 Product overview

The aim of the CLARA data record is to provide a comprehensive characterization of cloud properties, surface radiation components, surface albedo and top of atmosphere radiation budget components. An important boundary condition is imposed by the instrumentation: the passive Advanced High Resolution Radiometer (AVHRR) imager (and its successors) onboard Tiros-N, NOAA and Metop polar orbiting satellites with spectral channels described by tables Table 4-1 and 4-2. From the AVHRR sensor basic information about integrated cloud properties, radiation, properties near the tops of clouds and properties of the cloud-free Earth surface can be retrieved. Figure 4-1 describes the time periods when AVHRR on each satellite has been operational until 2018.

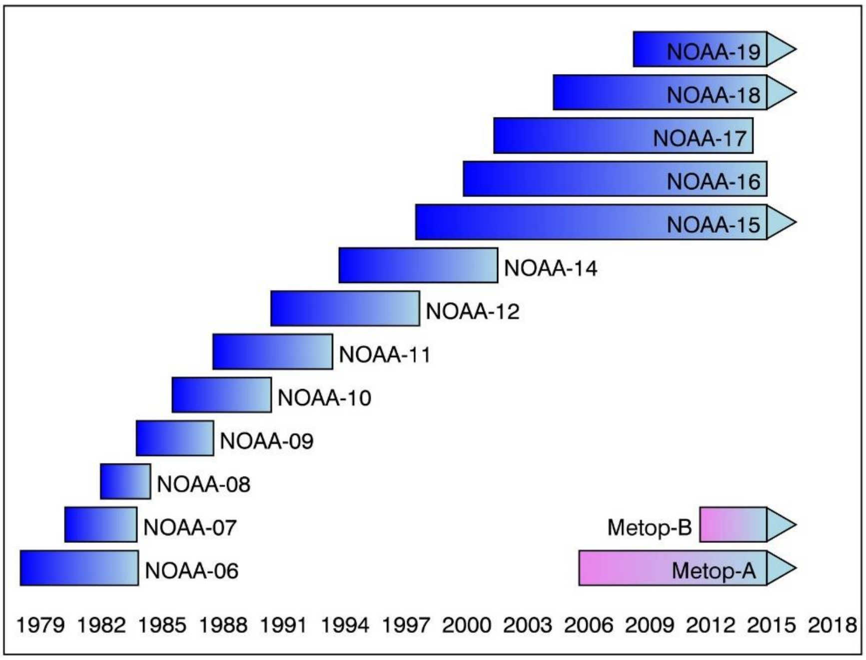

Figure 4-1: Overview of operation times for the AVHRR instrument on individual satellites from NOAA-6 in 1979 until 2018, although not including Metop-C being launched in November 2018. (From https://www.dlr.de/eoc/en/desktopdefault.aspx/tabid-9136/19476_read-45195/)

It is in general not possible to derive information about the vertical structure of clouds from passive imagery. There are exceptional cases in which information on the vertical structure can be obtained, such as: (i) identification of multilayer clouds and the (cloud top) properties of the respective layers if a relatively thin cirrus cloud overlies a low-level liquid cloud, (ii) retrieval of profile information on effective radius for specific cloud types by using different shortwave infrared wavelengths.However, this is still an area of active research and the encountered limitations met so far has led to the decision to not add such information to the planned cloud datasets.

Once cloud information has been retrieved, original AVHRR radiances and cloud information can be combined to derive radiation budget and surface albedo parameters.

Table 4-1: Spectral channels of the Advanced Very High Resolution Radiometer (AVHRR). The three different versions of the instrument are described as well as the corresponding satellites. Notice that channel 3A was only used continuously on NOAA-17 and on the Metop satellites. For the other satellites with AVHRR/3 it was used only for shorter periods.

Channel Number	**Wavelength (micrometers) AVHRR/1** Tiros-N, NOAA-6,8,10	**Wavelength (micrometers) AVHRR/2** NOAA-7,9,11,12,14	**Wavelength (micrometers) AVHRR/3** NOAA-15,16,17,18 NOAA-19, Metop-A, Metop-B, Metop-C
1	0.58-0.68	0.58-0.68	0.58-0.68
2	0.725-1.10	0.725-1.10	0.725-1.10
3A	-	-	1.58-1.64
3B	3.55-3.93	3.55-3.93	3.55-3.93
4	10.50-11.50	10.50-11.50	10.50-11.50
5	Channel 4 repeated	11.5-12.5	11.5-12.5

Table 4-2: Channel 3A and 3B activity for the AVHRR/3 instruments during daytime from launch date until present time (December 2023).

Satellite	**Channel 3a active**	**Channel 3b active**
NOAA-15		06/1998 – present
NOAA-16	10/2000 – 04/2003	05/2003 – 12/2011
NOAA-17	07/2002 – 02/2010	
NOAA-18		09/2005 – present
NOAA-19		06/2009 – present

Metop-A	09/2007 – 11/2021	
Metop-B	01/2013 – present	
Metop-C	11/2018 - present	

The CLARA-A3.5 data record contains the following products:

- Fractional cloud cover (CFC). On level-2 this involves the discrimination between cloudy and cloud-free pixels, i.e. a cloud mask. The instantaneous cloud masks are aggregated to level-3 cloud fraction.
- Cloud top level (CTO). This product includes the location of cloud tops expressed in three different ways: as cloud top pressure (CTP) in hPa, cloud top height (CTH) in m and cloud top temperature (CTT) in K.
- Cloud phase (CPH). This provides the dominant thermodynamic phase (liquid or ice) of particles near the top of the cloud.
- Liquid water path LWP). This is the vertically integrated amount of cloud water for pixels with liquid phase near the cloud top. The product contains the (liquid) cloud optical thickness (COT), particle effective radius (CRE), cloud droplet number concentration (CDNC), and cloud geometrical thickness (CGT) as additional layers.
- Ice water path (IWP). Same as liquid water path but then for pixels with ice phase near the cloud top. The product contains the (ice) cloud COT and CRE as additional layers.
- Joint cloud histogram (JCH). This is a combined histogram of CTP, COT and CPH, covering the solution space of these parameters. This gridded three-dimensional histogram (i.e., one histogram for each grid point) gives the absolute numbers of occurrences for specific COT-CTP-CPH combinations within specific bins.
- Surface Incoming Solar radiation (SIS). This provides the surface irradiance (also know as global radiation) and corresponds to the solar radiation (0.2 to 4 µm) that reaches the Earth surface on a horizontal plane.
- Black sky surface albedo (SAL). The value is the mean surface albedo value of the scenery of the pixel without any atmospheric contribution, but topography correction is taken into account in rough terrain.
- White-sky surface albedo (WAL). The value is the mean surface albedo value of the scenery of the pixel under perfectly isotropic illumination conditions, but topography correction is taken into account in rough terrain.
- Blue-sky surface albedo (BAL). The value is the mean surface albedo value of the scenery of the pixel in prevailing atmospheric conditions, but topography correction is taken into account in rough terrain.
- Surface downwelling longwave radiation (SDL). This provides the surface thermal (longwave) downwelling radiation (also know as counterradiation) with a wavelength larger than 4 µm reaching the Earth surface.
- Surface Net Solar radiation (SNS). This provides the net surface solar radiation estimated from the surface solar downwelling radiation and the surface albedo.

- Surface Net Longwave radiation (SNL). This provides the net surface longwave radiation based on the surface downweling and upwelling longwave radiation.
- Surface radiation budget (SRB). This provides the budget of the surface radiation, incl. shortwave (solar) and longwave (thermal) radiation.
- (Top of atmosphere) Reflected Solar Flux (RSF). RSF quantifies the total amount of solar radiation which is reflected back to space by the Earth and its atmosphere. The RSF is also sometime called shortwave flux. The incoming solar radiation is also provided as ancillary field in the data record. Those quantities are expressed as flux (density) in W/m².
- (Top of atmosphere) Outgoing Longwave Radiation (OLR). OLR quantifies the total amount of radiant energy which is (thermally) emitted in the Earth-atmosphere system and escapes the TOA toward space. OLR is also a flux in W/m². This quantity is also often call Outgoing Longwave Radiation (OLR) or longwave flux.

4.3 Recapitulating achievements in CLARA-A3 compared to the previous CLARA-A2 CDR

A number of changes and improvementshave been implemented in CLARA-A3 compared to the predecessor CLARA-A2, largely responding to requests from users and recommendations given at previous reviews:

- The time series have been extended from 1982–2015 (34 years) to 1979–2020 (42 years). This extension was accomplished by inclusion of data from four additional satellites carrying AVHRR/1 (see Table 5-1) and by extending the previous CLARA-A2 time series forward in time for satellites NOAA-18, NOAA-19 and all existing Metop satellites.
- An upgraded AVHRR GAC Fundamental Data Record (FDR) has been used. It consists of an updated and greatly revised visible calibration method provided by NOAA while infrared calibration is based on the same operational method as was used in previous CLARA editions. The calibrated AVHRR reflectances and brightness temperatures, used as a basis for the CLARA-A3 data record processing, have been compiled as a stand-alone dataset in a joint CM SAF/EUMETSAT effort. This dataset, provided by EUMETSAT is denoted the AVHRR FDR with the following dataset doi number: 10.15770/EUM_SEC_CLM_0060.
- Algorithms needing ancillary data on basic atmospheric and surface conditions have switched from using ERA-Interim data to the new reanalysis product ERA-5. It is important to notice that both the CFC product and the CTO product in CLARA-A3 are based on new statistical approaches (CFC is based on a Bayesian classifier and CTO on an artifial neural network). Consequently, both methods needed specific training when switching to ERA5 data.
- As mentioned above, a Bayesian concept for cloud masking was introduced. Cloud probabilities are now produced, replacing the previously used binary cloud mask, (a comprehensive method description is provided by Karlsson et al., 2020). This introduced a basic uncertainty measure for the CFC product and a way to more flexibly deal with cloud screening issues for downstream products. The Bayesian technique

also facilitated the processing of four-channel AVHRR data from the AVHRR/1 instrument which is not possible using the traditional thresholding method in PPS 2018.

- A new artificial neural network-based method for cloud top height retreival was introduced (described by Håkansson et al., 2018). The new method greatly improves cloud top height estimations . The method was also trained and adapted to AVHRR/1 data for which the previous PPS CTTH retrieval method in CLARA-A2 could not be used.
- The information about uncertainties of the products is enhanced. In particular, more error sources are taken into account for the estimation of uncertainties.
- Liquid cloud droplet number concentration (CDNC) and cloud geometrical thickness (CGT) products, based on the 3.7 μm CRE, were introduced along the lines of Bennartz and Rausch (2017).
- The retrieval of the surface irradiance is now based on the new top-of-the-atmosphere RSF product; besides ensuring consistency between the top-of-the-atmsophere and the surface radiation data records.
- Two new surface albedo products (WAL and BAL) are introduced in parallel with the SAL (Black-sky albedo) product.
- The monthly and pentad mean surface albedo values are now derived using the cloud probability information available for the whole month, instead of the previous use of an instantaneous binary cloud mask.
- The two top of atmosphere products (RSF and OLR) are new for CLARA-A3 and they have the following main features:
    - They are calculated for “all sky” conditions, i.e. no separate “clear-sky” product is provided.
    - Scene-dependent narrowband-to-broadband regressions between AVHRR and CERES-SSF are empirically derived from collocated/coangular observations, for RSF with channels 1 and 2, and for OLR with channel 4 (optionally also channel 5).
    - Broadband shortwave radiance is converted to flux by applying the CERES TRMM angular dependency models (ADM’s) (Loeb et al. (2003)), complemented by CERES TERRA ADM’s for snow and ice (Loeb et al., 2005). For longwave radiance, theoretical ADM’s was derived following Clerbaux et al. (2003).
    - Diurnal cycle is modelled by using method of Young et al. (1998).

The above list reflects the general improvements as outlined in the CDOP-3 proposal. They can be complemented with the following more specific improvements:

1. The addition of early satellite data (i.e., Tiros-N, NOAA-6, NOAA-8 and NOAA-10) have provided more realistic trends in CFC and all other parameters in the results based on all satellite data. In CLARA-A2 only satellites from afternoon orbit satellites were used in the first decade and this caused unrealistic trends in CFC and SIS.

2. CLARA-A2 did not provide uncertainties for all L3 cloud products but most products in CLARA-A3 have now associated uncertainty parameters.

3. The switch from ERA-Interim in CLARA-A2 to ERA-5 in CLARA-A3 as the basic reanalysis reference have lead to improved cloud detection (and subsequently an improved SIS retrieval) and cloud height assignment due to the improved horizontal, vertical and temporal resolution in addition to the overall effect of an improved ERA-5 data assimilation system.

4. CLARA-A2 CFC results over polar areas in the polar winter were greatly underestimated. Improvements are seen in CLARA-A3, although still limited mainly due to non-separability issues for clouds with similar cloud temperatures as the surface. However these problems are better reflected in CLARA-A3 uncertainty measures (cloud probabilities).

5. CLARA-A2 cloud top height results were previously oppositely biased, i.e., high clouds were assighed too low heights and low clouds were assigned too high heights. CLARA-A3 results has greatly reduced these opposite biases, e.g., resulting in improved reliability of Joint Cloud Histograms (JCH).

6. The albedo products have benefitted from the cloud probability information made available by the new probabilistic cloud product. This has improved the albedo retrieval especially in cloudy areas.

4.4 Planned improvements for CLARA-A3.5

4.4.1 Use of AVHRR-heritage channels from VIIRS data

A problem with CLARA-A3 is that the temporal coverage over the day varies over the covered period and that this coverage weakens, especially during the last decade. This is illustrated in Figure 4-2 showing the equator crossing times for the daytime observations for the satellites carrying the AVHRR sensor. Normally we have four observations per day (if including also the night-time observations) and they are fairly equally spaced over the day (although being exposed to some effects of orbital drift of the satellites some years after launch). The problem with the temporal coverage is shown in Figure 4-2 as a gradual loss of observations around 13:30 UTC in years after 2015. This is due to the orbital drift of satellites NOAA-18 and NOAA-19 and because no new satellites with AVHRR observations in this particular (afternoon) orbit have been or will be launched. Thus, instead of several observations approximately equally spaced over the day, we have ended up with a constellation practically giving us only observations with equator crossing times close to 09 and 21 local standard time (LST).

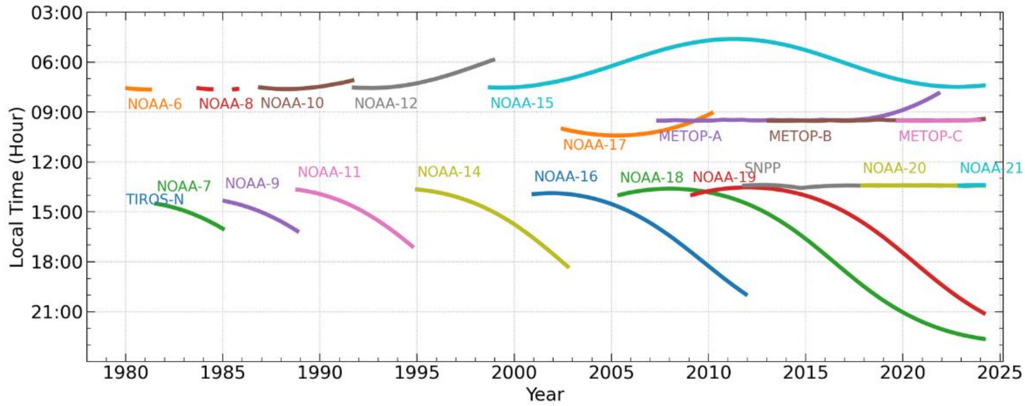

Figure 4-2: Local solar times of equator observations for all AVHRR-carrying NOAA satellites from TIROS-N to NOAA-19 and EUMETSAT's Metop A/B/C satellites. In addition, satellites with the VIIRS sensor (SNPP, NOAA-20 and NOAA-21) are also shown. The figure shows ascending (northbound) equator crossing times for afternoon satellites (starting with TIROS-N) and descending (southbound) equator crossing times for morning satellites (starting with NOAA-6). Corresponding night-time observations take place 12 hours earlier/later. (From Karlsson et al., 2023b)

The loss of the early afternoon observations means that the diurnal cycle of some parameters, (for example CFC, cloud cover) cannot be properly estimated anymore. Even more serious is that products related to reflected solar radiation in CLARA are now severely damaged or at least restricted in quality. More clearly, if observations are lacking at a time when the solar energy input to the Earth-Atmosphere is high, it becomes difficult to estimate parameters like the mean incoming solar radiation (SIS) or the mean reflected solar flux at the top of atmosphere (RSF). Another example is that CLARA surface albedo parameters need good illumination for being properly estimated and the loss of daytime observations will then severely reduce the frequency of available SAL observations. Consequently, the uncertainty increases for many parameters in the CLARA-A3 CDR during the last decade of CLARA-A3. The problem exists and will also grow even further for years after 2020 when the NOAA polar satellites with AVHRR (here, NOAA-18 and NOAA-19) will eventually be discontinued resulting in a situation with only access to AVHRR measurements from Metop satellites in a morning orbit. Additionally, this means that trend analyses after 2015 will be less representative for meteorological phenomena sensitive to diurnal cycle effects, such as cumulus convection. To be noted here is that CLARA-A3 improved the observational coverage for the first two decades in the CDR by adding observations from the very first version of AVHRR; AVHRR/1. This enables nominally four observations per day (i.e., two simultaneously operating satellites) for most of the years in these decades. For the last two decades, there are periods with more than two satellites operating simultaneously but the coverage of the diurnal cycle is only marginally improved since several satellites observe more or less in the same orbit with the same observation time as other satellites.

The proposed solution to the problem with the loss of early afternoon observations, is to ingest products based on new sensors having AVHRR-heritage channels. For CLARA-3.5 the plan is to introduce such products based on AVHRR-heritage channels of the Visible Infrared Imaging Radiometer Suite (VIIRS) carried by NOAA satellites Suomi-NPP (launched in 2011), NOAA-

20 (launched in 2018) and NOAA-21 (launched in 2022). Resampled VIIRS data with approximately the same horizontal resolution as AVHRR GAC is already available in the VGAC (VIIRS Global Area Coverage) format (Knapp et al., 2019). Satellites with VIIRS data (Suomi-NPP, NOAA-20 and NOAA-21) are kept in a stable orbit with equator crossing times at 13:30 LST (see Figure 4-2).

According to the CDOP-4 proposal, it was originally envisaged to view VGAC data as a fourth realization of AVHRR data and that CLARA-A3 methods would then need to be adapted to the available VIIRS channels. However, early prototyping has revealed that most of the AVHRR-heritage channels in VIIRS have only small deviations from the original AVHRR channels. This means that, by use of relatively simple spectral band adjustment factors (SBAFs), the AVHRR channels can be accurately simulated from VIIRS data. Consequently, the current strategy is to simulate NOAA-19 AVHRR channels from VIIRS data in order to minimize (and preferably avoid) specific adaptions of used CLARA-A3 retrieval methods. The choice of NOAA-19 is explained by the fact that NOAA-19 and Suomi-NPP operated in nearly identical orbits in the first few years of Suomi-NPP operations, thus creating ideal conditions for collocation of AVHRR and VIIRS data. This means that spectral band adjustment factors can be estimated directly based on collocated data. It is anticipated that all AVHRR channels except channel 2 at 0.9 microns will be simulated from simple linear relations between AVHRR and VIIRS while for channel 2 somewhat more complicated relations might be needed. Table 4-3 gives an overview of the chosen VIIRS channels for simulating the AVHRR channels of NOAA-19. However, notice that AVHRR channel 2 has a very broad spectral range which means that also possible contributions from VIIRS channel M6 (with spectral range 0.739-0.754 µm) could be considered.

Table 4-3: Description of AVHRR channels (two leftmost columns) and the presumed optimal AVHRR-heritage channels for VIIRS (two rightmost columns).

AVHRR channel	Spectral range (µm)	AVHRR-heritage VIIRS channel	Spectral range (µm)
Channel 1	0.58-0.68	M5	0.662-0.682
Channel 2	0.725-1.10	M6 M7	0.739-0.754 0.846-0.885
Channel 3b	3.55-3.93	M12	3.660-3.840
Channel 4	10.50-11.50	M15	10.263-11.263
Channel 5	11.50-12.50	M16	11.538-12.488

4.4.2 Calibration corrections for the transition from CLARA-A3 to CLARA-A3.5

A circumstance, that has added to the above-mentioned problems of lacking daytime observations for the last years of CLARA-A3, is the discovery of particular problems related to the calibration of AVHRR data during practically the same period in time. Since no on-board calibration mechanism exists for the visible AVHRR channels, vicarious calibration methods must be used based on comparisons with high-quality sensors (in this case MODIS) and invariant targets on the Earth surface. Most important here is to try to estimate the degradation rate for visible sensors which has shown to be quite different for the individual AVHRR instruments on different satellites. For this calibration correction to be accurate, several years of measurements must be at hand. In CLARA-A3, the latest update of the calibration method was made in 2017 (utilizing measurements up to 2015). It meant that only a few years worth of data was available for Metop-B (introduced in 2013) and this turned out to be insufficient for compensating in a realistic way for the degradation rate of corresponding visible channels. Recently (2023) a new calibration update has been issued and it is clear that also AVHRRs from other satellites than Metop-B need a correction before 2020 (including NOAA-19 and Metop-C which was launched in 2018). This update is clearly also essential for the processing of data after 2020.

An indication of the problems due to weaknesses of the AVHRR calibration of visible channels can be seen in Figure 4-3. It shows a time series of LWP derived from Metop-B AVHRR data compared to corresponding results from Terra MODIS observing at approximately the same time from a mid-morning orbit. We notice that CLARA-A3 LWP values start to deviate (i.e., decrease in both values and in amplitude) remarkably during the last years of the period. Since both Metop-B and Terra are in stable orbits, the mentioned calibration problems must then be the main cause for the deviation.. Figure 4-3 clearly illustrates that some corrections are necessary to fulfil compliance with LWP (and other) product requirements over the entire period.

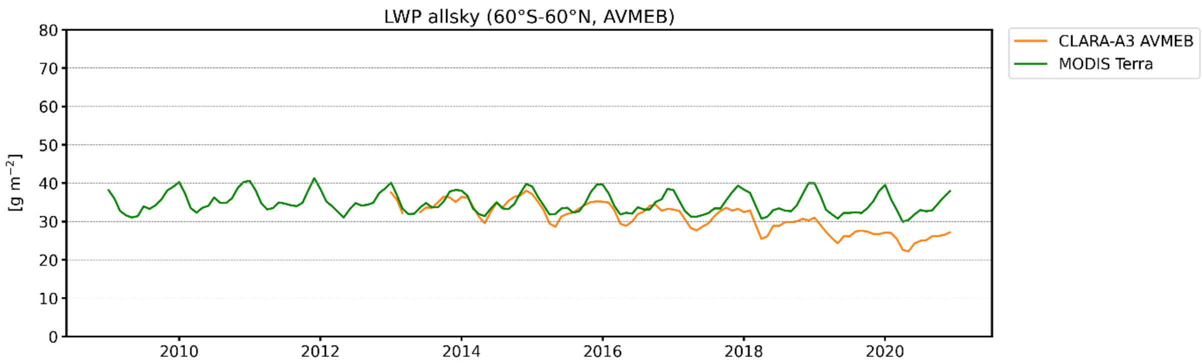

Figure 4-3: Time series of the 60°S-60°N monthly mean all-sky Liquid Water Path (g m^{-2}) based on CLARA-A3 Metop-B data (AVMEB) and the corresponding results from Terra MODIS data.

In conclusion, in addition to the obvious task of providing adequate calibration corrections for data after 2020 in CLARA-A3.5 (i.e., the additional years compared to CLARA-A3), measures must be taken to update the calibration of visible channels for some satellites (mainly Metop-B, Metop-C - the latter introduced in 2018 - and NOAA-19) for some years at the end of the

CLARA-A3 series. This must be done to get a seamless transition of results from satellites with the original AVHRR sensor for the years before and after 2020.

4.5 Traceability of requirements

The AVHRR GAC TCDRs serve various applications (see Section 5.2), many of which are related to global climate studies and model evaluation. Requirements for the use of Essential Climate Variables (ECVs) observations within the climate community have been formulated by the World Meteorological Organization (WMO) in the Global Climate Observing System (GCOS) report [GCOS-107] and its updates [GCOS-154 + GCOS-200 + GCOS-245]. However, note that GCOS-245 was published after the previous Requirements Review of CLARA-A3 which means that we cannot take these requirements into account for this extension of CLARA-A3 (i.e., requirements should be unchanged for the extension). These requirement reports focus on global applications and give target requirements in terms of horizontal, vertical, and temporal resolution, as well as 'accuracy' (to be interpreted as 'bias' in the terminology of this document) and stability (needed to detect expected long-term trends). [GCOS-200, Annex A] does not give requirements for (level-2) precision. Therefore, these requirements are added based on different sources.

4.5.1 Cloud products

For cloud properties the target horizontal and temporal resolution requirements in [GCOS-154] are set at 50 km and 3 hours, respectively. However, in climate research and particularly in regional climate studies, substantially higher spatial and temporal resolutions are requested. For example, in the World Climate Research Program (WCRP) Europe Coordinated Regional Downscaling Experiment (EURO-CORDEX) initiative (Jacob et al., 2014) regional climate simulations with a horizontal resolution of 12.5 km were presented. Therefore, the CM SAF aims to provide cloud products at a spatial resolution of ≈5 km (i.e., at nominal AVHRR GAC resolution). The monthly aggregated level-3 products will have a spatial resolution of 25 km, which is still finer than proposed by [GCOS-154].

As validation metrics we use generally the bias and the bias-corrected root-mean-square deviation (bc-RMS) to reflect systematic and random components of uncertainty, respectively (RD-1, Loew et al., 2017). These metrics are applied over the globe (or a collection of surface stations or a set of collocated orbits) with respect to a certain reference data record. Threshold, target and optimal values of the metrics are defined, which shall not be exceeded for any month in the CLARA-A3.5 record. This implies that locally (i.e. for subsets of the disk) larger deviations are possible. These deviations have to be reported in corresponding validation reports even if the global target values are fulfilled.

For level-2 the accuracy requirements are basically defined with the same metrics, also concerning the 'binary' products, cloud mask and cloud phase. Concerning the probabilistic cloud mask, a conversion to a binary mask is made prior to comparing it with reference datasets. This is consistent with how this product originally was trained (i.e., the target being an optimal performance at the 50 % probability level, see Karlsson et al., 2020). We propose to add one accuracy metric that is capable of giving a more complete picture of the efficiency of cloud screening, namely the Hanssen-Kuipers skill score (KSS, see e.g. Karlsson and Johansson, 2013). The KSS reflects how well events and no-events can be separated, and it is symmetrical in that respect. It is also a more neutral measure since it does not favor any of the two categories (if it is dominating) as a contrast to other measures like the Hit rate. It gives score values between -1 (complete discrimination failure producing anti-correlation) and 1 (perfect separation). Zero values imply that the method has no skill (i.e., producing random results).

The required accuracy for the respective cloud products is detailed below. The focus is on the target requirements. If not specified, the threshold and optimal requirements are normally set to twice and half the target requirement, respectively.

Fractional cloud cover (CM-11013)

In case of evaluating level-2 data with binary output, i.e. the cloud mask and cloud phase, we propose to use the Kuipers Skill Score (KSS) as a complement to the traditional bias and bc-RMS measures. A reasonable value for the target KSS requirement can be deduced by considering conditions under normal cloudiness conditions (i.e., mean CFC of 65 %) and the desired achievements in terms of probability of detection (POD) and false alarm rates (FAR). A reasonable requirement is to have POD(cloudy) exceeding 90 % and FAR(cloudy) below 15 %. Combining these POD and FAR values, this translates into a KSS of 0.6. Thus, we propose KSS=0.6 as the new target requirement, and analogously arrive at KSS=0.5 and 0.8 as threshold and optimal requirements, respectively.

In [GCOS-154] the accuracy requirement for cloud fraction was sharpened from 10 % (the value in [GCOS-107]) to a range of 1–5 %, dependent on cloud emissivity. For CLARA-A3.5 we will adopt the upper GCOS value of 5 %, while the optimal requirement is set to the lower GCOS value of 1%. Typically, we set the target for the level-3 bc-RMS, as a measure of precision, to twice that for the bias. For CFC daily and monthly means this implies a target bc-RMS of 10 %.

The temporal stability adviced by [GCOS-154] is a range of 0.3–3 %/decade. We propose a target stability of the bias that is somewhere in the middle of this range: 2 %/decade. The corresponding threshold and optimal values are set to 5 %/dec and 0.5 %/dec, respectively.

Overall, CLARA-A3.5 requirements are practically the same as for the previous CLARA-A2 dataset, although with an additional evaluation of the KSS scores for level-2 products.

Joint cloud histogram (CM-11023)

This combination of products was introduced for studying the evolution of various cloud regimes in time and space and stems from some pioneering International Satellite Cloud Climatology Project (ISCCP) work (e.g., by Jakob and Tselioudis, 2003). The main strength of the histograms is that they provide a very condensed and easily interpreted way of analyzing some of the most essential features of cloud appearance. To be noticed is that the joint histogram formulation is one of the cornerstones of the COSP satellite dataset simulators (Bodas-Salcedo et al., 2011). No separate requirements are formulated for the JCH product, since its accuracy depends on that of the underlying products CTP (part of CTO, CM-11033), COT (part of LWP/IWP, CM-11053/CM-11063), and CPH (CM-11043), which have their own requirements.

Cloud top level (CM-11033)

Just like cloud amount, cloud top pressure and cloud top temperature are two of the GCOS ECVs. Therefore, the same requirements guideline reflecting the needs for climate related research applies also in this case (GCOS-154). Cloud top height, pressure, and temperature are closely related. Therefore, a set of requirements for one of these quantities would be sufficient. However, in practice we use two sets of requirements, for CTP and CTH. The former is explicitly mentioned as ECV in [GCOS-154]. The latter is closest to what is primarily measured with active sensors (e.g., CALIPSO).

The envisaged target accuracy of the cloud top parameters is proposed as follows. For CTP the GCOS requirement is a range of 15-50 hPa [GCOS-154] dependent on cloud emissivity. We use the (slightly lowered) upper end of this range for the target bias, while the lower end of this range defines the optimum bias requirement. Thus, the target bias is set to a value of 45 hPa while the target bc-RMS is 85 hPa in case of level 3 products and 140 hPa for the unaveraged level 2 products, which is twice and three times the bias requirement, respectively. The GCOS stability requirement is 3–15 hPa/decade. We adopt the upper value of this range (15 hPa/dec) as target for the stability, while the optimal requirement is set close the lower value, namely to 5 hPa/dec.

In principle we aim to set the requirements for CTH at the same value as for CTP. For conversion from one unit to the other, we have chosen a reference height close to the border between middle and high clouds in the ISCCP definition (CTP ~ 400 hPa and CTH ~ 7.000 m). At this height a CTP deviation of 45 hPa corresponds to a CTH deviation of around 800 m. As a result, the CTP targets listed above translate to a target CTH bias of 800 m, and target bc-RMS values of 1600 m and 2400 m for level 3 and level 2 data, respectively. Similarly, the target CTH stability becomes 270 m/dec.

Overall, CLARA-A3.5 requirements for Cloud Top level products are slightly sharpened compared to requirements for previous CLARA-A2 dataset.

It should be noticed that decisions have been taken in the NWC SAF (regarding the PPS software which is used to derive some of the CLARA-A3.5 cloud products) to include measurements suitable for non-Gaussian error distributions alongside with the traditional mean errors and bc-RMS in the validation of the cloud top level product. The reason is that error distributions for cloud top retrievals (level-2) are typically irregular and far from Gaussian. Consequently, this makes the use of traditional measures difficult when judging whether product improvements are realized or not (as demonstrated by Håkansson et al., 2018). We will elaborate further on this in upcoming PCR and DRR reviews where results from alternative approaches (e.g. the use of median errors and inter-quartile ranges) will be presented together with results from traditional measures.

Cloud phase (CM-11043)

For level-2 cloud phase the NWCSAF [RD-14] employs POD and FAR as metrics. Their POD target for both liquid and ice cloud pixels is 80 %, while the FAR should not exceed 20 %. As argued for cloud cover, we propose to use the KSS as metric. Converting the POD and FAR into KSS using a typical liquid cloud fraction of about 50 %, yields KSS=0.6. This is the same value as obtained for the cloud mask. Therefore, we propose to also set the other requirements identical to those for the cloud mask, implying threshold and optimal requirements of KSS=0.5 and KSS=0.8, respectively.

Since CPH is not a GCOS ECV, no guidelines for target accuracy are available for this parameter. For CPH we propose to follow the cloud mask and define a target bias of 5 % for the fraction of water clouds (relative to the total cloud fraction), a target bc-RMS of twice this value, i.e. 10 %, and a target stability of 2 %/decade.

Liquid water path (CM-11053)

The GCOS accuracy requirement for LWP is 25% [GCOS-154]. Ohring et al. (2005) suggested very similar values. Our target accuracy closely follows these recommendations. Given a mean all-sky LWP of about 30 g/m^2 (e.g., RD-3), the GCOS target accuracy (bias) of 25 % translates to a bias of 7.5 g/m^2, which we slightly relax to 10 g/m^2 as target requirement. The target bc-RMS is set to twice this value, i.e. 20 g/m^2, for level-3. For stability, GCOS recommends a very challenging value of 5 %/dec, translating to 2 g/m^2/dec. We propose to relax this target to 3 g/m^2/dec, while the optimal requirement is set to 1 g/m^2/dec.

Ice water path (CM-11063)

The GCOS accuracy requirement for IWP is 25% [GCOS-154]. While this value is the same as for LWP, from a retrieval point of view the uncertainties in IWP are larger than in LWP, mainly because assumptions on ice crystal habits have to be made. Therefore, we apply relatively less strict requirements for IWP than for LWP. Given a mean all-sky IWP of about 40 g/m^2 (e.g., RD-3), the GCOS target accuracy (bias) of 25% translates to a bias of 10 g/m^2, while here a target bias of 20 g/m^2 is chosen. The target bc-RMS is set to twice this value, i.e. 40 g/m^2, and the target stability requirement is set to 6 g/m^2/dec.

4.5.2 Surface radiation products

Surface Incoming Solar Radiation (CM-11203)

The shortwave surface radiation is, as part of the surface radiation budget, an essential climate variable as identified by GCOS (GCOS-200, 2016). The CM SAF requirements are based on the recommendations by GCOS and on user feedback.

The target accuracy requirement for surface solar radiation data defined by GCOS is 1 W/m² (GCOS-200, 2016). The uncertainty of well-maintained ground measurements of shortwave radiation is estimated to be ±10 W/m² (hourly means) and ±4 W/m² (monthly means) (Raschke et al., 2012). In addition, the point to area–mean comparison adds further uncertainties to the validation process. Hence, the threshold accuracies of 9 / 18 W/m² (for SIS, monthly / daily) proposed here are based on the achieved accuracy of the CLARA-A2 data record. The optimum accuracies are set to 3 / 10 W/m² for SIS, monthly and daily, respectively.

The decadal stability requirement for surface solar radiation data defined by GCOS is 0.2 W/m²/dec [GCOS-200, 2016]. The optimal / target / threshold decadal stability of the CM SAF surface radiation data record (SIS) is 0.5 / 1 / 2 W/m²/dec, respectively. The target decadal stability is set to 1 W/m²/dec based on the documented changes in the surface solar radiation over the previous decades ('global brightening') from surface observations that are in the range from 1 W/m² to more than 10 W/m² (Wild, 2009). The stability of the new data record must be sufficient to be used for the assessment of these temporal changes. We consider a threshold stability of 2 W/m²/dec an appropriate compromise between the expected changes and the stability that can be promised to be achieved from satellite-based data. It is expected that the data record will be more stable than the optimal stability requirement for certain regions and time frames.

Surface Downwelling Longwave Radiation (CM-11263)

The longwave surface radiation is, as part of the surface radiation budget, an essential climate variable as identified by GCOS (GCOS-200, 2016). The target accuracy and decadal stability requirements for regional surface longwave radiation data defined by GCOS are 1 W/m² and 0.2 W/m²/dec, respectively.

The uncertainty of well-maintained ground measurements of longwave radiation is estimated to be ±2 W/m² for monthly averages (Raschke et al., 2012). In addition, the point to area–mean comparison adds further uncertainties to the validation process. Hence, the suggested threshold accuracy of 8 W/m² proposed here is close to the verifiable limit for gridded surface longwave radiation data, if the uncertainty of the reference measurements and the spatial variability are considered (GCOS-200, 2016).

Regarding the stability requirements, we have used the same values as for SIS, i.e., 0.5 W/m²/dec for the optimal stability, 1 W/m²/dec for the target stability and 2 W/m²/dec for the threshold stability.

Surface Net Solar radiation (CM-11282), Surface Net Longwave radiation (CM-11292), Surface Radiation Budget (CM-11273)

The surface radiation budget (SRB) is an essential climate variable as identified by GCOS (GCOS-200, 2016). The target accuracy and decadal stability requirements for the regional surface radiation budget defined by GCOS are 1 W/m² and 0.2 W/m²/dec, respectively. The solar and longwave net radiation (SNS / SNL) are derived from the corresponding downward and upward radiation components; the SRB is derived from the two net, shortwave (solar) and longwave (thermal), fluxes; the defined accuracies are based on the accuracies of the input data. Hence, we define the threshold, target, and optimal accuracy as 8 W/m^2, 5 W/m^2, and 3 W/m^2, respectively; the stability requirement also follows the corresponding requirements from CM-11263 and CM-11203.

4.5.3 Surface albedo products

Black-sky surface albedo SAL (CM-11226), White-sky surface albedo WAL (CM-11227) and Blue-sky surface albedo BAL (CM-11228).

The target GCOS accuracy requirement for black-sky and white-sky surface albedo is max (5% relative; 0.0025 absolute) [GCOS-154]. The stability target requirement is max (1%; 0.0001). As the TOA reflectance calibration accuracy for AVHRR channels 1 and 2 is not better than 2 – 3% [Heidinger et al., 2010], we use for the optimum accuracy for the surface albedo 5 % relative or 0.005 absolute and for the optimum relative decadal stability the value 2%. Since the cloud masking procedure has undergone a significant change in CLARA-A3, with potential effects downstream in SAL generation, we retain the CLARA-A2 target and threshold accuracy (bias) measures of 10% and 15% (respectively). The values are defined for flat land targets for 90% of observed cases. The target relative stability is set to 10 %. The reason for keeping a relatively high value here, despite the fact that achieved CLARA-A2 stability values were better than this, is because of expected higher radiometric noise and lower calibration accuracies of the AVHRR sensor data added in the beginning of the CLARA-A3.5 time series (e.g., from Tiros-N, NOAA-6, NOAA-8 and NOAA-10). For the newly developed white-sky and blue-sky albedo datasets, as the atmospheric correction, albedo retrieval methods and the geolocation uncertainty cause additional inaccuracy, the target relative accuracy is set to 25 % and the relative decadal stability 15 %, both defined for flat land and 90% of cases. The corresponding relative threshold values are 50% and 20%, respectively.

4.5.4 Top of Atmosphere radiation products (Reflected Solar Flux RSF CM-11313 and Outgoing Longwave Radiation OLR CM-11343)

TOA Earth radiation budget is one of the GCOS ECVs. [GCOS-154 and GCOS-200] documents the requirements for the corresponding CDRs in the frame of the observation of the global climate.

Spatial requirements and coverage

Concerning the spatial resolution, the proposed datasets will be provided at finer resolution (0.25°x0.25° lat-lon) than the GCOS requirement of 100 km. This fine spatial resolution aims to allow a better exploitation of the data, in particular when the TOA radiation is used to quantify cloud and aerosol forcing, and for impact studies involving small scale land cover and atmospheric processes. A fine spatial resolution also allows a better resampling of the data, for instance to match the grid of a climate model, and also a more frequent observation of clear sky flux. Furthermore, although not directly linked to the user requirements, a fine spatial resolution allows a better processing of the data, in particular to apply ADM (e.g. the CERES TRMM ADMs are derived from 10km footprints).

Although the datasets will be provided at 0.25°x0.25° spatial resolution, most of the validation will be performed at a coarser spatial resolution of 1°x1°. Therefore, the accuracy requirements proposed in the tables hereafter refer to the accuracy at this resolution. There are 2 reasons for this. The first one is that it is important to assess the product accuracy at the scale recommended by GCOS. The second reason is that the best-suited reference data for validation are the 1°x1° CERES products (see section 5.3.4 for details on the validation approach).

In accordance with the GCOS requirements, the datasets are global and will cover the entire surface of the Earth including both the North and South poles.

Temporal requirements

The temporal resolution required by GCOS is coarse (monthly mean), which might be appropriate for global climate studies, but appears inadequate for regional climate studies and other applications of TOA radiative fluxes, e.g. process studies. The Project team will therefore also generate and provide daily means.

The GCOS temporal requirement mentions that the diurnal cycle should be resolved, but does not specify how: either indirectly, by using smart interpolation techniques (modelling), or explicitly by frequent observation sampling. The latter is simply not feasible with polar-orbiting satellites which (in contrast to geostationary satellites) only provide observations during their overpass, limiting the actual daytime sampling to the number of satellites in orbit. Given the fact that simple models of the diurnal cycle are used, it is not foreseen to output the monthly mean diurnal cycle. This could be revisited in further editions, for instance using GeoRing FCDR.

Absolute radiometric level

The RSF and OLR products rely on empirical relations with CERES products, and hence their absolute radiometric level can be considered "tuned" (not independent). Therefore, we do not report a requirement, but rather state the absolute radiometric level of CERES, which is in the order of 1 W/m².

Concerning the reference level, the fluxes will be "scaled" to the 20km reference level that better suits the user needs (see Loeb et al., 2002).

Processing accuracy

The GCOS target accuracy for the instantaneous TOA fluxes at 100 km x 100 km resolution used to be 5 W/m² in 2006 [GCOS-107], and changed to 1 W/m² in 2011 [GCOS-154], probably following Ohring et al., 2005. Such a level of accuracy seems not to be feasible even after daily and monthly averaging, especially for the solar radiation. Therefore, the following elements are considered to set requirements for the products under review:

- The accuracies achieved for similar products issued by the CERES team. At first glance it could seem to make no sense to issue datasets with lower accuracy than the already available CERES datasets. In this view, the claimed accuracies of the CERES products would logically be threshold requirements. However, the datasets differ by their temporal coverage (41 years instead of 18) and spatial resolutions (0.25° in place of 1°). Also, it is worth to note that CERES uncertainties are generally reported for non-polar regions (60°S-60°N) and that higher error are expected near the Poles. Therefore, our threshold requirements will be less stringent than the actual CERES accuracies.

- The accuracies achieved for similar products issued by the University of Maryland (HIRS OLR CDR); this long-term CDR is based on the HIRS instrument onboard polar-orbiting satellites NOAA and MetOp, and produces daily and monthly OLR on a global grid of 1°x1°. The nature of the infrared channels (including CO2 and water vapour sensitive channels) allows obtaining accurate estimates of broadband longwave radiation.

CERES achievement in EBAF and SYN1deg.

The CERES EBAF product accuracy is summarized in [EBAF Ed.4 DQS]. For the EBAF monthly mean shortwave flux (i.e. RSF), the estimated regional uncertainty is 2.45 W/m² at 1 standard deviation. Most of the CERES uncertainty comes from the diurnal cycle correction (2 W/m²), while the errors due to the calibration of the instruments and due to the ADM's are both estimated at 1 W/m². For the monthly mean longwave flux (i.e. OLR), the estimated regional uncertainty is 2.40 W/m² at 1 standard deviation, from which the most important contributing error sources are the diurnal cycle correction (1.4 W/m²) as well as the CERES instrument calibration (1.8 W/m²), while the impact of the ADM is minor (0.75 W/m²). It is mentioned that the regional error can reach 5 W/m² in isolated regions of convection over south and central Africa and in the west Pacific Ocean region. Note that the above-mentioned uncertainty statistics were calculated for a particular area (60°S-60°N), ignoring 13.4% of Earth's surface (polar regions). The CERES SYN1deg product accuracy is summarized in [SYN1deg Ed.4A

DQS]. The combined monthly 1°x1° regional all-sky SW flux uncertainty is 3.8 W/m². The daily regional all-sky SW diurnal uncertainty is 8 W/m² (Doelling et al. 2013). The combined monthly regional all-sky LW flux uncertainty is 2.0 W/m². The daily regional all-sky LW diurnal uncertainties are 1.5 W/m² (Doelling et al. 2016). Those CERES achievements are set in the second and third last column of Table 5-3.

HIRS OLR CDR achievement in MM v02r07 and DM v01r02.

The latest information on the quality of the HIRS OLR CDR is provided in the document "QA Summary for OLR–Monthly and Daily CDR, Rev. 2.0, dated 08/31/2018", available through http://olr.umd.edu/. The document provides biases and RMSD with the CERES products.

The global mean OLR differences over the period March 2000 to Feb 2018 between the Monthly OLR CDR v02r07 and EBAF Ed4.0 is about -1.6 W/m², with the overall standard deviations is about 1.8 W/m² and RMSD of about 2.5 W/m².

The global mean OLR differences over the period March 2000 to Feb 2018 between the Daily OLR CDR v01r02 and EBAF Ed4.0 is about 2.3 W/m², with the overall standard deviations is about 1.5 W/m² and RMSDnces of about 2.8 W/m². However, those numbers are obtained after monthly integration. A more realistic estimate of the daily mean uncertainty is provided by comparison with the CERES SYN1deg-day product in (although this is not done for the latest v4.0 version of the CERES products). The reported RMSD is 5 W/m².

~~Currently, options are explored for scaling the CM SAF OLR product to the HIRS OLR CDR on 1°x1° pixel basis; this would mean that the added value of CM SAF OLR purely lies in its spatial resolution, and hence would constitute a spatially-refined version of the HIRS OLR CDR. For PCR 3.2 it will be decided if this option will be followed; if so, both the original CM SAF OLR as the HIRS-scaled CM SAF OLR will be provided to the user.~~

Proposed requirements for the processing accuracy

Compared to the CERES and HIRS OLR products, the CLARA-A3.5 RSF and OLR datasets will have additional sources of error, most importantly the narrowband-to-broadband conversion, a simplified diurnal cycle modelling (not involving geostationary satellites) and also less accurate ADM's ~~(the final set of ADMs were confirmed at PCR 3.2)~~. In contrast to the HIRS instrument, AVHRR has no water vapour and $C0_2$ sensitive infrared channels, which constitutes an additional source of uncertainty.

Given those additonal errors, our target requirements are set slightly higher than the reported uncertainties from the existing CERES and HIRS-OLR datasets. For both the RSF and OLR, a monthly mean accuracy of 4W/m² is targeted (see Table 4-4).

For the daily mean product, the targeted accuracy is 8 W/m² (a factor of about 2 is often reported between daily and monthly mean TOA radiation products). For the RSF, this value is similar to the CERES achievement in SYN1deg-day. For the OLR, this value is higher than the HIRS achievements of (5W/m²) to reflect the additonal uncertainties mentionned above.

It is proposed to set factor 2 between optimal, target and threshold requirements.

Table 4-4 summarizes the threshold, target and optimum requirements for CM-11313 (RSF) and CM-11343 (OLR) in terms of accuracy. For comparison, the last columns provide the achieved accuracies in the HIRS OLR datasets and in the CERES products.

Table 4-4: Accuracy requirements for TOA radiation products

Identifier	**Parameter**	**Temporal**	**Accuracy (mean absolute deviation) (W/m^2)**			**CERES EBAFv4**	**CERES SYNv4**	**HIRS OLR CDR**
			threshold	**target**	optimal	(W/m^2)	(W/m^2)	(W/m^2)
CM-11312	RSF	MM	**8**	**4**	**2**	2.45*	3.8*	-
		DM	**16**	**8**	**4**	-	8*	-
CM-11342	OLR	MM	**8**	**4**	**2**	2.40*	2* (?)	2.5**
		DM	**16**	**8**	**4**	-	1.5* (?)	5.0***

(*) uncertainty estimate on non-polar region (60°S-60°N);

(**) relative to CERES-EBAF Ed.4.0;

(***) relative to CERES SYN1deg-day ed 3A

(?) those number reported in the DQS are doubtful (maybe in percentage instead of W/m^2 unit)

Note: EBAF, SYN and HIRS OLR uncertainty provided at 1 standard deviation.

How these requirements meet the expected user's needs and application areas is further discussed in section 4.7.1. In general, the target accuracies between 4 W/m^2 and 8 W/m^2 proposed in Table 4-4 should allow the datasets to be useful for the various data usages. It is worth to mention that they are in the same order of magnitude as the achieved accuracies of the CERES products which are widely used (status as in Sept. 2018: 1,593 peer-reviewed journal papers and 52,390 citations to CERES papers).

The CERES and HIRS accuracies in Table 4-4 are provided at “1 standard deviation” (1σ) which means that, assuming a normal distribution of the error, about 68% of the grid values meets this accuracy. For consistency with the other CLARA-A3.5 radiation products, the accuracy requirements are given in terms of Mean Absolute Deviation (MAD), though both metrics are comparable. The requirements should obviously be met over most of the scene types, regions and illumination/observation geometries. If, in some conditions, the requirements are not fulfilled (or it can not be demonstrated they are fulfilled) the user shall be warned via the PUM and/or the data masked or flagged in the dataset (in case the threshold requirement is exceeded).

Stability

The GCOS stability requirement of 0.2 W/m²/decade [GCOS-107] was relaxed to 0.3 W/m²/decade in 2011 [GCOS-154], following Ohring et al., 2005. In 2016, this was again set to 0.2 W/m²/decade for OLR while for RSF it remained unchanged on 0.3 W/m² [GCOS-200].

The stability value refers to the maximum change of the systematic error over a period of 10 years (see Figure 4-4). The stability requirement put a constraint on the ageing present in the product, as well as on the discontinuities for instance when switching from one satellite to another. Following the [GCOS-200] we propose 0.2 and 0.3 W/m²/dec as optimal stability requirements for OLR and RSF, respectively. It is not expected that such a challenging stability can be reached (and demonstrated) with the AVHRR instruments. Therefore the target requirement is set to 0.6 W/m²/dec and the threshold requirement to 4 W/m²/dec, respectively. All stability requirements are listed in Table 4-5. However, achieving the target stability is directly subject to availability of stable FCDR data that will be confirmed for PCR 4.2. The value of 0.6W/m²/decade was set in between the optimum requirement and the stability achieved for surface incoming solar and thermal radiation in CLARA-A2 (<1 W/m²/decade, see Table 3-3 in RD 2). For the threshold, the relatively high tolerance of 4 W/m²/decade value is set as it is believed that in some applications of the data the stability will not be a crucial point (e.g. case studies).

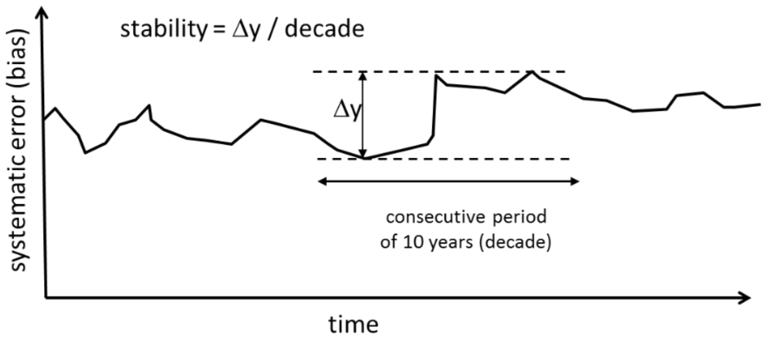

Figure 4-4: Definition of stability

The stability will be addressed by comparison with other datasets covering (part of) the dataset period (e.g. CERES EBAF, HIRS OLR dataset, ISCCP FD / FH, ERBE, PATMOS, ECMWF reanalysis) as well as “stable” Earth targets (deep convective clouds, desert). Those comparisons will provide reasonable evidence that the stability requirements are met (or not).

Stability requirements are only given for the monthly mean products. It is expected that the daily mean products will be characterized by the same stability. The stability will be evaluated at relatively large scale (e.g. in 5°x5° boxes) and the analysis should provide evidence that stability requirements are met over the principal scene types (clear ocean, vegetation, desert, cloud …).

Table 4-5: Stability requirements for TOA radiation products

Identifier	Parameter	Temporal	Decadal stability (W/m²/decade)		
			threshold	target	optimal
CM-11312	RSF	MM	4	0.6	0.3
CM-11342	OLR	MM	4	0.6	0.2

4.6 Validation approach

4.6.1 Cloud products

Validation of cloud products is a complicated task because for many cloud parameters no single data record exists that can serve as a true reference. An exception is data records of cloud cover, cloud-top phase and cloud-top height provided by the spaceborne lidar and radar sensors CALIPSO-CALIOP and Cloudsat-CPR. However, these instruments were not present prior to 2006 and they only provide global observations for two local times (1:30 a.m. and 1.30 p.m.). In addition, only a small fraction of all available NOAA/Metop orbits can be intercompared with these observations at high latitudes. Similarly, ground-based observations do not provide all cloud parameters and are normally restricted to a small number of surface sites, with limited coverage outside the developed world and over the ocean.

For these reasons, we aim at an evaluation approach, broader than strict validation, which characterizes the data products by comparison with various data records, taking the respective sensitivities into account. These comparisons can then complement each other, giving a more complete picture of the quality of the CLARA-A3.5 products.

In the following, the validation/evaluation approach and data sources are discussed per cloud product.

Fractional cloud cover (CM-11013)

The main source of validation observations for CFC for Level 2b products is the space-based CALIPSO-CALIOP lidar instrument. Cloud observations from this sensor are available from October 2006 onwards, and they provide more direct and easily interpreted observations of cloud detection and vertical cloud structure than passive methods. Also the CALIOP data are available in a format where the point measurements were aggregated to a horizontal resolution of 5 km which is very similar to the AVHRR GAC pixel size. As demonstrated by Karlsson and

Håkansson (2018) the CALIOP cloud optical thickness information can be used to determine the cloud detection sensitivity of passive imagers. In RD 3 and Karlsson et al. (2023a) extensive validation of the CLARA-A3 cloud mask with CALIOP was presented, and we intend to continue the same approach for CLARA-A3.5.

A problematic issue is that even if CALIOP observations were introduced in 2006 they cannot be used efficiently as a validation reference over the entire period thereafter. The reason is NOAA policies in how to operate their operational polar satellite system. NOAA is only maintaining a stable afternoon orbit (compatible with CALIPSO) for their prime satellites. In practice it means that shortly after a satellite is no longer a prime satellite, orbit-sustaining maneuvers are stopped and the satellites starts to drift in the orbit. The consequence is that this satellite cannot any longer be collocated globally with CALIPSO data and that collocations are now only available at high latitudes near 70 degrees. Thus, the introduction of the Suomi-NPP and NOAA-20 satellites in 2011 and 2017 (both declared prime satellites shortly after launch), respectively, meant that the last two AVHRR-carrying afternoon satellites NOAA-18 and NOAA-19 relatively soon lost their capability to be globally collocated and evaluated by use of CALIOP observations. For NOAA-18 the orbit started drifting in 2010 (NOAA-19 being prime satellite) and for NOAA-19 the orbit started drifting in 2013 (with Suomi-NPP as prime satellite). Notice that the Metop-satellites operate in a morning orbit which is kept stable by EUMETSAT. Unfortunately, since being in morning orbits, collocations for Metop-satellites will also be restricted to high latitudes. As a result of this limited availability of CALIOP validation data, global CALIOP validation of level-2 products for CLARA-A3 had to be carried out with almost the same collocation dataset as the one available for evaluation of CLARA-A2 (i.e., practically no additional data could be used). However, for the extended CLARA-A3.5 CDR, the situation improves considerably by the fact that the satellites carrying VIIRS are kept in a stable early afternoon orbit. This means that level-2 products for CLARA-A3.5 based on VIIRS can again be validated against CALIOP for full global orbits during the entire period from 2012 and until the end of CALIOP measurements in August 2023. Notice that not only the level-2 evaluation of fractional cloud cover will benefit from this but also the evaluation of products CTO and CPH.

For level-3 products from both CLARA-A3 and CLARA-A3.5, an important improvement Is nevertheless the fact that a much-improved level-3 product from CALIOP is now available as a reference covering a period of more than 15 years. Thus, more attention could be given to level-3 validation using CALIOP data for CLARA-A3, although no stability studies could be achieved due to the short period with CALIOP data. In CLARA-A3.5, level-3 datasets from CALIOP can be used for a few additional years and could possibly also contribute to stability studies.

Concerning other observation references than CALIOP, cloud observations made at meteorological surface synoptic stations (SYNOP) will be used as input for the validation of cloud cover. Drawbacks of SYNOP observations are that they are performed in varying ways (e.g., human observers or ceilometers with different sensitivities to high clouds), that their quality is not uniform, and that they have limited coverage outside the developed world and over the ocean. However, especially due to their long-term availability, they remain a useful reference data record suitable for monitoring and validating space-based estimations of cloud coverage.

Two other AVHRR-based CFC CDRs will be compared with CLARA-A3.5: PATMOS-X version 6 and ESA-CLOUD_CCI version 3. Both datasets were released after the release of CLARA-A2 and needs to be referred to in this context.

Finally, we will also compare to level-3 CFC-products from ISCCP-H and MODIS. ISCCP-H is an improved high resolution version of the ISCCP dataset which also has been released after the release of CLARA-A2 (Young et al., 2018). Regarding the MODIS products, MODIS-based Level 3 parameters, i.e. the official cloud products from MODIS (Platnick et al., 2017), will be used as a reference for the Level 3 product evaluation. MODIS uses the same measurement principle as AVHRR, but it has many more channels and is mounted on the polar orbiters Terra and Aqua. Therefore, it is very well suited not only to evaluate the level 2 and 3 products for the AVHRR field of view. As a contrast to the CLARA-A2 comparison with MODIS Collection 6 data, we will use an updated version of the MODIS dataset; MODIS Collection 6.1.

Joint cloud histogram (CM-11023)

The Joint Cloud Histogram will be not be validated separately as it consists of the histogram components CTP, COT, and CPH. However, JCH will be inter-compared with similar histogram data from the official MODIS product.

Cloud top level (CM-11033)

The main validation data source for the cloud top level products will be CALIPSO (see also the description of the availability of CALIPSO-CALIOP data in the discussion of validation of Cloud Fractional Cover above). With the vertically resolved cloud top data from CALIOP it is possible to analyze the effective detection range of a passive instrument such as AVHRR. In RD-3 an extensive validation of the CLARA-A3 cloud top level products with CALIOP was presented, and we intend to continue the same approach for CLARA-A3.5.

As additional evaluation, the AVHRR-derived monthly mean products will be evaluated with a comparable sensor in terms of measurement technique and footprint., Here we will use corresponding results from MODIS (C6.1), ESA-Cloud-CCI v3, PATMOS-X (version 6) and ISCCP-H.

Cloud phase (CM-11043)

As for CFC and CTO, CALIPSO will also be used as the main reference to validate the CPH product. This validation will be complemented by comparisons with MODIS, ESA-Cloud-CCI v3, PATMOS-X and ISCCP-H data.

Liquid water path (CM-11053)

For LWP, passive microwave (PMW) imagers provide a useful reference. We plan to perform pixel-based comparisons with the Advanced Microwave Scanning Radiometer – EOS (AMSR-E). In addition, level-3 LWP will be compared with the MAC-LWP climatology presented in Elsaesser et al., (2017). Although these observations are a very useful reference, some of their limitations have to be acknowledged: PMW LWP observations are characterized by a number of systematic errors (e.g., Seethala and Horvath, 2010), have a considerably coarser resolution than the SEVIRI observations, and are rather uncertain for precipitating clouds, and are available over ocean only.

MODIS, PATMOS-x, ESA-CLOUD-CCI v3 and ISCCP-H LWP retrievals will be used for additional evaluation, as they constitute important references to study longer-term homogeneity, as well as to pinpoint potential algorithm deficiencies.

Ice water path (CM-11064)

For IWP, the DARDAR product (Delanoë and Hogan, 2010) is probably the best reference, as it combines the sensitivities of the CALIPSO lidar to thin ice clouds with that of Cloudsat to thicker clouds. DARDAR will be used for the validation of CLARA-A3.5 level-2 IWP, while comparisons with MODIS, PATMOS-X, ESA-CLOUD-CCI v3 and ISCCP-H will be used for further evaluation as for the other cloud products.

4.6.2 Surface radiation products

Surface Incoming Solar Radiation (CM-11203)

Surface Downwelling Longwave Radiation (CM-11263)

Surface Net Solar radiation (CM-11282)

Surface Net Longwave radiation (CM-11292) Surface Radiation Budget (CM-11273)

The validation of the surface radiation data records will be conducted against high-quality surface reference measurements from the Baseline Surface Radiation Network (BSRN). The measures will be evaluated, analyzed and compiled to provide the complete error and uncertainty information in a consistent manner. The mean absolute deviation will be used to quantify the accuracy of the data records, the temporal stability of the bias against the surface observations will be used to assess the compliance of the data records with the stability requirement.

In the validation assessment the uncertainty of the reference measurements has to be considered [GCOS-200, 2016]. For the BSRN surface measurements, the uncertainty of the monthly mean data has been determined to be +/- 4 W/m^2 and +/- 2 W/m^2 for the solar and thermal radiation, respectively (Raschke et al., 2012]). However, this value strongly depends on the quality and the availability of the measurements within each particular month and the uncertainty can deviate from the reported mean value for individual months and BSRN stations. One specific factor to consider is the elevation difference between the BSRN Station and the CLARA-A3.5 topography in the Validation of SDL. There are also some issues with the BSRN SDL calibration (Nyeki et. al., 2018) which need some attention. The temporal stability of the measurements varies even more between the BSRN stations.

Although BSRN measurements will be the primary validation source, some evaluation of the results will also be considered comparing with data from other sources (e.g., GEBA, WRDC, buoys, etc.).

4.6.3 Surface albedo products

For albedo products, the satellite-based estimates shall be evaluated against quality-controlled in situ albedo observations from reference networks such as Baseline Surface Radiation Network (BSRN). Attention shall be paid in the selection of the evaluation sites to ensure the reference observations' spatial representativeness at the 0.25 degree resolution of the albedo products. Over sea ice and snow, select field campaigns will also be leveraged (SHEBA, Tara, etc.) to improve the evaluation coverage over the polar regions. Comparisons with existing satellite-based datasets will complement the validation and provide a spatiotemporally complete baseline for evaluation of possible differences.

4.6.4 Top of Atmosphere radiation products

Comparison with collocated satellite observations

Validations, verification and quality checks of the CLARA-A3.5 TOA radiation products will be performed by intercomparison with other CM SAF datasets (from MVIRI, SEVIRI and GERB) and with different CERES products (EBAF, SYN, SSF) and HIRS OLR following the methodology described in [SAF/CM/RMIB/VAL/GERB_DS]. In general, the comparison of various sources of TOA fluxes allows attributing the observed drifts or jumps in instrument's ratios to problems with one instrument or its processing.

To assess the accuracy, the CERES EBAF and SYN-1deg datasets will be the main references, but span only the 2000-2018 period (i.e. about the second half of the dataset), and will be used for validation of the monthly mean and the daily mean products, respectively.

For accuracy, daily and monthly "bias maps" are created (CM SAF minus CERES) on a 1°x1° grid, and across all grid boxes the Mean Absolute Deviation (MAD) is calculated in order to test the requirements.

For the thermal fluxes and its stability, it is planned to compare the CM SAF dataset with the HIRS OLR climate dataset (Lee et al., 2007). Intercomparison will be performed for the monthly mean products, but also on daily basis using the HIRS daily mean OLR CDR recently released by NCDC (access to data and C-ATBD available via http://www.ncdc.noaa.gov/cdr/operationalcdrs.html).

Finally, comparison with ERBE (ERBS - November 1984 through February 1990, NOAA-9 - February 1985 through January 1986, NOAA-10 - November 1986 through May 1989) data will also be done.

For stability assessment, intercomparison with ERBE Wide-FOV will be performed.

Verification with reanalysis

The comparison to the reanalysis (ERA5, ERA-interim, ERA-CLIM, NCEP/NCAR) data sets will be performed as additional check of the datasets, in particular for the stability criteria (e.g. to help to attribute if a trend exists in the dataset) and/or processing artifacts detection (e.g. switch from 1 satellite to another, effect of missing data, effect of the VZA near the Poles, ...). Although the CERES EBAF and SYN1deg data are our main references, comparison with

ERA5 reanalysis is expected to be useful to confirm the stability over the first part of the record. We have made a preliminary comparison between the global monthly mean TOA fluxes from ERA5 and CERES EBAF. It seems that ERA5 could be useful to detect jumps (e.g. at switch from one AVHRR instrument to another) of the order of > 0.5 W/m. However, it is noted that reanalysis products like ERA5 also have their flaws (e.g. lacking or simplified aerosol radiative effect). Rather than as an absolute stability measure, ERA5 is used for comparison together with other data records with the objective to increase confidence if multiple records confirm observed features.

Verification with ISCCP (-FD,-FH), GEWEX-SRB

Comparison with the ISCCP-FD (Zhang et al., 2004) and its successor ISCCP-FH (Zhang et al., 2017) will be performed. The overall uncertainties of the TOA monthly mean ISCCP-FD fluxes are estimated to 5-10W/m², which is a bit higher than our target accuracies. The ISCCP-FH product has similar uncertainties (≤~10W/m²).

Comparison with the GEWEX-SRB dataset (Stackhouse et al., 2011) will also be performed. Similar to the ISSCP-FD product, the overall uncertainty of the TOA monthly mean GEWEX-SRB fluxes is estimated to ~10W/m² which is a higher than our target accuracies.

4.7 Expected users and application areas

The users of the CLARA data records are mainly scientists performing climate studies but there are also many other applications. The previous CLARA releases have been used in scientific studies for various purposes. An overview of peer-reviewed papers in which CLARA data were used is given in Table 4-6 and Table 4-7. The former lists papers utilizing CLARA-A1 data and the latter papers utilizing CLARA-A2 data. Full references are given in sections 7.2 and 7.3. The lists include also a few papers from PT members utilizing CLARA data in validation studies or for development of new algorithms. In addition, Table 4-8 lists papers related to the use of CLARA-A3 data (with full references given in sections 7.1 and 7.4. This table is dominated by studies from the PT since CLARA-A3 was released less than one year ago (in May 2023).

Table 4-6: Overview of studies in which CM-SAF CLARA-A1 products have been used. The first and second column list the lead author and year of publication, respectively; full references can be found in Section sections 7.2. The remaining columns contain further details on which data was used for what application.

Author	Year	Parameter	Level	Region	Period	Application
Abera	2017	CFC	L3	Nile river	1994-2009	Water Budget calculations
Babar	2018	SIS	L3	Scandinavia	1982-2009	Evaluation CLARA-A1 radiation products
Blunden	2014	CFC	L3	Global	1982-2014	BAMS State of Climate

Author	Year	Parameter	Level	Region	Period	Application
Boccolari	2017	SDL	L3	Arctic	1982-2009	Longwave surface fluxes in the Arctic
Calbo	2016	CFC	L3	Black, Caspian and Aral Seas	1991-2010	Comparison with reanalyses and surface observations
Calbo	2017	SIS	L3	Iberian Peninsula	1988-2009	Assessing solar radiation stations
Cao	2015	SAL	L3	Northern Hemisphere	1982-2009	Sea Ice Albedo forcing studies
Cruz	2017	CFC	L3	Southeast Asia	1989-2008	CORDEX evaluation cumulus schemes
Duan	2015	SIS	L3	22 lakes	1982-2009	Lake heat budget calculations
Enriquez-Alonso	2016	CFC	L3	Mediterranean	1984-2005	CMIP-5 cloud cover study
Guo	2018	SAL	L3	Third Pole (central Asia)	1982-2009	CMIP5 snow-albedo feedback study
He	2014	SAL	L3	Global	1982-2009	Global assessment of surface albedo datasets
Hofer	2017	CFC	L3	Greenland	1982-2009	Relation CFC and loss of Greenland ice sheet
Karlsson	2013	SAL	L3	Arctic	1982-2004	Sea ice albedo studies CMIP-5
Karlsson	2013	CFC	L2	Global	2006-2009	CFC evaluation with CALIPSO data
Koenigk	2014	SAL	L3	Arctic	1982-2005	CMIP-5 model evaluation – sea ice
Koenigk	2015	CFC	L3	Arctic	1982-2005	Arctic modelling study (CORDEX)
Kotarba	2015	CFC	L3	Central Europe	2004-2009	Intercomparison with ISCCP and MODIS
Kotarba	2016	CFC	L3	Central Europe	2000-2009	Evaluation MODIS cloud climatology
Laine	2014	SAL	L3	Arctic	2003-2011	Arctic sea ice albedo studies
Laine	2011	SAL	L3	Arctic	2007	Development of MW-retrieval of SAL
Light	2015	SAL	L3	Arctic	1982-2009	Evaluation CCSM4 ice simulations
Loew	2016	SIS	L3	Global	1982-2009	Evaluation CMIP5 fluxes

Author	Year	Parameter	Level	Region	Period	Application
Obregon	2014	CFC, SAL, SIS	L3	Europe + Middle East	1982-2009	Use in WMO RA VI regional center
Qu	2015	SAL	L3	Global	1982-2009	Surface Broadband Albedo study
Quante	2016	CFC, SIS, ?	L3	North Sea region	1982-2009	Overview of North Sea region climate change
Riihelä	2015	SIS	L3	Finland + Sweden	1982-2009	Evaluation of surface fluxes using ground measurements
Räisanen	2014	SAL	L3	Northern Eurasia	1982-2006	ECHAM5.4 snow studies
Sanchez-Lorenzo	2017	CFC	L3	Mediterranean	1984-2009	Comparison climate simulations and satellite observations
Seo	2016	SAL	L3	Antarctica	1982-2009	Antarctic SAL study
Shao	2015	SAL	L3	Antarctica	1982-2009	Antarctic sea ice study
Sinitssyn	2018	SIS	L3	Global ocean	1982-2009	Ocean flux study
Sörensson	2018	SIS, SDL	L3	South America	1982-2009	Evapotranspiration study
Spangehl	2016	CFC, CTP, COT		Global	1982-2009	MiKlip climate simulation evaluation
Stengel	2015	CFC, CTP, CWP (COT, CRE)	L2	Global	2008	ESA-CLOUD-CCI Round Robin
Sun	2015	CFC	L3	USA	1982-2009	US cloud cover study
Tornow	2017	CFC	L3	Global	1982-2009	Assisting development of geostationary cloud detection
Volkova	2017	CFC	L3	Western Russia	1982-2009	Development and assessment of cloud detection methods
Yao	2016	SDL, SRB	L3	Arctic ocean	1982-2009	Evaluation of WRF model sea ice simulations
Zak	2015	SIS, SRB, SDL	L3	Czech Republic	1982-2009	Applications for Czech Republic
Zaninelli	2018	SIS	L3	South America	1982-2009	Regional climate study
Zhang	2016	SAL	L3	Arctic	1982-2009	Arctic Polar Vortex study
Zheng	2017	SAL	L3	China (Bohai Sea)	1992-2008	Sea Ice study

Table 4-7: Overview of studies in which CM-SAF CLARA-A2 products have been used. The first and second column list the lead author and year of publication, respectively; full references can be found in Section Section 7.3. The remaining columns contain further details on which data was used for what application.

Author	Year	Parameter	Level	Region	Period	Application
Anttila	2018	SAL	L3	Northern hemisphere	1982-2015	Changes in snowmelt timing and premelt albedo
Babar	2018	SIS	L2	Scandinavia	1982-2015	Intercomparing CLARA-A1/A2 for solar energy mapping
Benas	2018	CFC,LWP (COT, CRE)	L3	South China	2006-2015	Changes in cloudiness and cloud properties
Boers	2017	CFC	L3	The Netherlands	1982-2009	Solar radiation trends over the Netherlands
Bojanowskij	2020	CFC	L3	Meteosat disk	1991-2015	Effects of orbital drift of polar-orbiting satellites in climate datasets
Bruno	2020	CTO, CPH	L3	Global	2009-2013	Cloud Top Phase Partitioning in Different Cloud Types
Chen	2022	SAL	L3	China	1982-2015	Surface albedo feedback
Dong	2023	All cloud prods	L3	Global	1982-2015	Properties of stratus and stratocumulus clouds
Eliasson	2020	CFC, CTO, LWP, IWP, CER, JCH	L3, L2b	Global	1982-2015	CLARA-A2 simulator for COSP
Eyring	2022	SIS	L3	Switzerland	2008-2018	High-resolution electricity generation model demonstrates suitability of high-altitude floating solar power
Hartfield	2018	CFC	L3	Global	1982-2009	BAMS State of climate 2017
Jian	2018	SAL	L3	Global	2003-2015	Planetary albedo studies
Jääskeläinen	2017	SAL	L3	Global	1982-2014	Development of AOD SMAC atmospheric corrections
Jääskeläinen	2022	SAL	L3	Arctic Sea	1982-2015	Surface albedo of the Arctic Sea ice
Karlsson	2018	CFC	L2	Global	2006-2015	Evaluation of CLARA-A2 CFC
Karlsson	2018	CFC, CTP	L3	Global	1982-2009	Inter-comparison with PATMOS-X, ESA-CLOUD-CCI and ISCCP-H

Author	Year	Parameter	Level	Region	Period	Application
Kaushal	2021	CFC	L3	Indonesia	1990-2014	Coral Skeletal Luminescence Records
Manara	2020	SIS	L3	Italy	1990-2016	Comparison of Surface Solar Irradiance from Ground Observations and Satellite Data
Manninen	2019	SAL	L3	Northern Finland	1982-2015	Black and White-Sky Albedo Values of Snow
Palfreyman	2018	SIS	L3	Europe	1982-2009	Spread of zoonotic nematode Thelazia callipaeda
Pfeifroth	2018	SIS	L3	Europe	1983-2015	Validation with ground stations, analysis of trends
Pfeifroth	2018	CFC, SIS	L3	Europe	1982-2015	Trends in cloud cover and solar radiation
Pietkäinen	2018	SAL	L3	Scandinavia	1982-2015	REMO lake model studies
Riihelä	2017	CFC, CTO, CWP(COT, CRE)	L2	Arctic	2007	Arctic surface flux study
Riihelä	2018	SAL	L3	Global	1982-2015	Development of multi-sensor SAL
Riihelä	2019	SAL	L3	Greenland	1982-2015	Surface albedo of the Greenland Ice Sheet
Schwarz	2018	SIS	L3	Global	1982-2015	Point-to-Area measurement inter-comparison study
Sedlar	2018	SAL	L3	Arctic	2000-2015	Role of SW radiation in spring Arctic atmospheric preconditioning
Stengel	2023	CTO, CPH	L3	Global	2011	Temperature Dependence Cloud Ice Particle Effective Radius
Tang	2021	SIS	L3	Global	1983-2018	Satellite-Derived Surface Solar Radiation Products over Tropical Oceans
Tang	2022	SAL	L3	Global	1984-2018	Mapping long-term and high-resolution global gridded photosynthetically active radiation
Tong	2023	SDL	L3	China	2009-2012	Evaluation of downward shortwave radiation products
Tzallas	2019	CFC	L3	Europe	1984-2012	Comparing CLARA-A2 and ISCCP against surface observations

Author	Year	Parameter	Level	Region	Period	Application
Urraca	2017	SIS	L3	Europe	2005-2015	Validation surface radiation products
Urraca	2018	SIS	L3	Spain	2005-2015	Surface radiation network study
Urraca	2017	SIS	L3	Global	1982-2015	Quality control of surface radiation stations
Urraca	2018	SIS	L3	Global	1982-2015	Sources of uncertainty in global irradiance
Urraca	2019	SAL	L3	Global	1981-2015	Fitness of Satellite Albedo Products for Monitoring Snow Albedo Trends
Urraca	2020	SIS	L3	Europe	1983-2018	BQC: A free web service to quality control solar irradiance
Wang	2018	SIS	L3	China	1993-2015	Validation of surface solar radiation
Wang	2024	LWP, CRE	L3	China	1995-2015	Aerosol-cloud studies
Zhang	2023	CFC, LWP	L3	China	1980-2015	Precipitation and sensitivity to Cumulus parametrization
Zhao	2020	CFC, LWP, IWP	L3	China	2005-2017	Aerosol effects on cloud-to-ground lightning

Table 4-8: Overview of studies in which CM-SAF CLARA-A3 products have been used. The first and second column list the lead author and year of publication, respectively; full references can be found in Section 7.4. The remaining columns contain further details on which data was used for what application.

Author	Year	Parameter	Level	Region	Period	Application
Akkermans	2023	RSF, OLR	L3	Global	1979-2020	Evaluation of ToA fluxes
Devasthale	2023	CFC, CTO	L3	Global	2003-2020	Stabilty and trends of CFC and CTO
Devasthale	2023	CFC, CTO, SIS	L3	Global	1980-2020	Difference between Climate normals and Climatology
Karlsson	2023	CFC, CTO	L3	Global	1979-2020	Evaluation of cloudiness and cloud top information
Riihelä	2023	SAL, WAL, BAL	L3	Global	1979-2020	New SAL products in CLARA-A3
Xu	2023	CFC	L3	China	2017-2021	In-situ evaluation of night-time cloudiness
Wang	2018	SIS	L3	China	1993-2015	Validation of surface solar radiation

Author	Year	Parameter	Level	Region	Period	Application
Akkermans	2023	RSF, OLR	L3	Global	1979-2020	Evaluation of ToA fluxes
Devasthale	2023	CFC, CTO	L3	Global	2003-2020	Stabilty and trends of CFC and CTO
Devasthale	2023	CFC, CTO, SIS	L3	Global	1980-2020	Difference between Climate normals and Climatology
Karlsson	2023	CFC, CTO	L3	Global	1979-2020	Evaluation of cloudiness and cloud top information
Riihelä	2023	SAL, WAL, BAL	L3	Global	1979-2020	New SAL products in CLARA-A3
Zhan	2023	OLR	L3	Global	1979-2020	Evaluation of ToA fluxes

The applications can be grouped as follows, with the approximate (due to great overlap between topics) number of studies given in brackets:

- Arctic and Antarctic surface albedo and flux studies (15)
- Global (and regional) climate model evaluation (14)
- Global and regional climate monitoring (16)
- Evaluation of surface radiation climatologies and networks (23)
- Climate trend studies including inter-comparison of satellite data with other observations (20)
- Studies of physical processes (e.g., fluxes and evapotranspiration) (18)
- New validation methods and development of algorithms (13)
- Boreal snow studies (6)
- Biological studies (3)
- ToA flux studies (2)

The CLARA parameters have been used with varying frequency. Most frequently used are CFC, SAL and SIS products. There is a clear preference for using L3 data (86 studies) compared to L2 data (6 studies).

This analysis indicates a quite diverse group of scientific users with multiple application areas. Apart from this, there are many other users/applications with unpublished results. As an example, we mention applications in the solar energy sector, for which not only irradiance measurements but also information about clouds is highly important. Notice also the appearance of the new category “ToA flux studies”. These products are new for CLARA-A3 which explains why only one introductory paper is listed (see also the discussion in the following section). Overall, one can conclude that most CLARA parameters at both level-2 and level-3 are useful and should thus be continued in the next CLARA release.

4.7.1 Expected use of new Top of Atmosphere radiation products in CLARA-A3

The products from the CERES team are the current state-of-the-art for global TOA radiation CDRs: By a seamless combination of the CERES instrument onboard polar-orbiting satellites (providing broadband fluxes) with narrowband geostationary instruments (providing frequent temporal sampling for diurnal cycle), these highly accurate products are the *de facto* reference, to which most other scientific efforts are validated with, or at least compared to. However, there has been an increasing need for long-term, high-resolution TOA albedo products in monitoring the climate impacts of regional-scale events such as air pollution, urbanization, forest fires, and other small-scale land cover changes (Song et al., 2018), which can hardly be detected from data sets with coarse spatial resolution (Wang et al., 2016), and small scale atmospheric processes e.g. valley fog (Clerbaux et al., 2009). Furthermore, in absence of a global long term CERES-like CDR, many studies focusing on long term model validation or trend detection fall back to “surrogate datasets” such as reanalysis (e.g. ERA-Interim) or radiative transfer computations (e.g. ISSCP-FD), but would otherwise have preferred a more observation-based alternative. Concerning CERES, two major limitations can thus be identified: (1) the products are relatively recent, e.g. starting in year 2000 for the EBAF product, and (2) the products have a relatively coarse spatial resolution of 1°x1° (lat-lon equal angle grid). The current development within CM SAF aims to create a CDR that would resolve those two drawbacks, respectively by (1) a prolongation back in time to the late 70’s and (2) by increasing the spatial resolution to 0.25°x0.25°. A third advantage of the new CDRs lies in their synergy and compatibility with the other CDR’s from the CM SAF CLARA product family (cloud mask and other cloud parameters, surface radiation, surface albedo, etc.) which share common algorithms and processing chains. The following scientific topics are typically subject of published articles:

- **Understanding regional climate mechanisms:** improve the **understanding of regional climates** and **global climate teleconnections** and to **observe climate anomalies.** For example, Zhan and Davies (2017) show that June reflected solar radiation is closely related to the underlying sea-ice condition in that month, and can be used to achieve September sea-ice extent predictions with good accuracy. In addition to their CERES-based analysis, they also express the need to extend the analysis back in time (pre-CERES period) and therefore fall back to earlier broadband observations (ERBE) as well as to reanalyses, which offer a much longer period to evaluate the potential for a skilful forecast. The radiation anomalies in their study range from -15 to +15W/m², so a target requirement of 4W/m² would be more than sufficient to capture the signal. Tang and Leng (2013) investigate relations between temperature, precipitation, cloudiness and radiation using satellite-based products; however, the analysis period is 1982-2009 forcing the authors to also rely on GEWEX-SRB dataset despite their assessment of this dataset as “*lower quality*” and “*suffering from several known issues (…)*”. Longterm CDR’s of OLR are often used to identify tropical convective variability (Schreck et al., 2018). Chiodi and Harrison (2015) use two OLR CDR’s to identify El Nino and La Nina patterns, and clearly state their preference for the longest-running record.
- **Quantification of atmospheric processes:** For example, Schmidt et al. (2018) simulated time-series of global-mean volcanic effective radiative forcing from 1979 to 2015. Comparison with observations, however, is limited to the CERES and ERBS periods. The reported RSF radiation anomalies reach values of up to -2W/m² (“El

Chichon" eruption) and -3 W/m² ("Pinatubo" eruption). Such signal should be observed with the target 0.6 W/m²/decade for stability. Other examples are studies on the impact of desert (mineral) dust on the radiation budget. Those studies generally report radiative effects significantly higher than our target requirement for accuracy (e.g. up to 100 W/m² during daytime in Slingo et al., 2006).

- **Evaluation of climate models and reanalyses**: CLARA-A3.5 will be valuable for spatially explicit model validation at fine spatial resolution. Indeed, (regional) climate models and reanalysis are now performed at finer scale (e.g. ERA5 at 0.3°) that includes more and more small scale effects (e.g. surface variability, orography, …). Furthermore, long CDRs are preferred since the model output typically spans multiple decades, and often include a significant part during the pre-CERES era (1980s and 1990s). For example, Dolinar et al. (2015) evaluate their global multimodel ensemble of historical climate simulations (1979-2008) against CERES-EBAF, but are forced to temporally narrow down the analysis to the CERES period ("…*the NASA observations used in this study begin in March 2000. Therefore, the period between March 2000 and February 2008 is selected (….)*").
- **As boundary condition to calculate surface radiative fluxes**: A first step in estimating surface radiation consists often in an accurate estimation of TOA reflected radiation (e.g. the algorithm of Pinker and Laszlo (1992)). This approach is adopted in previous versions of CLARA and in GEWEX-SRB (Stackhouse et al., 2011).

The previously mentioned requirements are generally suited for those application areas.

4.8 Uniqueness of products

There are many previous data records available based on AVHRR GAC data and many more are under preparation (or being updated). This is explained by the long temporal coverage of AVHRR observations making it very interesting for climate monitoring applications. Data is used in different ways, either as standalone time series or as embedded data together with other geostationary data (e.g. ISCCP). For datasets based exclusively on AVHRR data, two other major datasets besides CLARA exists: PATMOS-x (Heidinger et al., 2014) and ESA-CLOUD-CCI (Stengel et al., 2017). However, these datasets are primarily cloud product datasets and do not include the surface radiation and surface albedo products. Notice also that CLARA-A3.5 is extended to include also top of atmosphere radiation products which allow total radiaton budget studies and cloud radiation effect studies (as discussed in section 4.7.1).

Method-wise the three different mentioned cloud CDRs differ in several ways, despite being based on the same basic input data. The development of respective methods have intensified during recent years. Competition has increased but it has also lead to rapid improvement of products for all involved parties. This has been accomplished by the use of common AVHRR FCDRs or FDRs and the access to high quality reference datasets (i.e. A-train data). PATMOS-x is released by NOAA and builds upon the agencies' knowledge heritage from being an AVHRR data provider. The EUMETSAT Metop-satellites were introduced starting from 2007 as a component of the joint EUMETSAT-NOAA polar satellite mission. This also motivated a European effort in trying to use data from Metop-satellites in climate monitoring applications which is one of the reasons for the development of the CLARA dataset. On a longer term a similar effort, as described earlier for including AVHRR-heritage information from the VIIRS sensor, is needed to incorporate AVHRR-heritage data from the next EUMETSAT imager Metimage into the long historic datasets after launch of the EPS-SG satellites.

The development of cloud retrieval methods continues in different ways, e.g. through introduction of new artificial neural network approaches, more accurate Bayesian approaches and by inclusion of sounding channels from the HIRS instrument in the processing ("fusion techniques").

As regards the CLARA-A3.5 products other than clouds, one must claim that there are few other (if any) datasets which include also the radiation and surface albedo products based on a consistent set of cloud products. In this respect, also the very high horizontal resolution of these additional products is a very strong point of the CLARA-A3.5 dataset. Comparable products are usually defined in a much coarser grid. Thus, the large and consistently derived product portfolio, defined at very high horizontal resolution, and over a very long time period makes CLARA-A3.5 unique.

4.8.1 Uniqueness of CLARA-A3 Top of Atmosphere radiation products

Since CLARA-A3 Top of Atmosphere products are new compared to previous CLARA versions, we give a separate discussion of these products' uniqueness in this section.

The following table provides an overview of the main TOA radiation CDRs available (or under development) for the 1978-2018 time period as L3 products:

Table 4-9: Overview of main TOA radiation CDRs

CDR	Organis.	Period	Res.	Global?	observation type	Instruments	Orbit	SW+LW?
ERBE/ERBS NS-WFOV Ed.3 Rev1	NASA LaRC	1985-1999	10°	No *(non-polar)*	**BB**	ERBS-WFOV	LEO	Yes
CERES-SYN, CERES-EBAF	NASA	2000-2018	1°	Yes	**BB**	CERES, (Multiple)	LEO+GEO	Yes
SEVIRI/GERB Data Record	CMSAF	2004-2015	9km	No	**BB**	GERB, SEVIRI	GEO	Yes
MVIRI/SEVIRI	CMSAF	1983-2015	0.05°	No	NB	MVIRI, SEVIRI	GEO	Yes
FORTH		1984-2004		Yes	RT model			Yes
ISCCP-FH	NCEI	1983-2015	110 km	Yes	RT model	(Multiple)	LEO+GEO	Yes

GEWEX-SRB	NASA LaRC	1983-2009	1°	Yes	NB	(Multiple) FCDR:ISCCP	LEO+GEO	Yes
HIRS OLR	UMD	1978-2018	1°	Yes	NB	HIRS, (Multiple)	LEO+GEO	No (LW)
PATMOS	NOAA NESDIS	1981-1999	1°	Yes	NB	**AVHRR**	LEO	Yes
NOAA Interpolated OLR	NOAA	1981-2018	2.5°	Yes	NB	**AVHRR**	LEO	No (LW)
APP-x	NCEI	1982-2018	25 km	No *(polar only)*	Neural net trained by RT model	**AVHRR**	LEO	Yes
TAL-AVHRR	UMD	1981-2018	0.05°	No *(land only)*	NB	**AVHRR**	LEO	No (SW)
CLARA-A3	**CMSAF**	**1979-2020**	**0.25°**	**Yes**	**NB**	**AVHRR**	**LEO**	**Yes**
BB = BroadBand, NB = NarrowBand, RT = Radiative Transfer, LEO = Low Earth Orbit, GEO = Geostationary.								

From all these available CDRs, the CLARA-A3.5 TOA radiative fluxes RSF and OLR stand out because of the unique combination of fine spatial resolution, long-term time span, observation based flux retrieval (although NB), global coverage, and complementarity with other CDRs (e.g. cloud mask).

5 ICDR

The ICDR regularly extends the associated CDR until present time. To the maximum extent possible the ICDR is based on the same input data, scientific approaches, algorithms and processing system as the CDR. The goal is that output from the ICDR is identical to output from the CDR if run in parallel. The intention is to provide to the users a consistent data record based on CDR and ICDR output.

The quality of the ICDR and how it relates to requirements is assessed in two steps:

1) ORR: the Operational Readiness Review takes place prior to the first release of the ICDR. Usually it is conducted in parallel to the DRR of the associated CDR. If both reviews are successfully passed and approved by SG, the combined CDR and ICDR data record is released. The objective of the ORR is to showcase the level of agreement between CDR and ICDR and a first impression on continuous quality of the ICDR after end of CDR. Thus, the ICDR is compared to the CDR using output over a mutual time period to assess the degree of similarity. Additional validation and/or comparisons to external (reference) data records are carried out for the period after the end of the CDR. The output from ORR does not define the Service Specifications. Requirements defined in this RR document are the baseline for this review and the initial Service Specifications.
2) OR: the Operations Review is carried out annually and assesses the compliance of operational CM SAF products, i.e., ICDRs, with Service Specifications. A key objective is to regularly showcase continuous quality and document it. Baseline for the ORs are the Service Specifications.
   During the ORR the focus is on the similarity between CDR and ICDR. With sufficient temporal coverage of the ICDR validation results presented during an early OR will then be used to fine tune the Service Specifications of the ICDR.

5.1.1 Traceability of requirements

The concept of fully consistent CDR and ICDR processing is not achievable given the latency constraint, availability of input data and efforts needed to guarantee quality of input at the same level as for the CDR. Consequently, differences between output from the ICDR and the CDR are expected. Thus, the threshold requirements of the CDR constitute the target requirements of the ICDR. Threshold and optimal requirements are not defined specifically for ICDR products.

5.1.2 Envisaged ICDR production

CLARA-A3.5 ICDR production will basically (method-wise) be identical to the CDR production. However, some changes are expected concerning input data due to the inability to have access to well-defined and climate-quality assured FCDR and ancillary datasets because of the short latency for delivery of products (one or two weeks). Typically this will concern the AVHRR and VGAC FDR datasets and ancillary datasets from reanalyses and other environmental data (e.g., ice cover maps). It is currently not possible to exactly specify what input data will be available at the time for ICDR products (scheduled for 2026) since also currently used datasets are developing over time.

The following is required:

- AVHRR FDR data from remaining Metop satellites in 2026
- VGAC data from NOAA satellites with VIIRS
- Reanalysis data
- Ice concentration maps

A final consideration is that at some point after 2026 also AVHRR-heritage information from the METimage sensor onboard EPS-SG satellites needs to be ingested into the ICDR production chain. Additional work (which is currently not planned) on this aspect is needed at the end of CDOP-4 or in the beginning of CDOP-5. Preferably, this should be done before going for a completely new edition of CLARA (tentatively CLARA-A4) to prevent a loss of data in the ICDR processing from the morning orbit when Metop-C is decommissioned.

5.1.3 Validation approach

During the ORR output from the ICDR will be compared to output from the CDR for an overlap period of approximately 1 year. This evaluation will document the level of CDR-ICDR consistency at the time of CDR-ICDR transition. During the subsequent, annual ORs the ICDR will be evaluated by comparisons to available reference data streams.

The reference data records for the ORs need to be available in February/March for the previous year every year in order to allow a timely validation until OR which typically takes place in April or May.

Reference data for cloud products are foreseen to be based on MODIS products (as long as they are available) but later on corresponding MODIS products being transferred by NOAA from MODIS to VIIRS. Note that the VIIRS-based reference products will be based on the full VIIRS channel set and not only AVHRR-heritage channels. Also surface observations from SYNOP (manual or automatic) can be used for some products.

For surface radiation and surface albedo products, reference measurements at BSRN stations will be used.

For the TOA flux products, the main reference data will consist of CERES-EBAF and CERES-SYN1deg (for both RSF and OLR).

During the sub-sequent ORs, the same validation/comparison excercises as during the ORR will be continued, except for the comparison to the CDR.

5.2 Expected users and application area

Since one essential purpose of the ICDR is to extend the CDR as close as possible to present time, the same expected users and applications as listed previously in Section 4.7 are valid also here. What adds to this are users at NMHSs who can use these results for near-real time climate monitoring, for example, for issuing monthly climate bulletins or climate anomaly products.

5.3 Uniqueness of products

The uniqueness is largely the same as listed previously in Section 4.8. What could possibly be added and emphasized is that these ICDR products create an ability to build operational applications for monitoring of climate anomalies based on satellite-derived products.

6 Summary and Conclusion

The planned CLARA-A3.5 extension of the CLARA-A3 CDR is described in this document together with applicable requirements (which basically are identical to previous CLARA-A3 requirements).

The CM SAF project team recommends to take the requirements as outlined in this document as baseline for the development of the CLARA-A3.5 CDRs and ICDRs.

The CDR product identifiers are CM-11013, CM-11023, CM-11033, CM-11043, CM-11053, CM-11063, CM-11203, CM-11263, CM-11273, CM-11282, CM-11292, CM-11226, CM-11227, CM-11228, CM-11313 and CM-11343. The corresponding ICDR product identifiers are CM-6012, CM-6022, CM-6032, CM-6042, CM-6052, CM-6062, CM-6212, CM-6262, CM-6272, CM-6282, CM-6292, CM-6226, CM-6227, CM-6228, CM-6332, and CM-6322.

The PRD entries for all CLARA-A3.5 CDR and ICDR products are detailed in Appendix A and B.

7 References

References are separated into three sub-sections: General references as well as published papers using CLARA-A1, CLARA-A2 and CLARA-A3.

7.1 General references

Bennartz, R. and Rausch, J.: Global and regional estimates of warm cloud droplet number concentration based on 13 years of AQUA-MODIS observations, Atmos. Chem. Phys., 17, 9815–9836, https://doi.org/10.5194/acp-17-9815-2017, 2017.

Bodas-Salcedo, A., Webb, M.J., Bony, S., Chepfer, H., Dufresne, J.-L., Klein, S.A., Zhang, Y., Marchand, R., Haynes, J.M., Pincus, R., and V.O. John, 2011: COSP: Satellite simulation software for model assessment. Bull. Amer. Meteorol. Soc., 92, 1023–1043. doi:10.1175/2011BAMS2856.1.

[CERES-EBAF DQS] CERES EBAF Ed.4.0 Data Quality Summary (March 7, 2017). *Available from http://ceres.larc.nasa.gov/*

[CERES-SYN DQS] CERES SYN1deg Ed.4A Data Quality Summary (September 13, 2017). *Available from* http://ceres.larc.nasa.gov/

Chiodi, A. M., & Harrison, D. E. 2015: Global seasonal precipitation anomalies robustly associated with El Niño and La Niña events—An OLR perspective. *J. Clim.*, **28**(15), 6133-6159.

Clerbaux, N., Dewitte, S., Gonzalez, L., Bertrand, C., Nicula, B., & Ipe, A., 2003: Outgoing longwave flux estimation: Improvement of angular modelling using spectral information. *Rem. Sens. Env.,* **85**(3), 389-395.

Dolinar, E. K., Dong, X., Xi, B., Jiang, J. H., & Su, H., 2015: Evaluation of CMIP5 simulated clouds and TOA radiation budgets using NASA satellite observations. *Clim. Dyn.,* **44**(7-8), 2229-2247.

Dybbroe, A., Thoss, A., and K.-G. Karlsson, 2005: NWCSAF AVHRR cloud detection and analysis using dynamic thresholds and radiative transfer modelling – Part I: algorithm description, J. Appl. Meteorol., 44, 39–54.

[GCOS-107] Systematic Observation Requirements for Satellite-based Products for Climate Supplemental details to the satellite-based component of the Implementation Plan for the Global Observing System for Climate in Support of the UNFCCC - *September 2006,* World Meteorological Organization, Geneva, Switzerland*. Available from http://www.wmo.int*

[GCOS-154] Systematic Observation Requirements for Satellite-based Products for Climate Supplemental details to the satellite-based component of the Implementation Plan for the Global Observing System for Climate in Support of the UNFCCC, 2011 Update*, December*

2011. World Meteorological Organization, Geneva, Switzerland*. Available from http://*www.wmo.int*.*

[GCOS-200] The Global Observing system for climate: Implementation needs, 2016, World Meteorological Organization, Geneva, Switzerland. Available from http://www.wmo.int.

[GCOS-245], The 2022 GCOS ECVs Requirements, *Available at: https://library.wmo.int/idurl/4/58111, Last access: 06/12/2023*

Heidinger, A. K., M. J. Foster, A. Walther, and X. Zhao, 2014: The Pathfinder Atmospheres Extended (PATMOS-x) AVHRR climate data set, B. Am. Meteorol. Soc., 95, doi:10.1175/BAMS-D-12-00246.1.

Heidinger, A.K., Straka, W.C., Molling, C.C., Sullivan, J.T. and Wu, X.Q.: Deriving an inter-sensor consistent calibration for the AVHRR solar reflectance data record. *Int. J. Rem. Sens.*, **31**(24), 6493-6517, 2010.

Håkansson, N., Adok, C., Thoss, A., Scheirer, R., and Hörnquist, S.: Neural network cloud top pressure and height for MODIS, Atmos. Meas. Tech., 11, 3177-3196, https://doi.org/10.5194/amt-11-3177-2018, 2018.

Jacob, D., Petersen, J., Eggert, B. et al., 2014: EURO-CORDEX: new high-resolution climate change projections for European impact research, Reg. Environ. Change, 14: 563, doi:10.1007/s10113-013-0499-2

Jakob, C., and G. Tselioudis, 2003: Objective Identification of cloud regimes in the Tropical Western Pacific. Geophys. Res. Let., 30, 2082, doi:10.1029/2003GL018367.

Karlsson, K.-G., Anttila, K., Trentmann, J., Stengel, M., Fokke Meirink, J., Devasthale, A., Hanschmann, T., Kothe, S., Jääskeläinen, E., Sedlar, J., Benas, N., van Zadelhoff, G.-J., Schlundt, C., Stein, D., Finkensieper, S., Håkansson, N., and Hollmann, R.: CLARA-A2: the second edition of the CM SAF cloud and radiation data record from 34 years of global AVHRR data, Atmos. Chem. Phys., 17, 5809-5828, https://doi.org/10.5194/acp-17-5809-2017, 2017.

Karlsson, K.-G., Johansson, E., Håkansson, N., Sedlar, J. and Eliasson, S.: Probabilistic Cloud Masking for the Generation of CM SAF Cloud Climate Data Records from AVHRR and SEVIRI Sensors. Remote Sens.12, 713. https://doi.org/10.3390/rs12040713, 2020.

Karlsson, K.-G., Riihelä, A., Müller, R., Meirink, J. F., Sedlar, J., Stengel, M., Lockhoff, M., Trentmann, J., Kaspar, F., Hollmann, R., and Wolters, E.: CLARA-A1: a cloud, albedo, and radiation dataset from 28 yr of global AVHRR data, Atmos. Chem. Phys., 13, 5351-5367, https://doi.org/10.5194/acp-13-5351-2013, 2013.

Karlsson, K.-G.; Devasthale, A.; Eliasson, S.: Global Cloudiness and Cloud Top Information from AVHRR in the 42-Year CLARA-A3 Climate Data Record Covering the Period 1979–2020. Remote Sens., 15, 3044. https://doi.org/10.3390/rs15123044, 2023a

Karlsson, K.-G., Stengel, M., Meirink, J. F., Riihelä, A., Trentmann, J., Akkermans, T., Stein, D., Devasthale, A., Eliasson, S., Johansson, E., Håkansson, N., Solodovnik, I., Benas, N., Clerbaux, N., Selbach, N., Schröder, M., and Hollmann, R.: CLARA-A3: The third edition of the AVHRR-based CM SAF climate data record on clouds, radiation and surface albedo covering the period 1979 to 2023, Earth Syst. Sci. Data, 15, 4901–4926, https://doi.org/10.5194/essd-15-4901-2023, 2023b.

Kato, S., Loeb, N. G., Rutan, D. A., & Rose, F. G., 2015: Clouds and the Earth's Radiant Energy System (CERES) data products for climate research. *J. Met. Soc. of Japan.* Ser. II, **93**(6), 597-612.

Knapp, K., Young, A., Inamdar, A. and Hankins, W.: ISCCP and VIIRS: Adapting new instruments to extend historical climate data regords—VGAC, https://ams.confex.com/ams/JOINTSATMET/mediafile/Handout/Paper360556/VGAC%20version%201%20-%20poster.pdf , 2019.

Lee, H., 2014: Climate Algorithm Theoretical Basis Document (C-ATBD): Outgoing Longwave Radiation (OLR) - Daily

Loeb, N. G., Manalo-Smith, N., Kato, S., Miller, W. F., Gupta, S. K., Minnis, P., & Wielicki, B. A., 2003: Angular distribution models for top-of-atmosphere radiative flux estimation from the Clouds and the Earth's Radiant Energy System instrument on the Tropical Rainfall Measuring Mission satellite. Part I: Methodology. *J. App. Meteor.*, **42**(2), 240-265.

Loeb, N.G., S. Kato, K. Loukachine, and N. Manalo-Smith, 2005: Angular Distribution Models for Top-of-Atmosphere Radiative Flux Estimation from the Clouds and the Earth's Radiant Energy System Instrument on the Terra Satellite. Part I: Methodology. *J. Atmos. Oceanic Technol.*, **22**, 338–351.

Loew, A., Bell, W., Brocca, L., Bulgin, C.E., Burdanowitz, J., Calbet, X., Donner, R.V., Ghent, D., Gruber, A., Kaminski, T., Kinzel, J., Klepp, C., Lambert, J.-C., Schaepman-Strub, G., Schröder, M., Verhoelst, T., 2017: Validation practices for satellite-based Earth observation data across communities, Rev. Geophys., 55, doi:10.1002/2017RG000562.

Nyeki, S., Wacker, S., Grbner, J., Finsterle, W., and Wild, M., 2017: Revising shortwave and longwave radiation archives in view of possible revisions of the WSG and WISG reference scales: methods and implications. *Atmos. Meas. Tech*., **10**, 3057-3071, doi:10.5194/amt-10-3057-2017.

Ohring, G., B. Wielicki, R. Spencer, B. Emery, and R. Datla, 2005: Satellite instrument calibration for measuring global climate change: report of a workshop. Bull. Amer. Meteorol. Soc., 86, 1303–1313.

Platnick, S., Meyer, K. G., D., K. M., Wind, G., Amarasinghe, N., Marchant, B., Arnold, G. T., Zhang, Z., Hubanks, P. A., Holz, R. E., Yang, P., Ridgway, W. L., and Riedi, J., 2017: The MODIS Cloud Optical and Microphysical Products: Collection 6 Updates and Examples From Terra and Aqua, IEEE T. Geosci. Remote, 55, 502–525, doi: 10.1109/TGRS.2016.2610522.

Raschke, E., S. Kinne, and P. Stackhouse, 2012: GEWEX Radiative Flux Assessment (RFA), Volume 1: Assessment, WCRP Report No. 19/2012.

Rossow, W.B.; Schiffer, R.A. Advances in understanding clouds from ISCCP, Bull. Amer. Meteorol. Soc. 1999, 80, 2261-2287, doi:10.1175/1520-0477(1999)080%3C2261:AIUCFI%3E2.0.CO;2

Schmidt, A., Mills, M. J., Ghan, S., Gregory, J. M., Allan, R. P., Andrews, T., ... & Portmann, R. W., 2018: Volcanic radiative forcing from 1979 to 2015. *J. Geoph. Res.: Atmospheres*, **123**, 12491-12508, https://doi.org/10.1029/2018JD028776.

Slingo, A., Ackerman, T.P., Allan, R.P., Kassianov, E.I., McFarlane, S.A., Robinson, G.J., Barnard, J.C., Miller, M.A., Harries, J.E., Russell, J.E., and Dewitte, S., 2006: Observations of the impact of a major Saharan dust storm on the atmospheric radiation balance. Geoph. Res. Lett., 33, L24817.

Song, Z., Liang, S., Wang, D., Zhou, Y., & Jia, A., 2018: Long-term record of top-of-atmosphere albedo over land generated from AVHRR data. *Rem. Sens. Env.,* **211**, 71-88.

Stackhouse Jr, P. W., Gupta, S. K., Cox, S. J., Zhang, T., Mikovitz, J. C., & Hinkelman, L. M., 2011: 24.5-year SRB data set released. *GEWEX News*, **21**(1), 10-12.

Stengel, M.; Stapelberg, S.; Sus, O.; Schlundt, C.; Poulsen, C.; Thomas, G.; Christensen, M.; Carbajal Henken, C.; Preusker, R.; Fischer, J.; Devasthale, A.; Willén, U.; Karlsson, K.-G.; McGarragh, G. R.; Proud, S.; Povey, A. C.; Grainger, R. G.; Meirink, J. F.; Feofilov, A.; Bennartz, R.; Bojanowski, J. S.; Hollmann, R., 2017: Cloud property datasets retrieved from AVHRR, MODIS, AATSR and MERIS in the framework of the Cloud_cci project, *Earth Syst. Sci. Data*, **9**, 881-904, https://doi.org/10.5194/essd-9-881-2017.

Tang, Q., & Leng, G., 2013: Changes in cloud cover, precipitation, and summer temperature in North America from 1982 to 2009. J. Clim., 26(5), 1733-1744.

Wang, D., & Liang, S., 2016: Estimating high-resolution top of atmosphere albedo from Moderate Resolution Imaging Spectroradiometer data. Rem. Sens. Env., 178, 93-103.

Wielicki, B. A., Young, D. F., Mlynczak, M. G., Thome, K. J., Leroy, S., Corliss, J., ... & Bowman, K., 2013: Achieving climate change absolute accuracy in orbit. *Bull. Amer. Met. Soc.,* **94**(10), 1519-1539.

Wild, M., 2009: Global dimming and brightening: A review, *J. Geophys. Res.,* 114, D00D16, doi: 10.1029/2008JD01147.

Young, A.H.; Knapp, K.R., Inamdar, A., Hankins, W., and Rossow, W.B., 2018b: The International Cloud Climatology Project H-Series climate data record product, Earth Syst. Sci. Data, 2018, 10, 583-593, doi: 10.5194/essd-10-583-2018.

Young, D. F., Minnis, P., Doelling, D. R., Gibson, G. G., & Wong, T., 1998: Temporal interpolation methods for the Clouds and the Earth's Radiant Energy System (CERES) experiment. *J. Appl. Meteor.*, **37**(6), 572-590.

Zhan, Y., & Davies, R., 2017: September Arctic sea ice extent indicated by June reflected solar radiation. *J. Geoph. Res.: Atmospheres*, **122**(4), 2194-2202.

Zhang, Y. and Rossow, W., 2017: ISCCP-FH Radiative Flux Profile Product C-ATBD.

7.2 Published Papers using CLARA-A1 (Status 15.12.2023)

1. Abera, W., G. Formetta, L. Brocca, and R. Rigon (2017), Modeling the water budget of the Upper Blue Nile basin using the JGrass-NewAge model system and satellite data, *Hydrol. Earth Syst. Sci.*, *21*(6), 3145-3165, doi:10.5194/hess-21-3145-2017.
2. Babar, B., R. Graversen, and T. Boström (2018), Evaluating CM-SAF solar radiation CLARA-A1 and CLARA-A2 datasets in Scandinavia, *Solar Energy*, *170*, 76-85, doi:10.1016/j.solener.2018.05.009.
3. Blunden, J., and D. S. Arndt (2015), State of the Climate in 2014, *Bulletin of the American Meteorological Society*, *96*(7), S1-S267, doi:10.1175/2015BAMSStateoftheClimate.1.
4. Boccolari, M., and F. Parmiggiani (2017), Seasonal co-variability of surface downwelling longwave radiation for the 1982–2009 period in the Arctic, *Adv. Sci. Res.*, *14*, 139-143, doi:10.5194/asr-14-139-2017.
5. Boccolari, M., and F. Parmiggiani (2018), Trends and variability of cloud fraction cover in the Arctic, 1982–2009, *Theoretical and Applied Climatology*, *132*(3-4), 739-749, doi:10.1007/s00704-017-2125-6.
6. Calbó, J., J. Badosa, J.-A. González, L. Dmitrieva, V. Khan, A. Enríquez-Alonso, and A. Sanchez-Lorenzo (2016), Climatology and changes in cloud cover in the area of the Black, Caspian, and Aral seas (1991-2010): a comparison of surface observations with satellite and reanalysis products, *International Journal of Climatology*, *36*(3), 1428-1443, doi:10.1002/joc.4435.
7. Calbó, J., J.-A. González, and A. Sanchez-Lorenzo (2017), Building global and diffuse solar radiation series and assessing decadal trends in Girona (NE Iberian Peninsula), *Theoretical and Applied Climatology*, *129*(3), 1003-1015, doi:10.1007/s00704-016-1829-3.
8. Cao, Y., S. Liang, X. Chen, and T. He (2015), Assessment of Sea Ice Albedo Radiative Forcing and Feedback over the Northern Hemisphere from 1982 to 2009 Using Satellite and Reanalysis Data, *Journal of Climate*, *28*(3), 1248-1259, doi:10.1175/jcli-d-14-00389.1.
9. Cruz, F. T., et al. Sensitivity of temperature to physical parameterization schemes of RegCM4 over the CORDEX-Southeast Asia region, *International Journal of Climatology*, doi:10.1002/joc.5151.
10. Duan, Z., and W. G. M. Bastiaanssen (2015), A new empirical procedure for estimating intra-annual heat storage changes in lakes and reservoirs: Review and analysis of 22 lakes, *Remote Sensing of Environment*, *156*, 143-156, doi:10.1016/j.rse.2014.09.009.
11. Enriquez-Alonso, A., A. Sanchez-Lorenzo, J. Calbó, J.-A. González, and J. R. Norris (2015), Cloud cover climatologies in the Mediterranean obtained from satellites, surface observations, reanalyses, and CMIP5 simulations: validation and future scenarios, *Climate Dynamics*, doi:10.1007/s00382-015-2834-4.
12. Guo, H., X. Wang, T. Wang, Y. Ma, J. Ryder, T. Zhang, D. Liu, J. Ding, Y. Li, and S. Piao (2018), Spring Snow-Albedo Feedback Analysis Over the Third Pole: Results From Satellite Observation and CMIP5 Model Simulations, *Journal of Geophysical Research: Atmospheres*, *123*, 750 - 763, doi:10.1002/2017JD027846.

13. He, T., S. Liang, and D.-X. Song (2014), Analysis of global land surface albedo climatology and spatial-temporal variation during 1981–2010 from multiple satellite products, *Journal of Geophysical Research*, *119*, 10281-10298, doi:10.1002/2014JD021667.
14. Hofer, S., A. J. Tedstone, X. Fettweis, and J. L. Bamber (2017), Decreasing cloud cover drives the recent mass loss on the Greenland Ice Sheet, *Science Advances*, *3*(6), doi:10.1126/sciadv.1700584.
15. Karlsson, J., and G. Svensson (2013), Consequences of poor representation of Arctic sea-ice albedo and cloud-radiation interactions in the CMIP5 model ensemble, *Geophysical Research Letters*, *40*(16), 4374-4379, doi:10.1002/grl.50768.
16. Karlsson, K. G., and E. Johansson (2013), On the optimal method for evaluating cloud products from passive satellite imagery using CALIPSO-CALIOP data: example investigating the CM SAF CLARA-A1 dataset, *Atmospheric Measurement Techniques*, *6*(5), 1271-1286, doi:10.5194/amt-6-1271-2013.
17. Karlsson, K. G., E. Johansson, and A. Devasthale (2015), Advancing the uncertainty characterisation of cloud masking in passive satellite imagery: Probabilistic formulations for NOAA AVHRR data, *Remote Sensing of Environment*, *158*, 126-139, doi:10.1016/j.rse.2014.10.028.
18. Karlsson, K. G., et al. (2013), CLARA-A1: a cloud, albedo, and radiation dataset from 28 yr of global AVHRR data, *Atmospheric Chemistry and Physics*, *13*(10), 5351-5367, doi:10.5194/acp-13-5351-2013.
19. Koenigk, T., P. Berg, and R. Döscher (2015), Arctic climate change in an ensemble of regional CORDEX simulations, *Polar Research*, *34*(0), doi:10.3402/polar.v34.24603.
20. Koenigk, T., A. Devasthale, and K. G. Karlsson (2014), Summer Arctic sea ice albedo in CMIP5 models, *Atmospheric Chemistry and Physics*, *14*(4), 1987-1998, doi:10.5194/acp-14-1987-2014.
21. Kotarba, A. Z. (2015), Evaluation of ISCCP cloud amount with MODIS observations, *Atmospheric Research*, *153*, 310-317, doi:https://doi.org/10.1016/j.atmosres.2014.09.006.
22. Kotarba, A. Z. (2016), Regional high-resolution cloud climatology based on MODIS cloud detection data, *International Journal of Climatology*, *36*(8), 3105-3115, doi:10.1002/joc.4539.
23. Laine, V., T. Manninen, and A. Riihelä (2014), High temporal resolution estimations of the Arctic sea ice albedo during the melting and refreezing periods of the years 2003-2011, *Remote Sensing of Environment*, *140*, 604-613, doi:10.1016/j.rse.2013.10.001.
24. Laine, V., T. Manninen, A. Riihelä, and K. Andersson (2011), Shortwave broadband black-sky surface albedo estimation for Arctic sea ice using passive microwave radiometer data, *Journal of Geophysical Research*, *116*(D16), doi:10.1029/2011jd015700.
25. Light, B., S. Dickinson, D. K. Perovich, and M. M. Holland (2015), Evolution of summer Arctic sea ice albedo in CCSM4 simulations: Episodic summer snowfall and frozen summers, *Journal of Geophysical Research: Oceans*, *120*(1), 284-303, doi:10.1002/2014jc010149.
26. Loew, A., A. Andersson, J. Trentmann, and M. Schröder (2016), Assessing Surface Solar Radiation Fluxes in the CMIP Ensembles, *Journal of Climate*, *29*(20), 7231-7246, doi:10.1175/jcli-d-14-00503.1.
27. Obregón, A., H. Nitsche, M. Körber, A. Kreis, P. Bissolli, K. Friedrich, and S. Rösner (2014), Satellite-based climate information within the WMO RA VI Regional Climate Centre on

Climate Monitoring, *Advances in Science and Research*, *11*, 25-33, doi:10.5194/asr-11-25-2014.

28. Qu, Y., S. Liang, Q. Liu, T. He, S. Liu, and X. Li (2015), Mapping Surface Broadband Albedo from Satellite Observations: A Review of Literatures on Algorithms and Products, *Remote Sensing*, *7*(1), 990-1020, doi:10.3390/rs70100990.
29. Quante, M., et al. (2016), Introduction to the Assessment—Characteristics of the Region, in *North Sea Region Climate Change Assessment*, edited by M. Quante and F. Colijn, pp. 1-52, doi:10.1007/978-3-319-39745-0_1.
30. Räisänen, P., et al. (2014), Evaluation of North Eurasian snow-off dates in the ECHAM5.4 atmospheric general circulation model, *Geoscientific Model Development*, *7*(6), 3037-3057, doi:10.5194/gmd-7-3037-2014.
31. Riihelä, A., T. Carlund, J. Trentmann, R. Müller, and A. V. Lindfors (2015), Validation of CM SAF Surface Solar Radiation Datasets over Finland and Sweden, *Remote Sensing*, *7*, 6663-6682, doi:10.3390/rs70606663.
32. Riihelä, A., T. Manninen, and V. Laine (2013), Observed changes in the albedo of the Arctic sea-ice zone for the period 1982–2009, *Nature Climate Change*, *3*(10), 895-898, doi:10.1038/nclimate1963.
33. Riihelä, A., T. Manninen, V. Laine, K. Andersson, and F. Kaspar (2013), CLARA-SAL: a global 28 yr timeseries of Earth's black-sky surface albedo, *Atmospheric Chemistry and Physics*, *13*(7), 3743-3762, doi:10.5194/acp-13-3743-2013.
34. Sanchez-Lorenzo, A., A. Enriquez-Alonso, J. Calbó, J.-A. González, M. Wild, D. Folini, J. R. Norris, and S. M. Vicente-Serrano (2017), Fewer clouds in the Mediterranean: consistency of observations and climate simulations, *Scientific Reports*, *7*, 41475, doi:10.1038/srep41475.
35. Seo, M., H.-C. Kim, M. Huh, J.-M. Yeom, C. Lee, K.-S. Lee, S. Choi, and K.-S. Han (2016), Long-Term Variability of Surface Albedo and Its Correlation with Climatic Variables over Antarctica, *Remote Sensing*, *8*(12), 981, doi:10.3390/rs8120981.
36. Shao, Z.-D., and C.-Q. Ke (2015), Spring–summer albedo variations of Antarctic sea ice from 1982 to 2009, *Environmental Research Letters*, *10*(6), 064001, doi:10.1088/1748-9326/10/6/064001.
37. Sinitssyn, A. V., and S. K. Gulev (2018), Comparative Analysis of Satellite Databases of Incoming Short-Wavelength Fluxes to the World Ocean Surface, *Oceanology*, *58*(5), 635-640, doi:10.1134/s0001437018050168.
38. Sörensson, A. A., and R. C. Ruscica (2018), Intercomparison and Uncertainty Assessment of Nine Evapotranspiration Estimates Over South America, *Water Resources Research*, *54*(4), 2891-2908, doi:10.1002/2017WR021682.
39. Spangehl, T., M. Schröder, S. Stolzenberger, R. Glowienka-Hense, A. Mazurkiewicz, and A. Hense (2016), Evaluation of the MiKlip decadal prediction system using satellite based cloud products, *Meteorologische Zeitschrift*, *26*(6), 695-707, doi:10.1127/metz/2015/0602.
40. Stengel, M., et al. (2015), The Clouds Climate Change Initiative: Assessment of state-of-the-art cloud property retrieval schemes applied to AVHRR heritage measurements, *Remote Sensing of Environment*, *162*, 363-379, doi:10.1016/j.rse.2013.10.035.
41. Sun, B., M. Free, H. L. Yoo, M. J. Foster, A. Heidinger, and K.-G. Karlsson (2015), Variability and Trends in U.S. Cloud Cover: ISCCP, PATMOS-x, and CLARA-A1 Compared

to Homogeneity-Adjusted Weather Observations, *Journal of Climate*, *28*(11), 4373-4389, doi:10.1175/jcli-d-14-00805.1.
42. Tornow, F., N. Clerbaux, A. Ipe, and M. Urbain (2017), An improved method to estimate reference cloud-free images for the visible band of geostationary satellites, *International Journal of Remote Sensing*, *38*(23), 7220-7241, doi:10.1080/01431161.2017.1372859.
43. Volkova, E. V., and A. B. Uspensky (2017), Detection and assessment of cloud cover and precipitation parameters using data of scanning radiometers of polar–orbiting and geostationary meteorological satellites, *Izvestiya, Atmospheric and Oceanic Physics*, *52*(9), 1097-1109, doi:10.1134/s0001433816090280.
44. Werkmeister, A., M. Lockhoff, M. Schrempf, K. Tohsing, B. Liley, and G. Seckmeyer (2015), Comparing satellite- to ground-based automated and manual cloud coverage observations – a case study, *Atmospheric Measurement Techniques*, *8*(5), 2001-2015, doi:10.5194/amt-8-2001-2015.
45. Yao, Y., J. Huang, Y. Luo, and Z. Zhao (2016), Improving the WRF model's (version 3.6.1) simulation over sea ice surface through coupling with a complex thermodynamic sea ice model (HIGHTSI), *Geoscientific Model Development*, *9*(6), 2239-2254, doi:10.5194/gmd-9-2239-2016.
46. Žák, M., J. Mikšovský, and P. Pišoft (2015), CMSAF Radiation Data: New Possibilities for Climatological Applications in the Czech Republic, *Remote Sensing*, *7*(11), 14445-14457, doi:10.3390/rs71114445.
47. Zaninelli, P. G., C. G. Menéndez, M. Falco, N. López-Franca, and A. F. Carril (2018), Future hydroclimatological changes in South America based on an ensemble of regional climate models, *Climate Dynamics*, doi:10.1007/s00382-018-4225-0.
48. Zhang, J., Tian, W., Chipperfield, M. P., Xie, F. and Huang, J., 2016: Persistent shift of the Arctic polar vortex towards the Eurasian continent in recent decades, Nature Climate Change, 6, 1094-1099, https://dx.doi.org/10.1038/nclimate3136
49. Zheng, J., C. Ke, and Z. Shao (2017), Winter sea ice albedo variations in the Bohai Sea of China, *Acta Oceanologica Sinica*, *36*(1), 56-63, doi:10.1007/s13131-017-0993-3.

7.3 Published Papers using CLARA-A2 (Status 15.12.2023)

1. Anttila, K., T. Manninen, E. Jääskeläinen, A. Riihelä, and P. Lahtinen (2018), The Role of Climate and Land Use in the Changes in Surface Albedo Prior to Snow Melt and the Timing of Melt Season of Seasonal Snow in Northern Land Areas of 40°N–80°N during 1982–2015, Remote Sensing, 10(10), 1619.
2. Babar, B., R. Graversen, and T. Boström (2018), Evaluating CM-SAF solar radiation CLARA-A1 and CLARA-A2 datasets in Scandinavia, Solar Energy, 170, 76-85, doi:10.1016/j.solener.2018.05.009.
3. Benas, N., J. F. Meirink, K.-G. Karlsson, M. Stengel, and P. Stammes (2018), Satellite observations of aerosols and clouds over South China from 2006 to 2015: analysis of changes and possible interactions, Atmospheric Chemistry and Physics Discussions, 1-21, doi:10.5194/acp-2018-554.

4. Boers, R., T. Brandsma, and A. P. Siebesma (2017), Impact of aerosols and clouds on decadal trends in all-sky solar radiation over the Netherlands (1966–2015), Atmos. Chem. Phys., 17(13), 8081-8100, doi:10.5194/acp-17-8081-2017.
5. Bojanowski, J. S. and Musiał, J. P.: Dissecting effects of orbital drift of polar-orbiting satellites on accuracy and trends of climate data records of cloud fractional cover, Atmos. Meas. Tech., 13, 6771–6788, https://doi.org/10.5194/amt-13-6771-2020, 2020.
6. Bruno, O., Hoose, C., Storelvmo, T., Coopman, Q., & Stengel, M. (2021). Exploring the cloud top phase partitioning in different cloud types using active and passive satellite sensors. Geophysical Research Letters, 48, e2020GL089863. https://doi.org/10.1029/2020GL089863
7. Chen, Y., Ji, D., Moore, J.C., Hu, J. and He, Y. (2022): Observational constraint on the contribution of surface albedo feedback to the amplified Tibetan Plateau surface warming. J. Geoph. Res. Atmos., 127.e2021JD036085. https://doi.org/10.1029/2021IJD036085.
8. Dong, X. and Minnis, P., 2023: Stratus, Stratocumulus and Remote Sensing, Chapter 6, Geophysical Monograph Series, https://doi.org/10.1002/9781119529019.ch6.
9. Eliasson, S., Karlsson, K.-G., and Willén, U.: A simulator for the CLARA-A2 cloud climate data record and its application to assess EC-Earth polar cloudiness, Geosci. Model Dev., 13, 297–314, https://doi.org/10.5194/gmd-13-297-2020, 2020.
10. Eyring, N., and Kittner, N.: High-resolution electricity generation model demonstrates suitability of high-altitude floating solar power, iScience, Volume 25, Issue 6, 2022,104394,ISSN 2589-0042, https://doi.org/10.1016/j.isci.2022.104394.
11. Hartfield, G., J. Blunden, and D. S. Arndt (2018), State of the Climate in 2017, Bulletin of the American Meteorological Society, 99(8), Si-S310, doi:10.1175/2018BAMSStateoftheClimate.1.
12. Jian, B., Li., J., Wang, G., He, Y., Han, Y., Zhang, M. and Huang, J., 2018: The impacts of atmospheric and surface parameters on long-term variations in the planetary albedo, J. Clim., 31, 8705-8718, DOI: 10.1175/JCLI-D-17-0848.1.
13. Jääskeläinen, E., T. Manninen, J. Tamminen, and M. Laine (2017), The Aerosol Index and Land Cover Class Based Atmospheric Correction Aerosol Optical Depth Time Series 1982–2014 for the SMAC Algorithm, Remote Sensing, 9(11), 1095.
14. Jääskeläinen, E., Manninen, T., Hakkarainen, J. and Tamminen, J.: Filling gaps of black-sky surface albedo of the Arctic sea ice using gradient boosting and brightness temperature data, International Journal of Applied Earth Observation and Geoinformation, Volume 107, 2022, 102701, ISSN 1569-8432, https://doi.org/10.1016/j.jag.2022.102701.
15. Karlsson, K. G., et al. (2017), CLARA-A2: the second edition of the CM SAF cloud and radiation data record from 34 years of global AVHRR data, Atmos. Chem. Phys., 17(9), 5809-5828, doi:10.5194/acp-17-5809-2017.
16. Karlsson, K. G., and N. Håkansson (2018), Characterization of AVHRR global cloud detection sensitivity based on CALIPSO-CALIOP cloud optical thickness information: demonstration of results based on the CM SAF CLARA-A2 climate data record, Atmos. Meas. Tech., 11(1), 633-649, doi:10.5194/amt-11-633-2018.
17. Karlsson, K.-G., and A. Devasthale (2018), Inter-Comparison and Evaluation of the Four Longest Satellite-Derived Cloud Climate Data Records: CLARA-A2, ESA Cloud CCI V3, ISCCP-HGM, and PATMOS-x, Remote Sensing, 10(10), 1567.

18. Kaushal, N., Sanwlani, N., Tanzil, J. T. I., Cherukuru, N., Sahar, S., Müller, M., et al. (2021). Coral skeletal luminescence records changes in terrestrial chromophoric dissolved organic matter in tropical coastal waters. Geophysical Research Letters, 48, e2020GL092130. https://doi.org/10.1029/2020GL092130
19. Manara, V.; Stocco, E.; Brunetti, M.; Diolaiuti, G.A.; Fugazza, D.; Pfeifroth, U.; Senese, A.; Trentmann, J.; Maugeri, M. Comparison of Surface Solar Irradiance from Ground Observations and Satellite Data (1990–2016) over a Complex Orography Region (Piedmont—Northwest Italy). Remote Sens. 2020, 12, 3882. https://doi.org/10.3390/rs12233882
20. Manninen, T., Emmihenna Jääskeläinen & Aku Riihelä (2019) Black and White-Sky Albedo Values of Snow: In Situ Relationships for AVHRR-Based Estimation Using CLARA-A2 SAL, Canadian Journal of Remote Sensing, 45:3-4, 350-367, DOI: 10.1080/07038992.2019.1632177
21. Palfreyman, J., J. Graham-Brown, C. Caminade, P. Gilmore, D. Otranto, and D. J. L. Williams (2018), Predicting the distribution of Phortica variegata and potential for Thelazia callipaeda transmission in Europe and the United Kingdom, Parasites & Vectors, 11(1), 272, doi:10.1186/s13071-018-2842-4.
22. Pfeifroth, U., J. S. Bojanowski, N. Clerbaux, V. Manara, A. Sanchez-Lorenzo, J. Trentmann, J. P. Walawender, and R. Hollmann (2018), Satellite-based trends of solar radiation and cloud parameters in Europe, Adv. Sci. Res., 15, 31-37, doi:10.5194/asr-15-31-2018.
23. Pfeifroth, U., A. Sanchez-Lorenzo, V. Manara, J. Trentmann, and R. Hollmann (2018), Trends and Variability of Surface Solar Radiation in Europe based on Surface- and Satellite-based Data Records, Journal of Geophysical Research: Atmospheres, 123, 1735-1754, doi:10.1002/2017JD027418.
24. Pietikäinen, J. P., et al. (2018), The regional climate model REMO (v2015) coupled with the 1-D freshwater lake model FLake (v1): Fenno-Scandinavian climate and lakes, Geosci. Model Dev., 11(4), 1321-1342, doi:10.5194/gmd-11-1321-2018.
25. Riihelä, A., J. R. Key, J. F. Meirink, P. K. Munneke, T. Palo, and K. G. Karlsson (2017), An intercomparison and validation of satellite-based surface radiative energy flux estimates over the Arctic, Journal of Geophysical Research: Atmospheres, 122(9), 4829-4848, doi:10.1002/2016JD026443.
26. Riihelä, A., T. Manninen, J. Key, Q. Sun, M. Sütterlin, A. Lattanzio, and C. Schaaf (2018), A Multisensor Approach to Global Retrievals of Land Surface Albedo, Remote Sensing, 10(6), 848.
27. Riihelä, A., King, M. D., and Anttila, K.: The surface albedo of the Greenland Ice Sheet between 1982 and 2015 from the CLARA-A2 dataset and its relationship to the ice sheet's surface mass balance, The Cryosphere, 13, 2597–2614, https://doi.org/10.5194/tc-13-2597-2019, 2019.
28. Schwarz, M., D. Folini, M. Z. Hakuba, and M. Wild (2018), From Point to Area: Worldwide Assessment of the Representativeness of Monthly Surface Solar Radiation Records, 123, doi:10.1029/2018JD029169.
29. Sedlar, J. (2018), Spring Arctic Atmospheric Preconditioning: Do Not Rule Out Shortwave Radiation Just Yet, Journal of Climate, 31(11), 4225-4240, doi:10.1175/jcli-d-17-0710.1.

30. Stengel, M., Meirink, J.F. & Eliasson, S. (2023). On the temperature dependence of the cloud ice particle effective radius – a satellite perspective, Geoph. Res. Lett., 50, e2022GL102521, https://doi.org/10.1029/2022GL102521.
31. Tang, W., Qin, J., Yang, K., Jiang, Y., and Pan, W.: Mapping long-term and high-resolution global gridded photosynthetically active radiation using the ISCCP H-series cloud product and reanalysis data, Earth Syst. Sci. Data, 14, 2007–2019, https://doi.org/10.5194/essd-14-2007-2022, 2022.
32. Tang, W., Yang, K., Qin, J., Li, J. and Ye, J. (2021) How accurate are satellite-derived surface solar radiation products over tropical oceans?, J. Atm. Ocean. Tech., 38, 283-291, https://doi.org/10.1175/JTECH-D-20-0099.1
33. Tong, L., Tao He, Yichuan Ma & Xiaotong Zhang (2023) Evaluation and intercomparison of multiple satellite-derived and reanalysis downward shortwave radiation products in China, International Journal of Digital Earth, 16:1, 1853-1884, DOI: 10.1080/17538947.2023.2212918
34. Tzallas, V.; Hatzianastassiou, N.; Benas, N.; Meirink, J.F.; Matsoukas, C.; Stackhouse, P., Jr.; Vardavas, I. Evaluation of CLARA-A2 and ISCCP-H Cloud Cover Climate Data Records over Europe with ECA&D Ground-Based Measurements. Remote Sens. 2019, 11, 212. https://doi.org/10.3390/rs11020212
35. Urraca, R., A. M. Gracia-Amillo, E. Koubli, T. Huld, J. Trentmann, A. Riihelä, A. V. Lindfors, D. Palmer, R. Gottschalg, and F. Antonanzas-Torres (2017), Extensive validation of CM SAF surface radiation products over Europe, Remote Sensing of Environment, 199, 171-186, doi:10.1016/j.rse.2017.07.013.
36. Urraca, R., J. Antonanzas, A. Sanz-Garcia, A. Aldama, and F. J. Martinez-de-Pison (2018), An algorithm based on satellite observations to quality control ground solar sensors: Analysis of Spanish meteorological networks, in Hybrid Artificial Intelligent Systems, HAIS 2018. Lecture Notes in Computer Science, edited by F. J. d. C. Juez, J. R. Villar, E. A. d. l. Cal, Á. Herrero, H. Quintián, J. A. Sáez and E. Corchado, Springer, Cham.
37. Urraca, R., A. M. Gracia-Amillo, T. Huld, F. J. Martinez-de-Pison, J. Trentmann, A. V. Lindfors, A. Riihelä, and A. Sanz-Garcia (2017), Quality control of global solar radiation data with satellite-based products, Solar Energy, 158, 49-62, doi:10.1016/j.solener.2017.09.032.
38. Urraca, R., T. Huld, F. J. Martinez-de-Pison, and A. Sanz-Garcia (2018), Sources of uncertainty in annual global horizontal irradiance data, Solar Energy, 170, 873-884, doi:10.1016/j.solener.2018.06.005.
39. R. Urraca, C. Lanconelli, F. Cappucci and N. Gobron, "Assessing the Fitness of Satellite Albedo Products for Monitoring Snow Albedo Trends," in IEEE Transactions on Geoscience and Remote Sensing, vol. 61, pp. 1-17, 2023, Art no. 4404817, doi: 10.1109/TGRS.2023.3281188.
40. Urraca, R., Sanz-Garcia, A. and Sanz-Garcia, I.: BQC: A free web service to quality control solar irradiance measurements across Europe, Solar Energy, Volume 211, 2020, Pages 1-10, ISSN 0038-092X, https://doi.org/10.1016/j.solener.2020.09.055.
41. Wang, Y., J. Trentmann, W. Yuan, and M. Wild (2018), Validation of CM SAF CLARA-A2 and SARAH-E Surface Solar Radiation Datasets over China, Remote Sensing, 10(12), 1977, doi:10.3390/rs10121977.

42. Wang, Y., Zhao, P. Xiao, H. and Zhang, P., 2024: Aerosol effects on liquid cloud microphysical properties in south China: Land–ocean contrasts, Atmospheric Pollution Research, Volume 15, Issue 3,102032, ISSN 1309-1042, https://doi.org/10.1016/j.apr.2023.102032
43. Zhao, P., Li, Z., Xiao, H., Wu, F., Zheng, Y., Cribb, M. C., Jin, X., and Zhou, Y.: Distinct aerosol effects on cloud-to-ground lightning in the plateau and basin regions of Sichuan, Southwest China, Atmos. Chem. Phys., 20, 13379–13397, https://doi.org/10.5194/acp-20-13379-2020, 2020.

7.4 Published Papers using CLARA-A3 (Status 15.12.2023)

1. Akkermans, T. and Clerbaux, N. (2023): Validation of the CLARA-A3 Top-of-Atmosphere Radiative Fluxes Climate Data Record. J. Atm. Ocean. Tech., 40, 1523-1539, https://doi.org/10.1175/JTECH-D-23-0065.1.
2. Devasthale, A.; Karlsson, K.-G. Decadal Stability and Trends in the Global Cloud Amount and Cloud Top Temperature in the Satellite-Based Climate Data Records. Remote Sens. 2023, 15, 3819. https://doi.org/10.3390/rs15153819
3. Devasthale, A.; Karlsson, K.-G.; Andersson, S.; Engström, E. Difference between WMO Climate Normal and Climatology: Insights from a Satellite-Based Global Cloud and Radiation Climate Data Record. Remote Sens. 2023, 15, 5598. https://doi.org/10.3390/rs15235598
4. Karlsson, K.-G.; Devasthale, A.; Eliasson, S. Global Cloudiness and Cloud Top Information from AVHRR in the 42-Year CLARA-A3 Climate Data Record Covering the Period 1979–2020. Remote Sens. 2023, 15, 3044. https://doi.org/10.3390/rs15123044
5. Riihelä, A., Jääskeläinen, E., and Kallio-Myers, V.: Four decades of global surface albedo estimates in the third edition of the CLARA climate data record, Earth Syst. Sci. Data Discuss. [preprint], https://doi.org/10.5194/essd-2023-282, in review, 2023.
6. Xu et al., 2023: Site-testing at the Muztagh-ata Site V. Nighttime Cloud Amount during the Last Five Years, Res. Astron. Astrophys. 23 045015 DOI 10.1088/1674-4527/acc29b
7. Zhan, C., Yang, J., Li, Y., Chen, Y., Miao, Z., Zeng, X., & Li, J. (2023). Evaluation of Five Global Top-of-Atmosphere Outgoing Longwave Radiation Products. Remote Sensing, 15(15), 3722.

8 List of abbreviations

Acronym	Explanation
AMSR-E	Advanced Microwave Scanning Radiometer for EOS
ADM	Angular Directional Model
AOD	Aerosol Optical Depth
ATBD	Algorithm Theoretical Baseline Document
AVHRR	Advanced Very High Resolution Radiometer
BAL	Blue-sky Albedo
BB	Broadband
bc-RMS	Bias-Corrected Root-Mean-Square Deviation
BSRN	Baseline Surface Radiation Network
CALIOP	Cloud-Aerosol Lidar with Orthogonal Polarisation
CALIPSO	Cloud-Aerosol Lidar and Infrared Pathfinder Satellite Observations
CDNC	Cloud Droplet Number Concentration
CDOP	Continuous Development and Operations Phase (taking place 2007-2012)
CDOP-2	2012-2017
CDOP-3	2017-2022
CDOP-4	2022-2027
CDR	Climate Data Record
CERES	Cloud and the Earth's Radiant Energy System
CF	Climate and Forecast
CFC	Fractional Cloud Cover
CFMIP	Cloud Feedback Model Intercomparison Project
CLARA-A	CM SAF Cloud, Albedo, Radiation dataset, AVHRR-based
CM SAF	Satellite Application Facility on Climate Monitoring

CMIP	Climate Model Intercomparison Project
CNRS	Centre National de la Recherche Scientifique, France
CO_2	Carbon Dioxide
CORDEX	Coordinated Regional Downscaling Experiment
COSP	CFMIP Observation Simulator Package
CS	Clear Sky
COT	Cloud Optical Thickness
CPH	Cloud Phase
CPP	Cloud Physical Properties
CRE	Particle effective radius
CTH	Cloud Top Height
CTP	Cloud Top Pressure
CTO	Cloud Top product
CTTH	Cloud Top Temperature and Height
DRR	Delivery Readiness Review
DWD	Deutscher Wetterdienst
ECMWF	European Center for Medium-Range Weather Forecasts
ECV	Essential Climate Variable
EOS	Earth Observing System (NASA satellite series)
EPS	Eumetsat Polar System
EPS-SG	EPS Second Generation satellites
ERA	ECMWF Re-Analysis
ESA	European Space Agency
ESA-CCI	Climate Change Initiative (ESA)
ESA-CLOUD-CCI	CCI project for Cloud parameters (ESA)
ERBE	Earth Radiation Budget Experiment

EUMETSAT	European Organisation for the Exploitation of Meteorological Satellites
FAR	False Alarm Rate
FCDR	Fundamental Climate Data Record
FMI	Finnish Meteorological Institute
FOV	Field Of View
GAC	Global Area Coverage (5 km resampled AVHRR)
GCOS	Global Climate Observing System
GEBA	Global Energy Balance Archive
GERB	Geostationary Earth Radiation Budget
GEWEX	Global Energy and Water Exchanges Project
GSICS	Global Space-based Inter-Calibration System
HIRS	High resolution Infrared Sounder
HR	High Resolution
ICDR	Interim Climate Data Record
ICWG	International Clouds Working Group
IR	Infrared
ISCCP	International Satellite Cloud Climatology Project
IWP	Ice Water Path
JCH	Joint Cloud Histogram (normally COT vs CTP)
KNMI	Royal Netherlands Meteorological Institute
KSS	Hanssen-Kuipers skill score
LST	Local Standard Time
LUT	Look Up Table
LWP	Liquid Water Path
MAB	Mean Absolut Bias
MERIS	Medium Resolution Imaging Spectrometer

METEOSAT	Meteorological Satellite(s) series operated by EUMETSAT
MeteoSwiss	The Meteorological Service of Switzerland
Metop	Polar orbiting meteorological satellites, EUMETSAT
MODIS	Moderate Resolution Imaging Spectroradiometer
MSG	Meteosat Second Generation
MVIRI	Meteosat Visible and Infrared Imager
NASA	National Aeronautics and Space Administration
NCAR	National Center for Atmospheric Research, USA
NCEP	National Center for Environmental Prediction, USA
NIR	Near IR
NMHSs	National Meteorological and Hydrological services
NOAA	National Oceanographic and Atmospheric Administration
NWC SAF	Nowcasting Satellite Application Facility
NWP	Numerical Weather Prediction
OLR	Outgoing Longwave Radiation
ORR	Operational Readiness Review
PATMOS-x	Pathfinder Atmospheres Extended
PCR	Product Consolidation Review
PMW	Passive Microwave
POD	Probability of Detection
PP	Project Plan
PPS	Polar Platform System cloud processing package
PRD	Product Requirements Document
PT	Project Team
PUM	Product User Manual
RD	Reference Document

RMIB	Royal Meteorological Institute of Belgium
RMSD	Root Mean Square Deviation
RMSE	Root Mean Square Error
RR	Requirements Review
RSF	Top of Atmosphere Reflected Solar radiation (flux)
SAF	Satellite Application Facility
SAL	Surface Albedo
SDL	Downwelling Longwave radiation at Surface
SEVIRI	Spinning Enhanced Visible and Infrared Imager
SG	Steering Group
SIS	Solar Incoming radiation at Surface
SMHI	Swedish Meteorological and Hydrological Institute
SSF	Single Satellite Footprint
SSI	Surface Solar Irradiance
SRB	Surface Radiation Budget
SW	Shortwave
SYNOP	Surface Synoptic Observations
SZA	Solar Zenith Angle
TCDR	Thematic Climate Data Record
TOA	Top Of Atmosphere
TRMM	Tropical Rainfall Monitoring Mission
RSF	Top of Atmosphere Reflected Solar radiation (flux)
UTC	Universal Time Coordinated
UK Metoffice	The Meteorological Service of the United Kingdom
VIIRS	Visible and Infrared
VZA	Viewing Zenith Angle

WAL	White-sky Albedo
WCRP	World Climate Research Program
WMO	World Meteorological Organization
WRDC	World Radiation Data Centre
WV	Water Vapour

9 Appendix A: Product requirements tables for the CDR data records

This section provides the requirements for CLARA-A3.5 CDRs, with proposed modifications indicated in **red**. It is noted that most of the changes are based on missing information and outdated entries in PRD 4.2. An explanation of the applied changes is given in the comments.

The project team recommends to take the updated requirements as discussed in section 4 and presented here as baseline for the implementation and the development.

CM-11013	CLARA-A3.5 Fractional Cloud Cover (CFC) TCDR	CFC_R4_CLARA_35_TCDR

Type

Dataset

Input Satellite Data	*Application Areas*
Operational Satellite:AVHRR GAC	Climate Research
Operational Satellte: VIIRS	National Meteorological and/or Hydrological Services
Others:ECMWF	Private Sector
	Public Sector and Government Agencies

Dissemination Information

Distribution format	*Generation frequency*
L3, L2b:NetCDF-CF	N/A
	Generation timeliness

Spatio-temporal Information

Spatial Coverage	*Spatial Resolution*
L3, L2b:Global, Polar areas	L3, Global:HORIZONTAL:(0.25°)²

L3, Polar: HORIZONTAL: (25 km)[2]

L2b: HORIZONTAL: (0.05°)[2]

Temporal Resolution	*Temporal Coverage*
L2b:Daily:Per satellite	Start:01/01/1979
L3:Monthly+Daily:Mean	End:12/31/2024

Uncertainty Characteristics			Optimum	Target	Threshold
CFC-L2b	ACCURACY	bias	1%	5%	10%
CFC-L2b	PRECISION	KSS	0.8	0.6	0.5
CFC-L2b	PRECISION	bc-RMS	10%	20%	40%
CFC-Daily Mean	ACCURACY	bias	1%	5%	10%
CFC-Daily Mean	PRECISION	bc-RMS	5%	10%	20%
CFC-Daily Mean	STABILITY	decadal	0.5%	2%	5%
CFC-Monthly Mean	ACCURACY	bias	1%	5%	10%
CFC-Monthly Mean	PRECISION	bc-RMS	5%	10%	20%
CFC-Monthly Mean	STABILITY	decadal	0.5%	2%	5%

Verification:

Primarily comparisons with SYNOP and CALIPSO-CALIOP;

Consistency checks against MODIS C6.1, ISCCP-H, ESA-CLOUD-CCI v3 and PATMOS-x version 6. For L2b comparisons will be made with SNO-matched CALIPSO-CALIOP observations

Comment:

The accuracy is defined as the mean error (i.e, defined in % cloud amount units) and precision is defined as the bc-RMS.

For the polar areas, CFC products will be provided defined in EASE-grid projection (25 km for level3)).

Daily level2b files (per satellite in asc./desc. node).

CM-11023	CLARA-A3.5 Joint Cloud Histograms (JCH) TCDR	JCH_R4_CLARA_35_TCDR

Type

Dataset

Input Satellite Data	*Application Areas*
CM-SAF Product:CM-11033	Climate Research
CM-SAF Product:CM-11043	
CM-SAF Product:CM-11053	

Dissemination Information

Distribution format	*Generation frequency*
L3:NetCDF-CF	N/A
	Generation timeliness

Spatio-temporal Information

Spatial Coverage	*Spatial Resolution*
L3:Global	L3:HORIZONTAL:$(1°)^2$
	L3:VERTICAL:n/a
Temporal Resolution	*Temporal Coverage*
L3:Monthly:Histogram	Start:01/01/1979
	End:12/31/2024

Uncertainty Characteristics	Optimum	Target	Threshold

JCH-Monthly Histogram	N/A	N/A	N/A

Verification:

Comment:

No specific verification as this product is being composed of already validated CM SAF products (Cloud Top, Cloud Optical Thickness, and Cloud Phase).

CM-11033	CLARA-A3.5 Cloud Top Level (CTO) TCDR	CTO_R4_CLARA_35_TCDR

Type

Dataset

Input Satellite Data

Operational Satellite:AVHRR GAC

Operational Satellte: VIIRS

Others:ECMWF

Application Areas

Climate Research

National Meteorological and/or Hydrological Services

Dissemination Information

Distribution format

L3, L2b:NetCDF-CF

Generation frequency

N/A

Generation timeliness

Spatio-temporal Information

Spatial Coverage

L3, L2b:Global, Polar areas

Spatial Resolution

L3, Global:HORIZONTAL:$(0.25°)^2$

L3, Polar: HORIZONTAL: $(25\ km)^2$

L2b: HORIZONTAL$(0.05°)^2$

Temporal Resolution

L2b:Daily:Per satellite

L3:Daily+Monthly:Mean

Temporal Coverage

Start:01/01/1979

End:12/31/2024

Uncertainty Characteristics			Optimum	Target	Threshold
CTH-L2b	ACCURACY	bias	500 m	800 m	1800 m
CTH-L2b	PRECISION	bc-RMS	1500 m	2400 m	4000 m
CTH-Daily Mean	ACCURACY	bias	500 m	800 m	1300 m
CTH-Daily Mean	PRECISION	bc-RMS	1300 m	2000 m	3500 m
CTH-Daily Mean	STABILITY	decadal	150 m	270 m	400 m
CTH-Monthly Mean	ACCURACY	bias	500 m	800 m	1300 m
CTH-Monthly Mean	PRECISION	bc-RMS	1200 m	1600 m	3000 m
CTH-Monthly Mean	STABILITY	decadal	150 m	270 m	400 m
CTP-L2b	ACCURACY	bias	20 hPa	45 hPa	100 hPa
CTP-L2b	PRECISION	bc-RMS	110 hPa	140 hPa	170 hPa
CTP-Daily Mean	ACCURACY	bias	20 hPa	45 hPa	100 hPa
CTP-Daily Mean	PRECISION	bc-RMS	70 hPa	100 hPa	130 hPa
CTP-Daily Mean	STABILITY	decadal	5 hPa	15 hPa	30 hPa
CTP-Monthly Mean	ACCURACY	bias	20 hPa	45 hPa	100 hPa
CTP-Monthly Mean	PRECISION	bc-RMS	50 hPa	85 hPa	110 hPa
CTP-Monthly Mean	STABILITY	decadal	5 hPa	15 hPa	30 hPa

Verification:

comparison with ISCCP-H;

comparison with MODIS C6.1;

comparison with Cloudsat/Calipso;

comparison with PATMOS-X version 6

comparison with ESA-CLOUD-CCI v3

Comment:

For CTT: no specific requirement as it represents same information in different units.

For the polar areas, CTO products will be provided defined in EASE-grid projection (25 km for level3)).

CM-11043	CLARA-A3.5 Cloud Phase (CPH) CPH_R4_CLARA_35_TCDR TCDR

Type

Dataset

Input Satellite Data	*Application Areas*
Operational Satellite:AVHRR GAC	Climate Research
Operational Satellte: VIIRS	National Meteorological and/or Hydrological Services
Others:ECMWF	

Dissemination Information

Distribution format	*Generation frequency*
L3, L2b:NetCDF-CF	N/A
	Generation timeliness

Spatio-temporal Information

Spatial Coverage	*Spatial Resolution*
L3, L2b:Global	L3:HORIZONTAL:$(0.25°)^2$
	L2b:$(0.05°)^2$

Temporal Resolution	*Temporal Coverage*
L2b:Daily:Per satellite	Start:01/01/1979
L3:Daily+Monthly:Mean	End:12/31/2024

Uncertainty Characteristics	Optimum	Target	Threshold

CPH-L2b	ACCURACY	bias	1%	5%	10%
CPH-L2b	PRECISION	KSS	0.8	0.6	0.5
CPH-Daily Mean	ACCURACY	bias	1%	5%	10%
CPH-Daily Mean	PRECISION	bc-RMS	5%	10%	20%
CPH-Daily Mean	STABILITY	decadal	0.5%	2%	5%
CPH-Monthly Mean	ACCURACY	bias	1%	5%	10%
CPH-Monthly Mean	PRECISION	bc-RMS	5%	10%	20%
CPH-Monthly Mean	STABILITY	decadal	0.5%	2%	5%

Verification:

comparison with ISCCP-H;

comparison with MODIS C6.1;

comparison with Cloudsat/Calipso;

comparison with PATMOS-X version 6.

comparison with ESA-CLOUD-CCI v3.

Comment:

Additional layers: CPH for daytime and nighttime L2b contains extended cloud phase with more categories (supercooled, overlap, cirrus, ..).

Bias and bc-RMS are expressed in absolute units (% liquid clouds relative to all clouds).

CM-11053 CLARA-A3.5 Liquid Water Path (LWP) TCDR LWP_R4_CLARA_35_TCDR

Type

Dataset

Input Satellite Data

Operational Satellite:AVHRR GAC

Operational Satellte: VIIRS

Others:ECMWF

Application Areas

Climate Research

National Meteorological and/or Hydrological Services

Private Sector

Public Sector and Government Agencies

Dissemination Information

Distribution format

L3, L2b:NetCDF-CF

Generation frequency

N/A

Generation timeliness

Spatio-temporal Information

Spatial Coverage

L3, L2b:Global

Spatial Resolution

L3:HORIZONTAL:$(0.25°)^2$

L2b: HORIZONTAL: $(0.05°)^2$

Temporal Resolution

L2b: Daily: Per satellite

L3:Daily:Mean

L3:Monthly:Mean

Temporal Coverage

Start:01/01/1979

End:12/31/2024

Uncertainty Characteristics			Optimum	Target	Threshold
LWP-L2b	ACCURACY	bias	5 g/m²	10 g/m²	20 g/m²
LWP-L2b	PRECISION	bc-RMS	20 g/m²	50 g/m²	100 g/m²
LWP-Daily Mean	ACCURACY	bias	5 g/m²	10 g/m²	20 g/m²
LWP-Daily Mean	PRECISION	bc-RMS	15 g/m²	30 g/m²	60 g/m²
LWP-Daily Mean	STABILITY	decadal	1 g/m²	3 g/m²	6 g/m²
LWP-Monthly Mean	ACCURACY	bias	5 g/m²	10 g/m²	20 g/m²
LWP-Monthly Mean	PRECISION	bc-RMS	10 g/m²	20 g/m²	40 g/m²
LWP-Monthly Mean	STABILITY	decadal	1 g/m²	3 g/m²	6 g/m²

Verification:

comparison with satellite-based MWR retrieved LWP over ocean (e.g. AMSR-E);

comparison with PATMOS-X version 6;

comparison with ESA-CLOUD-CCI v3;

comparison with MODIS C6.1;

comparison with ISCCP-H

Comment:

Contains as additional layers: COT (cloud optical thickness), CRE (particle effective radius), and CDNC (cloud droplet number concentration). CDNC only for instruments with 3.7 micron channel active during daytime.

LWP averaged over cloudy sky and all sky.

COT expressed as linear and logarithmic average.

CM-11063	CLARA-A3.5 Ice Water Path (IWP) TCDR	IWP_R4_CLARA_35_TCDR

Type

Dataset

Input Satellite Data	*Application Areas*
Operational Satellite:AVHRR GAC	Climate Research
Operational Satellte: VIIRS	National Meteorological and/or Hydrological Services
Others:ECMWF	Private Sector
	Public Sector and Government Agencies

Dissemination Information

Distribution format	*Generation frequency*
L3, L2b:NetCDF-CF	N/A
	Generation timeliness

Spatio-temporal Information

Spatial Coverage	*Spatial Resolution*
L3, L2b:Global	L3:HORIZONTAL:$(0.25°)^2$
	L2b: HORIZONTAL: $(0.05°)^2$

Temporal Resolution	*Temporal Coverage*
L2b: Daily: Per satellite	Start:01/01/1979
L3, L2b:Daily+Monthly:Mean	End:12/31/2024

Uncertainty Characteristics	Optimum	Target	Threshold

IWP-L2b	ACCURACY	bias	10 g/m²	20 g/m²	40 g/m²
IWP-L2b	PRECISION	bc-RMS	40 g/m²	100 g/m²	200 g/m²
IWP-Daily Mean	ACCURACY	bias	10 g/m²	20 g/m²	40 g/m²
IWP-Daily Mean	PRECISION	bc-RMS	30 g/m²	60 g/m²	120 g/m²
IWP-Daily Mean	STABILITY	decadal	2 g/m²	6 g/m²	12 g/m²
IWP-Monthly Mean	ACCURACY	bias	10 g/m²	20 g/m²	40 g/m²
IWP-Monthly Mean	PRECISION	bc-RMS	20 g/m²	40 g/m²	80 g/m²
IWP-Monthly Mean	STABILITY	decadal	2 g/m²	6 g/m²	12 g/m²

Verification:

comparison with CloudSat/CALIPSO (DARDAR);

comparison with PATMOS-X version 6;

comparison with ESA-CLOUD-CCI v3;

comparison with MODIS C6.1;

comparison with ISCCP-H

Comment:

Contains as additional layers: COT (cloud optical thickness) and CRE (particle effective radius).

IWP averaged over cloudy sky and all sky

COT expressed as linear and logarithmic average.

CM-11203	CLARA-A3.5 Surface Incoming Solar Radiation TCDR	SIS_R4_CLARA_35_TCDR

Type

Dataset

Input Satellite Data	*Application Areas*
Operational Satellite:AVHRR GAC	Climate Change Analysis
Operational Satellte: VIIRS	Climate Impact Analysis
Others: ToA reflected solar flux (RSF L2)	Climate Modelling and Evaluation
	Public Sector and Government Agencies

Dissemination Information

Distribution format	*Generation frequency*
L3:NetCDF4	
	Generation timeliness

Spatio-temporal Information

Spatial Coverage	*Spatial Resolution*
L3:Global	L3:HORIZONTAL:$(0.25)^2$
Temporal Resolution	*Temporal Coverage*
L3:Daily+Monthly:Mean	Start:01/01/1979
	End:12/31/2024

Uncertainty Characteristics			Optimum	Target	Threshold
SIS-Daily Mean	ACCURACY	MAB	10 W/m²	15 W/m²	18 W/m²

SIS-Daily Mean	STABILITY	decadal	0.5 W/m²	1 W/m²	2 W/m²
SIS-Monthly Mean	ACCURACY	MAB	3 W/m²	5 W/m²	9 W/m²
SIS-Monthly Mean	STABILITY	decadal	0.5W/m²	1 W/m²	2 W/m²

Verification:

comparison with BSRN

Comment:

CM-11226	CLARA-A3.5 Surface Albedo (SAL) TCDR	SAL_R4_CLARA_35_TCDR

Type

Dataset

Input Satellite Data

Others:AOD

Operational Satellite:AVHRR GAC

Operational Satellte: VIIRS

Others:DEM

Others:cloud mask

Others:co-ordinates

Others:land cover information

Others:ozone

Others:water vapour

Others: wind speed

Others: sea ice concentration

Others: surface pressure

Application Areas

Climate Research

National Meteorological and/or Hydrological Services

Public Sector and Government Agencies

Dissemination Information

Distribution format

L3:NetCDF-CF

Generation frequency

N/A

Generation timeliness

Spatio-temporal Information	
Spatial Coverage	*Spatial Resolution*
L3:Global, Polar areas	L3, Global:HORIZONTAL:(0.25º)^2
	L3, Polar: HORIZONTAL: (25 km)^2
Temporal Resolution	*Temporal Coverage*
L3:Monthly:Mean	Start:01/01/1979
L3:Pentad:Mean	End:12/31/2024

Uncertainty Characteristics			Optimum	Target	Threshold
SAL-Pentad Mean	ACCURACY	bias	5 % rel.	10 % rel.	15 % rel.
SAL-Pentad Mean	PRECISION	bc-RMS	0.05	0.10	0.15
SAL-Pentad Mean	STABILITY	decadal	2% rel.	15% rel.	20 % rel.
SAL-Monthly Mean	ACCURACY	bias	5 % rel.	10 % rel.	15 % rel.
SAL-Monthly Mean	PRECISION	bc-RMS	0.05	0.10	0.15
SAL-Monthly Mean	STABILITY	decadal	2% rel.	15% rel.	20 % rel.

Verification:

comparison with surface measurements for different regions

Comment:

Atmospheric correction with SMAC, BRDF correction for vegetation with Roujean-Li method, narrow-to-broadband conversion after Liang. For snow, aggregation of observations with adaptable narrow-to-broadband conversion after Xiong. Topography correction, dynamic AOD background, empirical-based snow white/blue-sky albedo estimates.
For polar areas products will be provided in EASE-grid (25 km for level3).

Target and Threshold Accuracies are defined for flat land for 90% of cases.

Accuracy-Optimum: 5% or 0.005 absolute

CM-11227	CLARA-A3.5 White sky surface Albedo TCDR	SAW_R2_CLARA_35_TCDR

Type

Dataset

Input Satellite Data	*Application Areas*
Others:AOD	Climate Research
Operational Satellite:AVHRR GAC	National Meteorological and/or Hydrological Services
Operational Satellte: VIIRS	Public Sector and Government Agencies
Others:DEM	
Others:cloud mask	
Others:co-ordinates	
Others:land cover information	
Others:ozone	
Others:water vapour	
Others: wind speed	
Others: sea ice concentration	
Others: surface pressure	

Dissemination Information

Distribution format	*Generation frequency*
L3:NetCDF4	
	Generation timeliness

Spatio-temporal Information	
Spatial Coverage	*Spatial Resolution*
L3:Global, Polar areas	L3, Global:HORIZONTAL: $(0.25°)^2$
	L3, Polar: HORIZONTAL: $(25\ km)^2$
Temporal Resolution	*Temporal Coverage*
L3:Monthly:Mean	Start:01/01/1979
L3:Pentad:Mean	End:12/31/2024

Uncertainty Characteristics			Optimum	Target	Threshold
WAL-Pentad Mean	ACCURACY	bias	5% rel.	25% rel.	50% rel.
WAL-Pentad Mean	PRECISION	bc-RMS	0.05	0.10	0.15
WAL-Pentad Mean	STABILITY	decadal	2% rel.	15% rel.	20% rel.
WAL-Monthly Mean	ACCURACY	bias	5% rel.	25% rel.	50% rel.
WAL-Monthly Mean	PRECISION	bc-RMS	0.05	0.10	0.15
WAL-Monthly Mean	STABILITY	decadal	2% rel.	15% rel.	20% rel.

Verification:

comparison with surface measurements for different regions

Comment:

Atmospheric correction with SMAC, BRDF correction for vegetation with Roujean-Li method, narrow-to-broadband conversion after Liang. For snow, aggregation of observations with adaptable narrow-to-broadband conversion after Xiong. Topography correction, dynamic AOD background, empirical-based snow white/blue-sky albedo estimates.

Target and Threshold Accuracies are defined for flat land for 90% of cases.

Accuracy-Optimum: 5% or 0.005 absolute

For polar areas products will be provided in EASE-grid (25 km for level3).

CM-11228	CLARA-A3.5 Blue sky surface Albedo TCDR	SAB_R2_CLARA_35_TCDR

Type

Dataset

Input Satellite Data

Others:AOD

Operational Satellite:AVHRR GAC

Operational Satellte: VIIRS

Others:DEM

Others:cloud mask

Others:co-ordinates

Others:land cover information

Others:ozone

Others:water vapour

Others: wind speed

Others: sea ice concentration

Others: surface pressure

Application Areas

Climate Research

National Meteorological and/or Hydrological Services

Public Sector and Government Agencies

Dissemination Information

Distribution format

L3:NetCDF4

Generation frequency

Generation timeliness

Spatio-temporal Information	
Spatial Coverage	*Spatial Resolution*
L3:Global, Polar areas	L3, Global:HORIZONTAL: $(0.25°)^2$
	L3, Polar: HORIZONTAL: $(25\ km)^2$
	L3:VERTICAL:N/A
Temporal Resolution	*Temporal Coverage*
L3:Monthly:Mean	Start:01/01/1979
L3:Pentad:Mean	End:12/31/2024

Uncertainty Characteristics			Optimum	Target	Threshold
BAL-Monthly Mean	ACCURACY	bias	5 % rel.	25 % rel.	50 % rel.
BAL-Monthly Mean	PRECISION	bc-RMS	0.05	0.10	0.15
BAL-Monthly Mean	STABILITY	decadal	2% rel.	15% rel.	20 % rel.
BAL-Monthly Mean	ACCURACY	bias	5 % rel.	25 % rel.	50 % rel.
BAL-Monthly Mean	PRECISION	bc-RMS	0.05	0.10	0.15
BAL-Monthly Mean	STABILITY	decadal	2% rel.	15% rel.	20 % rel.

Verification:

comparison with surface measurements for different regions

Comment:

Atmospheric correction with SMAC, BRDF correction for vegetation with Roujean-Li method, narrow-to-broadband conversion after Liang. For snow, aggregation of observations with adaptable narrow-to-broadband conversion after Xiong. Topography correction, dynamic AOD background, empirical-based snow white/blue-sky albedo estimates.

Target and Threshold Accuracies are defined for flat land for 90% of cases.

Accuracy-Optimum: 5% or 0.005 absolute

For polar areas products will be provided in EASE-grid (25 km for level3).

CM-11263	CLARA-A3.5 Surface Downwelling Longwave Radiation TCDR	SDL_R3_CLARA_35_TCDR

Type

Dataset

Input Satellite Data	*Application Areas*
Operational Satellite:AVHRR GAC	Cimate Monitoring
Operational Satellte: VIIRS	Climate Modelling and Evaluation

Dissemination Information

Distribution format	*Generation frequency*
L3:NetCDF4	
	Generation timeliness

Spatio-temporal Information

Spatial Coverage	*Spatial Resolution*
L3:Global	L3:HORIZONTAL:0.25^2
Temporal Resolution	*Temporal Coverage*
L3:Monthly:Mean	Start:01/01/1979
	End:12/31/2024

Uncertainty Characteristics			Optimum	Target	Threshold
SDL-Monthly Mean	ACCURACY	MAB	3 W/m²	5 W/m²	8 W/m²
SDL-Monthly Mean	STABILITY	decadal	0.5 W/m²	1 W/m²	2 W/m²

Verification:

comparison with BSRN

Comment:

CM-11273	CLARA-A3.5 Surface Radiation Budget TCDR	SRB_R3_CLARA_35_TCDR

Type

Dataset

Input Satellite Data	*Application Areas*
CM-SAF Product:CM-11222	Cimate Monitoring
CM SAF Product:CM-11262	Climate Modelling and Evaluation
CM SAF Product: CM-11202	

Dissemination Information

Distribution format	*Generation frequency*
L3:NetCDF4	
	Generation timeliness

Spatio-temporal Information

Spatial Coverage	*Spatial Resolution*
L3:Global	L3:HORIZONTAL:0.25²
Temporal Resolution	*Temporal Coverage*
L3:Monthly:Mean	Start:01/01/1979
	End:12/31/2024

Uncertainty Characteristics			Optimum	Target	Threshold
SRB-Monthly Mean	ACCURACY	MAB	3 W/m²	5 W/m²	8 W/m²
SRB-Monthly Mean	STABILITY	decadal	0.5 W/m²	1 W/m²	2 W/m²

Verification:

comparison with BSRN

Comment:

CM-11282	CLARA-A3.5 Surface Net Shortwave Radiation TCDR	SNS_R3_CLARA_35_TCDR

Type

Dataset

Input Satellite Data

Operational Satellite:AVHRR GAC

Operational Satellte: VIIRS

Application Areas

Climate Change Analysis

Climate Impact Analysis

Climate Modelling and Evaluation

Public Sector and Government Agencies

Dissemination Information

Distribution format

L3:NetCDF4

Generation frequency

Generation timeliness

Spatio-temporal Information

Spatial Coverage

L3:Global

Spatial Resolution

L3:HORIZONTAL:$(0.25)^2$

Temporal Resolution	*Temporal Coverage*
~~L3:Daily:Mean~~	01/01/1979
L3:Monthly:Mean	12/31/2024

Uncertainty Characteristics			Optimum	Target	Threshold
~~SNS-Daily Mean~~	~~ACCURACY~~	~~bias~~	~~3 W/m²~~	~~5 W/m²~~	~~8 W/m²~~
~~SNS-Daily Mean~~	~~STABILITY~~	~~decadal~~	~~0.5 W/m²~~	~~1 W/m²~~	~~2 W/m²~~
SNS-Monthly Mean	ACCURACY	MAB	3 W/m²	5 W/m²	8 W/m²
SNS-Monthly Mean	STABILITY	decadal	0.5 W/m²	1 W/m²	2 W/m²

Verification:

comparison with BSRN

Comment:

CM-11292	CLARA-A3.5 Surface Net Longwave Radiation TCDR	SNL_R3_CLARA_35_TCDR

Type

Dataset

Input Satellite Data	*Application Areas*
Operational Satellite:AVHRR GAC	Climate Change Analysis
Operational Satellte: VIIRS	Climate Impact Analysis
	Climate Modelling and Evaluation
	Public Sector and Government Agencies

Dissemination Information

Distribution format	*Generation frequency*
L3:NetCDF4	
	Generation timeliness

Spatio-temporal Information

Spatial Coverage	*Spatial Resolution*
L3:Global	L3:HORIZONTAL:(0.25)²

Temporal Resolution	*Temporal Coverage*
~~L3:Daily:Mean~~	01/01/1979
L3:Monthly:Mean	12/31/2024

Uncertainty Characteristics	Optimum	Target	Threshold

~~SNL-Daily Mean~~	~~ACCURACY~~	~~bias~~	~~3 W/m²~~	~~5 W/m²~~	~~8 W/m²~~
~~SNL-Daily Mean~~	~~STABILITY~~	~~decadal~~	~~0.5 W/m²~~	~~1 W/m²~~	~~2 W/m²~~
SNL-Monthly Mean	ACCURACY	MAB	3 W/m²	5 W/m²	8 W/m²
SNL-Monthly Mean	STABILITY	decadal	0.5 W/m²	1 W/m²	2 W/m²

Verification:

comparison with BSRN

Comment:

CM-11313	CLARA-A3.5 ToA Reflected Shortwave Flux TCDR	RSF_R2_CLARA_35_TCDR

Type

Dataset

Input Satellite Data	*Application Areas*
Operational Satellite:AVHRR GAC	Climate Research
Operational Satellite: VIIRS	

Dissemination Information

Distribution format	*Generation frequency*
L3:NetCDF4	
	Generation timeliness

Spatio-temporal Information

Spatial Coverage	*Spatial Resolution*
L3:Global	L3:HORIZONTAL:0.25°

Temporal Resolution	*Temporal Coverage*
L3:Daily:Mean	Start:01/01/1979
L3:Monthly:Mean	End:12/31/2024

Uncertainty Characteristics			Optimum	Target	Threshold
RSF-Daily Mean	PRECISION	MAB	4 W/m²	8 W/m²	16 W/m²
RSF-Daily Mean	STABILITY	decadal	0.3 W/m²	0.6 W/m²	4 W/m²
RSF-Monthly Mean	PRECISION	MAB	2 W/m²	4 W/m²	8 W/m²

RSF-Monthly Mean	STABILITY	decadal	0.3 W/m²	0.6 W/m²	4 W/m²

Verification:

Comparison with CERES (EBAF,SYN), reanalysis (ERA5), ISCCP-DF, GEWEX-SRB

Comparison with CM SAF GERB CDR (CM-21301) and MVIRI/SEVIRI ToA Radiation CDR (CM-23311)

Comment:

CM-11343	CLARA-A3.5 ToA Outgoing Longwave Radiation TCDR	OLR_R2_CLARA_35_TCDR

Type

Dataset

Input Satellite Data	*Application Areas*
Operational Satellite:AVHRR GAC	Climate Research
Operational Satellite: VIIRS	

Dissemination Information

Distribution format	*Generation frequency*
L3:NetCDF4	
	Generation timeliness

Spatio-temporal Information

Spatial Coverage	*Spatial Resolution*
L3:Global	L3:HORIZONTAL: 0.25°
Temporal Resolution	*Temporal Coverage*
L3:Daily:Mean	Start:01/01/1979
L3:Monthly:Mean	End:12/31/2024

Uncertainty Characteristics			Optimum	Target	Threshold
OLR-Daily Mean	PRECISION	MAB	4 W/m²	8 W/m²	16 W/m²
OLR-Daily Mean	STABILITY	decadal	0.2 W/m²	0.6 W/m²	4 W/m²
OLR-Monthly Mean	PRECISION	MAB	2 W/m²	4 W/m²	8 W/m²

OLR-Monthly Mean	STABILITY	decadal	0.2 W/m²	0.6 W/m²	4 W/m²

Verification:

Comparison with CERES (EBAF,SYN), reanalysis (ERA5), HIRS OLR, ISCCP-DF, GEWEX-SRB

Comparison with CM SAF GERB CDR (CM-21331) and MVIRI/SEVIRI ToA Radiation CDR (CM-23341)

Comment:

10 Appendix B: Product requirements tables for the ICDR data records

This section provides the requirements for CLARA-A3.5 ICDRs. Baseline for these requirements are section 5 and the CDR requirement tables in Appendix A.

The project team recommends to take the updated requirements as discussed in section 4 and presented here as baseline for the implementation and the development.

CM-6012	CLARA-A3.5 Fractional Cloud Cover ICDR R4	CFC_R4_CLARA_35_ICDR
Type Dataset		
Input Satellite Data Operational Satellite:AVHRR GAC Operational Satellte: VIIRS Others:ECMWF	*Application Areas* Climate monitoring	
Dissemination Information		
Distribution format L3, L2b:NetCDF-CF	*Generation frequency* 1 day, 1 month *Generation timeliness* 10 days (95%), 15 days (100%)	
Spatio-temporal Information		
Spatial Coverage L3, L2b:Global, Polar areas	*Spatial Resolution* L3, Global:HORIZONTAL:$(0.25°)^2$ L3, Polar: HORIZONTAL: $(25 km)^2$ L2b: HORIZONTAL: $(0.05°)^2$	

Temporal Resolution	*Temporal Coverage*
L2b:Daily:Per satellite	01 January 2025 onwards
L3:Monthly+Daily:Mean	

Uncertainty Characteristics			Optimum	Target	Threshold
CFC-L2b	ACCURACY	bias	--	10%	--
CFC-L2b	PRECISION	KSS	--	0.5	--
CFC-L2b	PRECISION	bc-RMS	--	40%	--
CFC-Daily Mean	ACCURACY	bias	--	10%	--
CFC-Daily Mean	PRECISION	bc-RMS	--	20%	--
CFC-Monthly Mean	ACCURACY	bias	--	10%	--
CFC-Monthly Mean	PRECISION	bc-RMS	--	20%	--

Verification:

Comparisons with SYNOP and MODIS C6.1

Comment:

The accuracy is defined as the mean error (i.e, defined in % cloud amount units) and precision is defined as the bc-RMS.

For the polar areas, CFC products will be provided defined in EASE-grid projection (25 km for level3)).

Daily level2b files (per satellite in asc./desc. node).

ICDR related to the CLARA-A3.5 CDR (CM-11013).

CM-6022	CLARA-A3.5 Joint Cloud Histograms ICDR R4	JCH_R4_CLARA_35_ICDR

Type

Dataset

Input Satellite Data	*Application Areas*
CM-SAF Product:CM-6032	Climate Monitoring
CM-SAF Product:CM-6042	
CM-SAF Product:CM-6052	

Dissemination Information

Distribution format	*Generation frequency*
L3:NetCDF-CF	1 day, 1 month
	Generation timeliness
	10 days (95%), 15 days (100%)

Spatio-temporal Information

Spatial Coverage	*Spatial Resolution*
L3:Global	L3:HORIZONTAL:$(1°)^2$
	L3:VERTICAL:n/a
Temporal Resolution	*Temporal Coverage*
L3:Monthly:Histogram	01 January 2025 onwards

Uncertainty Characteristics	Optimum	Target	Threshold
JCH-Monthly Histogram	--	N/A	--

Verification: see comment

Comment:

No specific verification as this product is being composed of already validated CM SAF products (Cloud Top, Cloud Optical Thickness, and Cloud Phase).

ICDR related to the CLARA-A3.5 CDR (CM-11023).

CM-6032	CLARA-A3.5 Cloud Top Level ICDR R4	CTO_R4_CLARA_35_ICDR

Type

Dataset

Input Satellite Data	*Application Areas*
Operational Satellite:AVHRR GAC	Climate Monitoring
Operational Satellte: VIIRS	
Others:ECMWF	

Dissemination Information

Distribution format	*Generation frequency*
L3, L2b:NetCDF-CF	1 day, 1 month
	Generation timeliness
	10 days (95%), 15 days (100%)

Spatio-temporal Information

Spatial Coverage	*Spatial Resolution*
L3, L2b:Global, Polar areas	L3, Global:HORIZONTAL:$(0.25°)^2$
	L3, Polar: HORIZONTAL: $(25\ km)^2$
	L2b: HORIZONTAL$(0.05°)^2$
Temporal Resolution	*Temporal Coverage*
L2b:Daily:Per satellite	01 January 2025 onwards
L3:Daily+Monthly:Mean	

Uncertainty Characteristics	Optimum	Target	Threshold

CTH-L2b	ACCURACY	bias	--	1800 m	--
CTH-L2b	PRECISION	bc-RMS	--	4000 m	--
CTH-Daily Mean	ACCURACY	bias	--	1300 m	--
CTH-Daily Mean	PRECISION	bc-RMS	--	3500 m	--
CTH-Monthly Mean	ACCURACY	bias	--	1300 m	--
CTH-Monthly Mean	PRECISION	bc-RMS	--	3000 m	--
CTP-L2b	ACCURACY	bias	--	100 hPa	--
CTP-L2b	PRECISION	bc-RMS	--	170 hPa	--
CTP-Daily Mean	ACCURACY	bias	--	100 hPa	-
CTP-Daily Mean	PRECISION	bc-RMS	--	130 hPa	--
CTP-Monthly Mean	ACCURACY	bias	--	100 hPa	--
CTP-Monthly Mean	PRECISION	bc-RMS	--	110 hPa	--

Verification:

Comparison with MODIS C6.1

Comment:

For CTT: no specific requirement as it represents same information in different units.

For the polar areas, CTO products will be provided defined in EASE-grid projection (25 km for level3)).

ICDR related to the CLARA-A3.5 CDR (CM-11033).

CM-6042	CLARA-A3.5 Cloud Phase ICDR R4	CPH_R4_CLARA_35_ICDR

Type

Dataset

Input Satellite Data	*Application Areas*
Operational Satellite:AVHRR GAC	Climate monitoring
Operational Satellte: VIIRS	
Others:ECMWF	

Dissemination Information

Distribution format	*Generation frequency*
L3, L2b:NetCDF-CF	1 day, 1 month
	Generation timeliness
	10 days (95%), 15 days (100%)

Spatio-temporal Information

Spatial Coverage	*Spatial Resolution*
L3, L2b:Global	L3:HORIZONTAL:$(0.25°)^2$
	L2b:$(0.05°)^2$

Temporal Resolution	*Temporal Coverage*
L2b:Daily:Per satellite	01 January 2025 onwards
L3:Daily+Monthly:Mean	

Uncertainty Characteristics			Optimum	Target	Threshold
CPH-L2b	ACCURACY	bias	--	10%	--
CPH-L2b	PRECISION	KSS	--	0.5	--

CPH-Daily Mean	ACCURACY	bias	--	10%	--
CPH-Daily Mean	PRECISION	bc-RMS	--	20%	--
CPH-Monthly Mean	ACCURACY	bias	--	10%	--
CPH-Monthly Mean	PRECISION	bc-RMS	--	20%	--

Verification:

Comparison with MODIS C6.1

Comment:

Additional layers: CPH for daytime and nighttime L2b contains extended cloud phase with more categories (supercooled, overlap, cirrus, ..).

Bias and bc-RMS are expressed in absolute units (% liquid clouds relative to all clouds).

ICDR related to the CLARA-A3.5 CDR (CM-11043).

CM-6052	CLARA-A3.5 Liquid Water Path ICDR R3	LWP_R4_CLARA_35_ICDR

Type

Dataset

Input Satellite Data	*Application Areas*
Operational Satellite:AVHRR GAC	Climate monitoring
Operational Satellte: VIIRS	
Others:ECMWF	

Dissemination Information

Distribution format	*Generation frequency*
L3, L2b:NetCDF-CF	1 day, 1 month
	Generation timeliness
	10 days (95%), 15 days (100%)

Spatio-temporal Information

Spatial Coverage	*Spatial Resolution*
L3, L2b:Global	L3:HORIZONTAL:$(0.25°)^2$
	L2b: HORIZONTAL: $(0.05°)^2$

Temporal Resolution	*Temporal Coverage*
L2b: Daily: Per satellite	01 January 2025 onwards
L3:Daily:Mean	
L3:Monthly:Mean	

Uncertainty Characteristics			Optimum	Target	Threshold
LWP-L2b	ACCURACY	bias	--	20 g/m²	--

LWP-L2b	PRECISION	bc-RMS	--	100 g/m²	--
LWP-Daily Mean	ACCURACY	bias	--	20 g/m²	--
LWP-Daily Mean	PRECISION	bc-RMS	--	60 g/m²	--
LWP-Monthly Mean	ACCURACY	bias	--	20 g/m²	--
LWP-Monthly Mean	PRECISION	bc-RMS	--	40 g/m²	--

Verification:

Comparison with MODIS C6.1

Comment:

Contains as additional layers: COT (cloud optical thickness), CRE (particle effective radius), and CDNC (cloud droplet number concentration). CDNC only for instruments with 3.7 micron channel active during daytime.

LWP averaged over cloudy sky and all sky.

COT expressed as linear and logarithmic average.

ICDR related to the CLARA-A3.5 CDR (CM-11053).

CM-6062	CLARA-A3.5 Ice Water Path ICDR R3	IWP_R4_CLARA_35_ICDR

Type

Dataset

Input Satellite Data	*Application Areas*
Operational Satellite:AVHRR GAC	Climate monitoring
Operational Satellte: VIIRS	
Others:ECMWF	

Dissemination Information

Distribution format	*Generation frequency*
L3, L2b:NetCDF-CF	1 day, 1 month
	Generation timeliness
	10 days (95%), 15 days (100%)

Spatio-temporal Information

Spatial Coverage	*Spatial Resolution*
L3, L2b:Global	L3:HORIZONTAL:$(0.25°)^2$
	L2b: HORIZONTAL: $(0.05°)^2$
Temporal Resolution	*Temporal Coverage*
L2b: Daily: Per satellite	01 January 2025 onwards
L3:Daily+Monthly:Mean	

Uncertainty Characteristics			Optimum	Target	Threshold
IWP-L2b	ACCURACY	bias	--	40 g/m²	--
IWP-L2b	PRECISION	bc-RMS	--	200 g/m²	--

IWP-Daily Mean	ACCURACY	bias	--	40 g/m²	--
IWP-Daily Mean	PRECISION	bc-RMS	--	120 g/m²	--
IWP-Monthly Mean	ACCURACY	bias	--	40 g/m²	--
IWP-Monthly Mean	PRECISION	bc-RMS	--	80 g/m²	--

Verification:

Comparison with MODIS C6.1

Comment:

Contains as additional layers: COT (cloud optical thickness) and CRE (particle effective radius).

IWP averaged over cloudy sky and all sky

COT expressed as linear and logarithmic average.

ICDR related to the CLARA-A3.5 CDR (CM-11063).

CM-6212	CLARA-A3.5 Surface Incoming Solar Radiation ICDR R3	SIS_R4_CLARA_35_ICDR

Type

Dataset

Input Satellite Data

Operational Satellite:AVHRR GAC

Operational Satellte: VIIRS

Others: ToA reflected solar flux (RSF L2)

Application Areas

Climate monitoring

Dissemination Information

Distribution format

L3:NetCDF4

Generation frequency

1 day, 1 month

Generation timeliness

10 days (95%), 15 days (100%)

Spatio-temporal Information

Spatial Coverage

L3:Global

Spatial Resolution

L3:HORIZONTAL:$(0.25)^2$

Temporal Resolution

L3:Daily+Monthly:Mean

Temporal Coverage

01 January 2025 onwards

Uncertainty Characteristics			Optimum	Target	Threshold
SIS-Daily Mean	ACCURACY	MAB	--	18 W/m²	--
SIS-Monthly Mean	ACCURACY	MAB	--	9 W/m²	--

Verification:

comparison with BSRN

Comment:

ICDR related to the CLARA-A3.5 CDR (CM-11203).

CM-6226	CLARA-A3.5 Surface Albedo ICDR R3	SAL_R4_CLARA_35_ICDR

Type

Dataset

Input Satellite Data	*Application Areas*
Others:AOD	Climate monitoring
Operational Satellite:AVHRR GAC	
Operational Satellte: VIIRS	
Others:DEM	
Others:cloud mask	
Others:co-ordinates	
Others:land cover information	
Others:ozone	
Others:water vapour	
Others: wind speed	
Others: sea ice concentration	
Others: surface pressure	

Dissemination Information

Distribution format	*Generation frequency*
L3:NetCDF-CF	1 day, 1 month
	Generation timeliness
	10 days (95%), 15 days (100%)

Spatio-temporal Information

Spatial Coverage

L3:Global, Polar areas

Spatial Resolution

L3, Global:HORIZONTAL:$(0.25^o)^2$

L3, Polar: HORIZONTAL: $(25\ km)^2$

Temporal Resolution

L3:Monthly:Mean

L3:Pentad:Mean

Temporal Coverage

01 January 2025 onwards

Uncertainty Characteristics			Optimum	Target	Threshold
SAL-Pentad Mean	ACCURACY	bias	--	15 % rel.	--
SAL-Pentad Mean	PRECISION	bc-RMS	--	0.15	--
SAL-Monthly Mean	ACCURACY	bias	--	15 % rel.	--
SAL-Monthly Mean	PRECISION	bc-RMS	--	0.15	--

Verification:

comparison with BSRN

Comment:

Atmospheric correction with SMAC, BRDF correction for vegetation with Roujean-Li method, narrow-to-broadband conversion after Liang. For snow, aggregation of observations with adaptable narrow-to-broadband conversion after Xiong. Topography correction, dynamic AOD background, empirical-based snow white/blue-sky albedo estimates.
For polar areas products will be provided in EASE-grid (25 km for level3).

Target and Threshold Accuracies are defined for flat land for 90% of cases.

Accuracy-Optimum: 5% or 0.005 absolute

ICDR related to the CLARA-A3.5 CDR (CM-11226).

CM-6227	CLARA-A3.5 White sky surface Albedo ICDR R3	SAW_R3_CLARA_35_ICDR

Type

Dataset

Input Satellite Data

Others:AOD

Operational Satellite:AVHRR GAC

Operational Satellte: VIIRS

Others:DEM

Others:cloud mask

Others:co-ordinates

Others:land cover information

Others:ozone

Others:water vapour

Others: wind speed

Others: sea ice concentration

Others: surface pressure

Application Areas

Climate monitoring

Dissemination Information

Distribution format

L3:NetCDF4

Generation frequency

1 day, 1 month

Generation timeliness

10 days (95%), 15 days (100%)

Spatio-temporal Information

Spatial Coverage

L3:Global, Polar areas

Spatial Resolution

L3, Global:HORIZONTAL: $(0.25°)^2$

L3, Polar: HORIZONTAL: $(25\ km)^2$

Temporal Resolution

L3:Monthly:Mean

L3:Pentad:Mean

Temporal Coverage

01 January 2025 onwards

Uncertainty Characteristics			Optimum	Target	Threshold
WAL-Pentad Mean	ACCURACY	bias	--	50% rel.	--
WAL-Pentad Mean	PRECISION	bc-RMS	--	0.15	--
WAL-Monthly Mean	ACCURACY	bias	--	50% rel.	--
WAL-Monthly Mean	PRECISION	bc-RMS		0.15	--

Verification:

comparison with BSRN

Comment:

Atmospheric correction with SMAC, BRDF correction for vegetation with Roujean-Li method, narrow-to-broadband conversion after Liang. For snow, aggregation of observations with adaptable narrow-to-broadband conversion after Xiong. Topography correction, dynamic AOD background, empirical-based snow white/blue-sky albedo estimates.

Target and Threshold Accuracies are defined for flat land for 90% of cases.

Accuracy-Optimum: 5% or 0.005 absolute

For polar areas products will be provided in EASE-grid (25 km for level3).

ICDR related to the CLARA-A3.5 CDR (CM-11227).

CM-6228	CLARA-A3.5 Blue sky surface Albedo ICDR R3	SAB_R3_CLARA_35_ICDR

Type

Dataset

Input Satellite Data

Others:AOD

Operational Satellite:AVHRR GAC

Operational Satellte: VIIRS

Others:DEM

Others:cloud mask

Others:co-ordinates

Others:land cover information

Others:ozone

Others:water vapour

Others: wind speed

Others: sea ice concentration

Others: surface pressure

Application Areas

Climate monitoring

Dissemination Information

Distribution format

L3:NetCDF4

Generation frequency

1 day, 1 month

Generation timeliness

10 days (95%), 15 days (100%)

Spatio-temporal Information	
Spatial Coverage	*Spatial Resolution*
L3:Global, Polar areas	L3, Global:HORIZONTAL: (0.25°)^2
	L3, Polar: HORIZONTAL: (25 km)^2
	L3:VERTICAL:N/A
Temporal Resolution	*Temporal Coverage*
L3:Monthly:Mean	01 January 2025 onwards
L3:Pentad:Mean	

Uncertainty Characteristics			Optimum	Target	Threshold
BAL-Monthly Mean	ACCURACY	bias	--	50 % rel.	--
BAL-Monthly Mean	PRECISION	bc-RMS	--	0.15	--
BAL-Monthly Mean	ACCURACY	bias	--	50 % rel.	--
BAL-Monthly Mean	PRECISION	bc-RMS	--	0.15	--

Verification:

comparison with BSRN

Comment:

Atmospheric correction with SMAC, BRDF correction for vegetation with Roujean-Li method, narrow-to-broadband conversion after Liang. For snow, aggregation of observations with adaptable narrow-to-broadband conversion after Xiong. Topography correction, dynamic AOD background, empirical-based snow white/blue-sky albedo estimates.

Target and Threshold Accuracies are defined for flat land for 90% of cases.

Accuracy-Optimum: 5% or 0.005 absolute

For polar areas products will be provided in EASE-grid (25 km for level3).

ICDR related to the CLARA-A3.5 CDR (CM-11228).

CM-6262	CLARA-A3.5 Surface Downwelling Longwave Radiation ICDR R2	SDL_R2_CLARA_35_ICDR

Type

Dataset

Input Satellite Data	*Application Areas*
Operational Satellite:AVHRR GAC	Cimate Monitoring
Operational Satellte: VIIRS	

Dissemination Information

Distribution format	*Generation frequency*
L3:NetCDF4	1 day, 1 month
	Generation timeliness
	10 days (95%), 15 days (100%)

Spatio-temporal Information

Spatial Coverage	*Spatial Resolution*
L3:Global	L3:HORIZONTAL:0.25²
Temporal Resolution	*Temporal Coverage*
L3:Monthly:Mean	01 January 2025 onwards

Uncertainty Characteristics			Optimum	Target	Threshold
SDL-Monthly Mean	ACCURACY	MAB	--	8 W/m²	--

Verification:

comparison with BSRN

Comment:

ICDR related to the CLARA-A3.5 CDR (CM-11263).

CM-6272	CLARA-A3.5 Surface Radiation Budget ICDR R2	SRB_R2_CLARA_35_ICDR

Type

Dataset

Input Satellite Data

CM-SAF Product:CM-11222

CM SAF Product:CM-11262

CM SAF Product: CM-11202

Application Areas

Cimate Monitoring

Dissemination Information

Distribution format

L3:NetCDF4

Generation frequency

1 day, 1 month

Generation timeliness

10 days (95%), 15 days (100%)

Spatio-temporal Information

Spatial Coverage

L3:Global

Spatial Resolution

L3:HORIZONTAL:0.25²

Temporal Resolution

L3:Monthly:Mean

Temporal Coverage

01 January 2025 onwards

Uncertainty Characteristics			Optimum	Target	Threshold
SRB-Monthly Mean	ACCURACY	MAB	--	8 W/m²	--

Verification:

comparison with BSRN

Comment:

ICDR related to the CLARA-A3.5 CDR (CM-11273).

CM-6282	CLARA-A3.5 Surface Net Shortwave Radiation ICDR	SNS_R3_CLARA_35_ICDR

Type

Dataset

Input Satellite Data

Operational Satellite:AVHRR GAC

Operational Satellte: VIIRS

Application Areas

Climate monitoring

Dissemination Information

Distribution format

L3:NetCDF4

Generation frequency

1 day, 1 month

Generation timeliness

10 days (95%), 15 days (100%)

Spatio-temporal Information

Spatial Coverage

L3:Global

Spatial Resolution

L3:HORIZONTAL:$(0.25)^2$

Temporal Resolution

~~L3:Daily:Mean~~

L3:Monthly:Mean

Temporal Coverage

01 January 2025 onwards

Uncertainty Characteristics			Optimum	Target	Threshold
~~SNS-Daily Mean~~	~~ACCURACY~~	~~bias~~	~~3 W/m²~~	~~5 W/m²~~	~~8 W/m²~~
~~SNS-Daily Mean~~	~~STABILITY~~	~~decadal~~	~~0.5 W/m²~~	~~1 W/m²~~	~~2 W/m²~~
SNS-Monthly Mean	ACCURACY	MAB	--	8 W/m²	--

Verification:

comparison with BSRN

Comment:

ICDR related to the CLARA-A3.5 CDR (CM-11282).

CM-6292	CLARA-A3.5 Surface Net Longwave Radiation ICDR R2	SNL_R2_CLARA_35_ICDR

Type

Dataset

Input Satellite Data

Operational Satellite:AVHRR GAC

Operational Satellte: VIIRS

Application Areas

Climate monitoring

Dissemination Information

Distribution format

L3:NetCDF4

Generation frequency

1 day, 1 month

Generation timeliness

10 days (95%), 15 days (100%)

Spatio-temporal Information

Spatial Coverage

L3:Global

Spatial Resolution

L3:HORIZONTAL:$(0.25)^2$

Temporal Resolution

~~L3:Daily:Mean~~

L3:Monthly:Mean

Temporal Coverage

01 January 2025 onwards

Uncertainty Characteristics			Optimum	Target	Threshold
~~SNL-Daily Mean~~	~~ACCURACY~~	~~bias~~	~~3 W/m²~~	~~5 W/m²~~	~~8 W/m²~~
~~SNL-Daily Mean~~	~~STABILITY~~	~~decadal~~	~~0.5 W/m²~~	~~1 W/m²~~	~~2 W/m²~~
SNL-Monthly Mean	ACCURACY	MAB	--	8 W/m²	--

Verification:

comparison with BSRN

Comment:

ICDR related to the CLARA-A3.5 CDR (CM-11292).

CM-6332	CLARA-A3.5 ToA Reflected Shortwave Flux ICDR R2	RSF_R2_CLARA_35_ICDR

Type

Dataset

Input Satellite Data	*Application Areas*
Operational Satellite:AVHRR GAC	Climate monitoring
Operational Satellite: VIIRS	

Dissemination Information

Distribution format	*Generation frequency*
L3:NetCDF4	1 day, 1 month
	Generation timeliness
	10 days (95%), 15 days (100%)

Spatio-temporal Information

Spatial Coverage	*Spatial Resolution*
L3:Global	L3:HORIZONTAL:0.25°
Temporal Resolution	*Temporal Coverage*
L3:Daily:Mean	01 January 2025 onwards
L3:Monthly:Mean	

Uncertainty Characteristics			Optimum	Target	Threshold
RSF-Daily Mean	PRECISION	MAB	--	16 W/m²	--
RSF-Monthly Mean	PRECISION	MAB	--	8 W/m²	--

Verification:

Comparison with CERES

Comment:

ICDR related to the CLARA-A3.5 CDR (CM-11313).

CM-6322	CLARA-A3.5 ToA Outgoing Longwave Radiation ICDR R2	OLR_R2_CLARA_35_ICDR

Type

Dataset

Input Satellite Data

Operational Satellite:AVHRR GAC

Operational Satellite: VIIRS

Application Areas

Climate monitoring

Dissemination Information

Distribution format

L3:NetCDF4

Generation frequency

1 day, 1 month

Generation timeliness

10 days (95%), 15 days (100%)

Spatio-temporal Information

Spatial Coverage

L3:Global

Spatial Resolution

L3:HORIZONTAL: 0.25°

Temporal Resolution

L3:Daily:Mean

L3:Monthly:Mean

Temporal Coverage

01 January 2025 onwards

Uncertainty Characteristics			Optimum	Target	Threshold
OLR-Daily Mean	PRECISION	MAB	--	16 W/m²	--
OLR-Monthly Mean	PRECISION	MAB	--	8 W/m²	--

Verification:

Comparison with CERES

Comment:

ICDR related to the CLARA-A3.5 CDR (CM-11343).